Identification of Novel Protein Interaction Partners of the Oxygen-sensing HIF Prolyl-4-hydroxylase 1 (PHD1) and Characterization of the Interactor Onconeural Cerebellar Degeneration-related Protein 2 (Cdr2)

Dissertation

zur

Erlangung der naturwissenschaftlichen Doktorwürde (Dr. sc. nat.)

vorgelegt der

Mathematisch-naturwissenschaftlichen Fakultät

der

Universität Zürich

von

Verena Simone Hofmann

aus Deutschland

Promotionskomitee

Prof. Dr. Roland H. Wenger (Vorsitz)
Dr. Gieri Camenisch (Leitung der Dissertation)
PD Dr. Ingo Flamme

Zürich, 2007

This work has been performed under the supervision of

Dr. Gieri Camenisch and

Prof. Dr. Roland H. Wenger

at the Institute of Physiology and Zürich Center for Integrative Human Physiology (ZIHP), University of Zürich, CH-8057 Zürich, Switzerland

Table of contents – Yeast two-hybrid screenings

Table of contents – The onconeural antigen Cdr2

Abbreviations

2-OG	2-oxoglutarate
Ang2	angiopoietin-2
AKT	Synonym for protein kinase B
APC	antigen-presenting cell
ARD1	arrest-defective-1
ARNT	aryl hydrocarbon receptor nuclear translocator
ATF-4	activating transcription factor-4
bHLH	basic helix-loop-helix
BSA	bovine serum albumin
C-TAD	carboxy-terminal transactivation domain
Cdr	cerebellar degeneration-related protein
ChIP	chromatin immunoprecipitation
CITED2	cAMP-responsive element-binding protein (CBP)/p300-interacting transactivators with glutamic acid (E) and aspartic acid (D)-rich tail
CODDD	c-terminal oxygen-dependent degradation domain
CTL	cytotoxic T lymphocyte
DC	dendritic cell
DFX	desferrioxamine
EGL	egg-laying abnormal
EPO	erythropoietin
ERK	extracellular signal-regulated protein kinase
ER	endoplasmatic reticulum
FIH	factor inhibiting HIF
FKBP38	FK506-binding protein 38
GSE	genetic supressor element
GST	glutathione-S-transferase
HDM2	human ortholog of mouse Mdm2
HIF	hypoxia-inducible factor
HLZ	helix-leucine zipper
HPH	HIF prolyl hydroxylase
HRE	hypoxia response element
ICAM-1	intercellular adhesion molecule 1
IGF1/2	insulin-like growth factor 1/2
ING4	inhibitor of growth family member 4
K_m	Michaelis Menten constant
NGF	nerve growth factor
NF-κB	nuclear factor kappa B
NLS	nuclear localization signal
NODDD	N-terminal oxygen-dependent degradation domain
NO	nitric oxide
NOS	nitric oxide synthase
N-TAD	amino-terminal transactivation domain
MAPK	mitogen-activated protein kinase
MDM2	mouse double minute 2
MEF	mouse embryonic fibroblast
MHC	major histocompatibility complex
mTOR	mammalian target of rapamycin
MCS	multiple cloning site
OD	optical density
ODDD	oxygen-dependent degradation domain
p300	300 kDa protein, histone acetyl transferase
PAS	PER/ARNT/SIM
PCD	paraneoplastic cerebellar degeneration
PER	*Drosophila* periodic protein
PDFG-B	platelet-derived growth factor B
PHD	prolyl-4-hydroxylase domain protein
PI3-K	phosphatidylinositol 3-kinase

PKC	protein kinase C
PKB	protein kinase B
PND	paraneoplastic neurological disease
PTEN	phosphatase and tensin homolog deleted on chromosome ten
Siah	seven in absentia homolog
SIM	*Drosophila* single-minded protein
SLE	systemic lupus erythematosus
SUMO	small ubiquitin-related modifier
TAD	transactivation domain
TAP	transporter associated with antigen processing
TCA	tricarboxylic acid
TCR	T cell receptor
TNF-α	tumor necrosis factor alpha
VCAM-1	vascular cell adhesion molecule 1
VEGF	vascular endothelial growth factor
pVHL	von Hippel-Lindau tumor suppressor protein
wt	wild-type

Zusammenfassung

Bis 1995 war der molekulare Mechanismus, wie Organismen sich an eine veränderte Sauerstoffverfügbarkeit anpassen, noch wenig verstanden. Ein wesentlicher Durchbruch gelang mit der Entdeckung des heterodimeren Transkriptionsfaktors Hypoxie-induzierbarer Faktor (HIF). Unter normoxischen Bedingungen ist die HIF-α Untereinheit aufgrund einer Prolylhydroxylierung durch HIF Prolyl-4-hydroxylasen (PHDs) instabil. Diese HIF-α Prolylhydroxylierung führt zur Erkennung und zur Bindung des von Hippel-Lindau Tumor-Suppressor Proteins (pVHL), einer Komponente eines E3-Ubiquitin-Ligase Komplexes. HIF-α wird polyubiquitinyliert und im Proteasom abgebaut. Unter Hypoxie fehlt den PHDs molekularer Sauerstoff als Kosubstrat für die Hydroxylierung, wodurch ihre Aktivität reduziert ist und dadurch die HIF-α Untereinheit stabilisiert wird. HIF-α transloziert in den Nukleus, heterodimerisiert dort mit HIF-β, rekrutiert zusätzliche Koaktivatoren und induziert schliesslich die Transkription von Zielgenen wie zum Beispiel Erythropoietin.

Die Hydroxylierungskapazität der PHDs ist im wesentlichen bestimmt durch die Sauerstoffverfügbarkeit, d.h. sie agieren als molekulare Sauerstoffsensoren innerhalb der Zelle. Bis heute sind drei verschiedene HIF PHDs bekannt. Obwohl alle drei fähig sind, HIF-α *in vitro* zu hydroxylieren, unterscheiden sie sich in der Gewebsverteilung, ihrer Induzierbarkeit unter Hypoxie und ihrer subzellulären Lokalisation. PHD1 wird überwiegend im Hoden, im Gehirn und in der Leber exprimiert. Im Gegensatz zur PHD2 und PHD3 ist die mRNA von PHD1 nicht durch Hypoxie induzierbar.

Ziel dieser Doktorarbeit war es, neue Interaktoren der PHD1 zu identifizieren. Hierfür haben wir zwei unabhängige Hefe Zwei-Hybrid Screenings durchgeführt. Wir wählten für das Screening eine Humane und eine Maus Hoden cDNA Bank und fanden unter anderem das onkoneurale Antigen Cerebellar degeneration-related protein 2 (Cdr2) als neuen Interaktor der PHD1. Cdr2 wurde benannt nach der Detektion seiner Antikörper in einer Krankheit namens paraneoplastische Kleinhirndegeneration (PCD). Dabei handelt es sich um eine seltene Autoimmunerkrankung, die auftritt, wenn Brust- oder Ovarialtumore das Cdr2 Protein exprimieren. Dieses Protein ist unter physiologischen Bedingungen nur im Kleinhirn und im Hoden vorzufinden. Die Folge ist eine durch

zytotoxische T-Killerzellen vermittelte Immunantwort, welche zu Tumorimmunität und zu einer Degeneration des Kleinhirns führt. Es wird angenommen, dass Cdr2-spezifische zytotoxische T-Killerzellen und Antikörper die Kleinhirndegeneration auslösen, indem sie die Bluthirnschranke überschreiten und im Kleinhirn exprimiertes Cdr2 als Antigen erkennen. PCD ist eine der wenige Fälle in der eine natürlich vorkommende Tumorimmunität sichtbar wird. Aufgrundessen stellt dieses Krankheitsbild ein interessantes Model zur Untersuchung und zum Verständnis von Tumorimmunität im Menschen dar.

In der vorliegenden Dissertation zeigte ich, dass Cdr2 in der Hefe und auch *in vitro* mit PHD1 interagiert. Während Cdr2 mRNA nicht sauerstoffabhängig reguliert ist, waren Cdr2 Proteinmengen in transienten Transfektionen unter Hypoxie und unter Hemmung der PHDs und des Proteasoms erhöht.

Aufgrund dieser Resultate nahmen wir an, dass Cdr2 ein neues Substrat der PHD1 ist und unter Normoxie hydroxyliert wird. Das Gehirn und der Hoden sind Organe mit relativ niedrigen Sauerstoffpartialdrücken. Desweiteren ist bekannt, dass solide Tumore, verglichen zu ihren gesunden Ursprungsgeweben, gering oxygeniert sind. Sollten also Cdr2 Proteinmengen hauptsächlich über die sauerstoffabhängige Hydroxylierung durch PHD1 reguliert sein, würde sich die Cdr2 Protein Stabilisierung in Ovarial- und Brusttumoren durch die Hemmung der PHD1 aufgrund geringer Oxygenierung des Gewebes erklären lassen.

Um die Regulation von endogenem Cdr2 Protein in Ovarial- und Brustkrebs Zellinien zu untersuchen, stellten wir poly- und monoklonale Antikörper gegen Cdr2 her. Entgegen unseren Erwartungen konnten wir die Stabilisierung von endogenem Cdr2 unter Hypoxie und PHD Hemmung nicht bestätigen.

Summary

Until 1995, the molecular mechanism by which organisms are able to adapt to low oxygen conditions was poorly understood. The discovery of the heterodimeric transcription factor hypoxia-inducible factor (HIF) represented a breakthrough in the understanding of transcriptional adaptation of the cell to changes in oxygen availability. Under normoxic conditions, the HIF-α subunit is unstable due to hydroxylation of prolyl residues catalyzed by HIF prolyl-4-hydroxylases (PHDs). Hydroxylated HIF-α prolyl residues are recognized and bound by the von Hippel-Lindau tumor suppressor protein (pVHL), a component of an E3 ubiquitin ligase complex. HIF-α becomes polyubiquitinated and is degraded via the proteasome. In contrast, under hypoxia, the PHDs are inhibited because the co-substrate oxygen is limiting and HIF-α is stabilized, translocates into the nucleus, recruits additional co-activators and finally induces the transcription of target genes such as erythropoietin.

The hydroxylation capacity of the PHDs is mainly determined by the oxygen availability, and thereby PHDs act as molecular oxygen sensors within the cell.

So far, three different PHDs are known and even though all three are able to hydroxylate HIF-α *in vitro*, they differ in their tissue distribution, their response to hypoxia and their subcellular localization. PHD1 is mainly found in testis, brain and liver. In contrast to PHD2 and PHD3, PHD1 mRNA is not induced under hypoxic conditions.

We carried out two independent yeast two-hybrid screenings to identify novel interactors of PHD1. We screened a human and a mouse testis cDNA library and identified among others the onconeural antigen cerebellar degeneration-related protein 2 (Cdr2) as a novel PHD1 interactor. The physiological function of Cdr2 is unknown, but anti-Cdr2 antibodies are found in a disease called paraneoplastic cerebellar degeneration (PCD). This uncommon autoimmune disease develops when breast or ovarian tumors start to express Cdr2 protein, which is under physiological conditions limited to the cerebellum and the testis. The consequence is a $CD8^+$ cytotoxic T cells-mediated immune response which leads to tumor immunity and cerebellar degeneration. It is believed that Cdr2 specific $CD8^+$ cytotoxic T cells and antibodies elicit the cerebellar degeneration. They seem to be able to pass the blood-brain-barrier and to recognize Cdr2 as

an antigen expressed in the cerebellum. PCD is one of the rare cases where naturally occurring tumor immunity becomes visible and thereby it represents an interesting model for studying tumor immunity in human beings.

I showed in my thesis that Cdr2 interacts in yeast and *in vitro* with PHD1. Whereas Cdr2 transcription is not regulated in an oxygen-dependent manner, Cdr2 protein levels were increased under hypoxic conditions as well as after inhibition of the PHD enzymes and the proteasome in transient transfection assays. Therefore, we hypothesized that Cdr2 might be a novel substrate of PHD1 which could hydroxylate Cdr2 under normoxic conditions. Brain and testis are organs with relatively low oxygen partial pressure and it is well established that also solid tumors are poorly oxygenated in comparison to their tissue of origin. If Cdr2 protein levels are mainly regulated by oxygen-dependent hydroxylation by PHD1, Cdr2 protein stabilization in ovarian and breast tumors might be due to inhibition of PHD1 by reduced tissue oxygenation.

We then generated polyclonal and monoclonal antibodies against Cdr2 to investigate the protein regulation of endogenous Cdr2 in ovary and breast cancer cell lines. Unfortunately, oxygen- and PHD-dependent regulation of endogenous Cdr2 protein levels could not be confirmed.

Introduction

1 The hypoxia-inducible factor (HIF)

1.1 Discovery and function of HIF

Oxygen is the final electron acceptor in the respiratory electron transport chain and thereby its abundance is crucial for the aerobic generation of energy in form of ATP within the cell. The oxygen homeostasis itself is tightly controlled to maintain intracellular oxygen levels necessary for metabolic processes and to avoid oxygen-mediated toxicity. Although specific oxygen-sensing mechanisms were defined in bacteria and yeast, until 1995 it was barely understood how higher organisms are able to adapt to a decrease in oxygen.

The discovery of the heterodimeric transcription factor hypoxia-inducible factor (HIF) more than one decade ago represented a breakthrough in the understanding how organisms respond and adapt to low oxygen conditions (hypoxia) (Wang and Semenza 1995). HIF was initially identified as transcription factor that upregulates erythropoietin gene expression in kidney tissues when oxygen availability is decreased. Over the last years more than 70 HIF target genes involved in oxygen-homeostasis, glucose-energy-metabolism, apoptosis and growth have been identified (Wenger *et al.* 2005). HIF binds to the conserved sequence 5'-RCGTG-3' in hypoxia-response elements (HREs) of these genes and thereby upregulates gene expression (Wenger *et al.* 2005). Table 1 shows few examples of HIF target genes.

	HIF target genes
Glucose metabolism	HK1, HK2, AMF/GPI, ENO1, GLUT1, GADPH, LDHA, PFKBF3, PFKL, PGK1, PKM, TPI
Angiogenesis	EG-VEGF, ENG, LEP, LRP1, TGF-β3, VEGF
Erythropoesis	EPO
Iron metabolism	Ceruloplasmin, Transferrin, Transferrin receptor
pH regulation	Carbonic anhydrase 9
Cell proliferation	Cyclin G2, IGF2, IGF-BP1, IGF-BP2, IGF-BP3, WAF1, TGF-α, TGF-β
Cell survival	ADM, EPO, IGF2, IGF-BP1, IGF-BP2, IGF-BP3, NOS2, TGF-α, VEGF
Apoptosis	NIP3, NIX, RTP801
Vascular tone	α_{1B}-adrenergic receptor, ADM, ET1, Haem oxygenase-1, NOS2
Cell adhesion	MIC2
Cytoskeletal structure	KRT14, KRT18, KRT19, VIM
Motility	AMF/GPI, c-MET, LRP1, TGF-α
Transcriptional regulation	DEC1, DEC2, ETS-1, NUR77

Regulation of HIF-1 activity	p35srj
Epithelial homeostasis	Intestinal trefoil factor
Drug resistance	MDR1
Nucleotide metabolism	Adenylate kinase 3
Extracellular-matrix metabolism	CATHD, Collagen type V (α1), FN1, MMP2, PAI1, Collagen prolyl-4-hydroxylase α (I), UPAR
Energy metabolism	LEP
Amino-acid metabolism	Transglutaminase 2

Table 1: HIF target genes *(Semenza 2003). ADM, adrenomedullin; ALDA, aldolase A; ALDC, aldolase C; AMF, autocrine motility factor; CATHD, cathepsin D; EG-VEGF, endocrine-gland-derived VEGF; ENG, endoglin; ET1, endothelin-1; ENO1, enolase 1; EPO, erythropoietin; FN1, fibronectin 1; GLUT1, glucose transporter 1; GLUT3, glucose transporter 3; GAPDH, glyceraldehyde-3-P-dehydrogenase; HK1, hexokinase 1; HK2, hexokinase 2; IGF2, insulin-like growth-factor 2; IGF-BP1, IGF-factor-binding-protein 1; IGF-BP2, IGF-factor-binding-protein 2; IGF-BP3, IGF-factor-binding-protein 3; KRT14, keratin 14; KRT18, keratin 18; KRT19, keratin 19; LDHA, lactate dehydrogenase A; LEP, leptin; LRP1, LDL-receptor-related protein 1; MDR1, multidrug resistance 1; MMP2, matrix metalloproteinase 2; NOS2, nitric oxide synthase 2; PFKBF3, 6-phosphofructo-2-kinase/fructose-2,6-biphosphatase-3; PFKL, phosphofructokinase L; PGK 1, phosphoglycerate kinase 1; PAI1, plasminogen-activator inhibitor 1; PKM, pyruvate kinase M; TGF-α, transforming growth factor-α; TGF-β3, transforming growth factor-β3; TPI, triosephosphate isomerase; VEGF, vascular endothelial growth factor; UPAR, urokinase plasminogen activator receptor; VEGFR2, VEGF receptor-2; VIM, Vimentin*

1.2 Composition of the HIF complex

HIF is a heterodimeric protein complex, which consists of oxygen sensitive HIF-α subunits (HIF-1α, HIF-2α or HIF-3α) and a constitutively expressed HIF-1β subunit, also known as ARNT (aryl hydrocarbon receptor nuclear translocator). Both α and β subunits are members of the basic helix-loop-helix Per/Arnt/Sim (bHLH-PAS) transcription factor family (Wang and Semenza 1995).

HIF-α consists of an N-terminal basic helix-loop-helix domain (bHLH), which is necessary for DNA binding, followed by the PAS domain that is essential for dimerization with ARNT (Jiang *et al.* 1996). HIF-α undergoes oxygen-regulated degradation which is dependent on the presence of two independently functioning domains, called NODDD and CODDD, standing for N-terminal and C-terminal oxygen-dependent degradation domain, respectively (ODDD). The ODDD contains two proline residues (P402 and P564) (numbering according to human HIF-1α). Two transactivation domains (TAD), an N-terminal and a C-terminal, complete the domain structure in the C-terminal part of HIF-1α and HIF-2α whereas HIF-3α lacks a C-terminal TAD. In addition, a nuclear localization signal (NLS) is also found within the C-terminal part of HIF-1α and HIF-2α. Figure 1 indicates the domain structure of the three HIF-α isoforms.

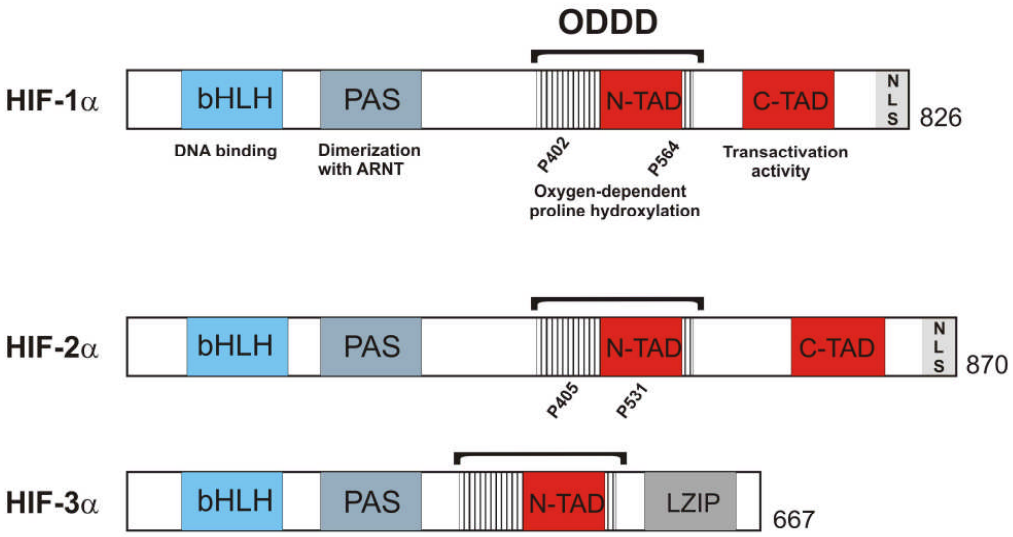

***Figure 1: Domain structure of HIF-α isoforms**. HIF-α isoforms share bHLH, PAS domain and the ODDD which contains the N-terminal TAD. Two proline residues within the ODDD are hydroxylated in normoxia. HIF-1α and HIF-2α possess additionally the C-terminal transactivation domain, whereas HIF-3α contains a leucine zipper in the C-terminus. In addition the nuclear localization sequence is shown (NLS).*

1.3 Regulation of HIF-1α by oxygen

1.3.1 Oxygen-dependent regulation of HIF-1α protein stability

HIF-1α and HIF-1β mRNAs are both constitutively and oxygen-independently expressed. In contrast, HIF-1α protein undergoes oxygen-regulated degradation. In normoxia, PHDs hydroxylate two conserved proline residues, proline 402 and 564 within the HIF-1α ODDD which mediate the binding of von Hippel-Lindau tumor suppressor protein (pVHL), the substrate recognition component of an E3 ubiquitin ligase complex. Polyubiquitination of HIF-1α takes place and the subunit is targeted for proteasomal degradation (Maxwell *et al.* 1999). In patients, suffering from the von Hippel-Lindau disease, a rare hereditary cancer syndrome, one allele of the VHL gene is mutated. In case of loss or somatic inactivation of the wild-type allele, these patients loose VHL function and hence develop sporadic renal cell carcinomas (Gnarra *et al.* 1994). Constant HIF upregulation in the absence of pVHL in these carcinomas suggested that pVHL-dependent proteolysis is the prime oxygen-dependent degradation pathway (Maxwell *et al.* 1999). Under hypoxic conditions, PHD activity is reduced because molecular dioxygen is limited and α subunits become stabilized.

1.3.2 Oxygen-dependent regulation of the HIF-1α transactivation activity

In addition to prolyl hydroxylation under normoxia, hydroxylation of an asparagine residue (Asn803) in the C-terminal transactivation domain by factor inhibiting HIF (FIH) takes place. Asn803 hydroxylation blocks the recruitment of coactivators such as p300 and CREB-binding protein and thereby inhibits transactivation activity (Lando *et al.* 2002). Like PHDs, FIH is also inhibited under hypoxia due to limited molecular oxygen, and the C-terminal TAD undergoes no modification and stays active. HIF-1α translocates into the nucleus and heterodimerizes with its HIF-1β subunit. A functional transcriptional complex is formed, which binds to the consensus sequence in the HREs of its target genes and induces their expression (Metzen and Ratcliffe 2004). Figure 2 shows the oxygen-dependent regulation of HIF by PHDs and FIH.

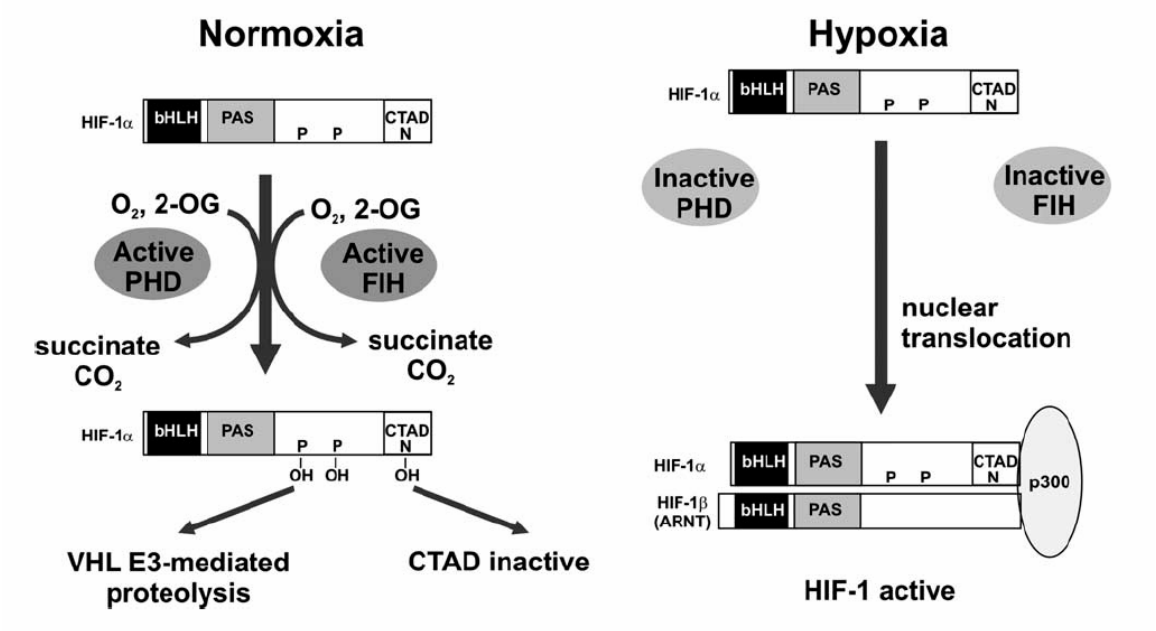

Figure 2: Oxygen-dependent regulation of HIF-1α *(Metzen and Ratcliffe 2004)*
Under normoxia, HIF-1α is unstable and inactive due to hydroxylation of proline and asparagine residues by PHDs and FIH. HIF-1α undergoes VHL-mediated ubiquitination and proteolysis. Under hypoxia, the hydroxylases are inhibited and HIF-1α becomes stabilized, translocates to the nucleus and recruits coactivators for transactivation of its target genes.

1.4 Additional positive and negative regulators of HIF

HIF-1α is induced by a variety of growth factors and cytokines such as insulin, insulin-like growth factors (IGF1/2), endothelial growth factor (EGF) or tumor necrosis factor alpha (TNF-α). Most of these stimuli act through PI3-K/Akt/PKB

and MAPK signaling cascades and are oxygen independent (Semenza 2002). Within the PI3-K/Akt signaling pathway, HIF-1α is upregulated through PI3-K itself, PTEN, Akt and also through some insulin signaling downstream targets like HDM2 and mTOR (Zundel *et al.* 2000; Stiehl *et al.* 2002). The second pathway known to be involved in oxygen-independent upregulation of HIF-1 is the MAPK pathway. Inhibition of MAP kinase results in downregulation of HIF-1 transcriptional activity. Although ERK1/2 MAP kinases have been suggested to be able to phosphorylate HIF-1α, no specific phosphorylation sites had been identified (Richard *et al.* 1999). Treatment of cells with the unselective tyrosine kinase inhibitor genistein led to lower HIF-1 DNA-binding activity and reduced HIF-1α stabilization under hypoxia. Likewise, treatment with the unspecific phosphatase inhibitor sodium orthovanadate increased HIF-1α phosphorylation and thereby enhanced DNA-binding activity. These results suggest that HIF-1α phosphorylation might be a potential way of modulating HIF-dependent signaling pathways (Wang *et al.* 1995).

In 2004, Bae *et al.* reported a novel post-translational modification that influences HIF-1α stability as well as transcriptional activity. Small ubiquitin-related modifier-1 (SUMO) modifies its target proteins similar to the ubiquitination process. Although the underlying mechanism is not clear, sumoylation of the lysines 391, 477 and 532 upregulates HIF-1α protein level as well transcriptional activity, resulting in higher expression of VEGF (Bae *et al.* 2004).

The influence of the immune regulator and inflammatory molecule nitric oxide (NO) on HIF-1α is controversially discussed. Some studies report that NO inhibits HIF in hypoxia, others observe HIF-1α upregulation in response to NO in normoxia (Huang *et al.* 1999; Sandau *et al.* 2001). HIF-1α cysteine 300 S-nitrosylation has been shown *in vitro* and in cell culture experiments, but the biological role and function of this modification remains unclear (Sumbayev *et al.* 2003).

The function of the tumor suppressor protein p53 in the regulation of HIF-1α is widely discussed. HIF-1α dependent p53 degradation as well as HIF-dependent p53 induction have been reported (An *et al.* 1998; Ravi *et al.* 2000). However, our group provided evidence that hypoxic upregulation of HIF-1α is not sufficient

for oxygen-regulated p53 induction (Wenger *et al.* 1998). Only near anoxic conditions, mimicked through treatment of cells with the iron chelator and PHD inhibitor desferrioxamine (DFX), induced p53. Furthermore, p53 upregulation was observed even in HIF-1α-deficient cells, suggesting that oxygen-dependent p53 induction is HIF-1α independent.

The N-acetyltransferase arrest-defective-1 (ARD1) was reported to acetylate HIF and it has been suggested that inhibition of ARD1 is sufficient to stabilize HIF-1α protein (Jeong *et al.* 2002). In contrast, Fisher *et al.* recently showed that inhibition of ARD1 did neither increase HIF protein levels nor expression of HIF target genes (Fisher *et al.* 2005). In addition, other research groups were unable to reproduce ARD1-dependent HIF-1α regulation (Arnesen *et al.* 2005; Bilton *et al.* 2005).

Another negative regulator of HIF-1α is a p300-binding protein called CITED2 (cAMP-responsive element-binding protein (CBP)/p300-interacting transactivators with glutamic acid (E) and aspartic acid (D)-rich tail 2). CITED2 protein is bound within the cell by p300 and therefore competes with HIF-1α for p300 binding. This means that the interaction of CITED2 with p300 blocks the HIF-1α-p300 interaction and thereby the transactivation of HIF-1α. The fact that CITED2 expression is upregulated by hypoxia led to the assumption that a negative feedback loop may exist which downregulates HIF-1-mediated transactivation under hypoxia (Bhattacharya *et al.* 1999).

2 The HIF prolyl-4-hydroxylases function as oxygen sensors

2.1 The HIF prolyl-4-hydroxylases (PHDs)

In 2001, Epstein and colleagues described a family of three human and mouse HIF prolyl-4-hydroxylases which showed high homology to the egg-laying abnormal-9 (EGL9) family in *Caenorhabditis elegans* (*C. elegans*) (Epstein *et al.* 2001). They termed the three isoforms of HIF prolyl-4-hydroxylases PHD1, PHD2 and PHD3, standing for prolyl-4-hydroxylase domain-containing protein. These enzymes have alternatively been termed HIF prolyl hydroxylase (HPH3, HPH2 and HPH1) or egg laying abnormal nine homolog (EGLN2, EGLN1 and EGLN3) (Bruick and McKnight 2001; Ivan *et al.* 2002). Each of the three PHD isoforms contains a conserved gene structure, suggesting duplication in the lineage leading to vertebrates (Taylor 2001). The three HIF prolyl hydroxylases show 42 to 59% sequence identity to each other but no distinct sequence similarity to the well known collagen prolyl-4-hydroxylases (Hirsilä *et al.* 2003). Only one HIF prolyl hydroxylase orthologue has been identified in *Drosophila melanogaster* (*D. melanogaster*) (Bruick and McKnight 2001).

PHD1, also known and discovered as the mouse orthologue Falkor (Erez *et al.* 2002), is located on chromosome 19q13.2 and encodes a predicted open reading frame of 407 amino acids (Bruick and McKnight 2001). PHD1 is able to hydroxylate both Pro402 and Pro564 of human HIF-1α *in vitro* (Epstein *et al.* 2001). When fused to green fluorescent protein (GFP), PHD1 is found exclusively in the nucleus of the cell (Metzen *et al.* 2003). In contrast, a recent publication of Soilleux *et al.* used novel monoclonal antibodies against PHD1 and observed predominantly cytoplasmic staining in normal tissue. Furthermore bronchogenic and breast carcinoma showed similar staining for PHD1 (Soilleux *et al.* 2005).

PHD2 is located on chromosome 1q42-43 (Dupuy *et al.* 2000) and GFP-PHD2 is found predominantly in the cytoplasm of the cell (Metzen *et al.* 2003). Berra *et al.* showed that regulation of HIF-1α protein stability seems to be mainly dependent on PHD2 (Berra *et al.* 2003). Soilleux *et al.* detected endogenous PHD2 mainly in the cytoplasm (Soilleux *et al.* 2005).

PHD3 was originally termed SM-20 and found to be upregulated in rat smooth muscle cells after stimulation with platelet-derived growth factor (Wax *et al.* 1994). With 239 amino acids, PHD3 represents the shortest of the three PHDs. Overexpressed GFP-PHD3 was found both in the nucleus and the cytoplasm (Metzen *et al.* 2003). Endogenous PHD3 was as well observed in the nucleus and the cytoplasm (Soilleux *et al.* 2005).

Recently a fourth prolyl hydroxylase termed PH-4 was found through a database search approach. Despite a high similarity to the other three PHDs and suppression of HIF-2α accumulation as well as HIF-dependent reporter gene activation in PH-4 overexpressing cells, this isoform did not show any activity in a HIF-1α-pVHL *in vitro* interaction assay (Oehme *et al.* 2002).

2.2 PHD mRNA expression pattern

PHD1, PHD2 and PHD3 mRNA was found to be expressed in all tissues albeit at different levels (Cioffi *et al.* 2003). PHD1 mRNA is mostly detected in testis and PHD2 and PHD3 mRNA in heart and liver (Lieb *et al.* 2002). Recently, Hirsilä *et al.* identified alternatively spliced isoforms of PHD2 and PHD3, which showed no enzymatic activity. The levels of expression of these splice variants were, in comparison to the mRNAs containing all exons, lower in all tissues examined (Hirsilä *et al.* 2003).

2.3 Enzymatic activity and catalytic mechanism of the PHDs

PHDs are iron- and 2-oxoglutarate (2-OG) dependent dioxygenases and catalyze the hydroxylation of specific prolyl residues within the ODDD of HIF-α subunits. They need oxygen as co-substrate and ascorbate as co-factor. The requirement of molecular oxygen for the hydroxylation of proline residues presents their O_2-sensing function. Figure 3 shows the proposed mechanism of prolyl hydroxylation by PHDs.

During the enzymatic reaction, one oxygen atom is added to a peptidyl proline to form hydroxyproline. In a coupled decarboxylation reaction that converts 2-oxoglutarate to succinate the second oxygen atom is incoporated into succinate (Welford *et al.* 2005). Within the enzyme Fe(II) is bound through a triad of two histidinyl residues and one aspartyl residue. Three remaining coordination sites are occupied by two to three labile water molecules. The detailed mechanism of

the catalysis by HIF prolyl hydroxylases is still not clear. One common suggested mechanism is that an enzyme-Fe(II) complex first binds 2-oxoglutarate. As a next step 2-OG substitutes a water molecule that is co-ordinated to the Fe(II) and thereby triggers the reaction with molecular oxygen. The next step is thought to be the oxidative decarboxylation of 2-oxoglutarate, which produces succinate and a ferryl species at the iron centre. The generated highly reactive intermediate is then able to oxidize the prime substrate (RH), a peptidyl proline (Costas *et al.* 2004; Hausinger 2004).

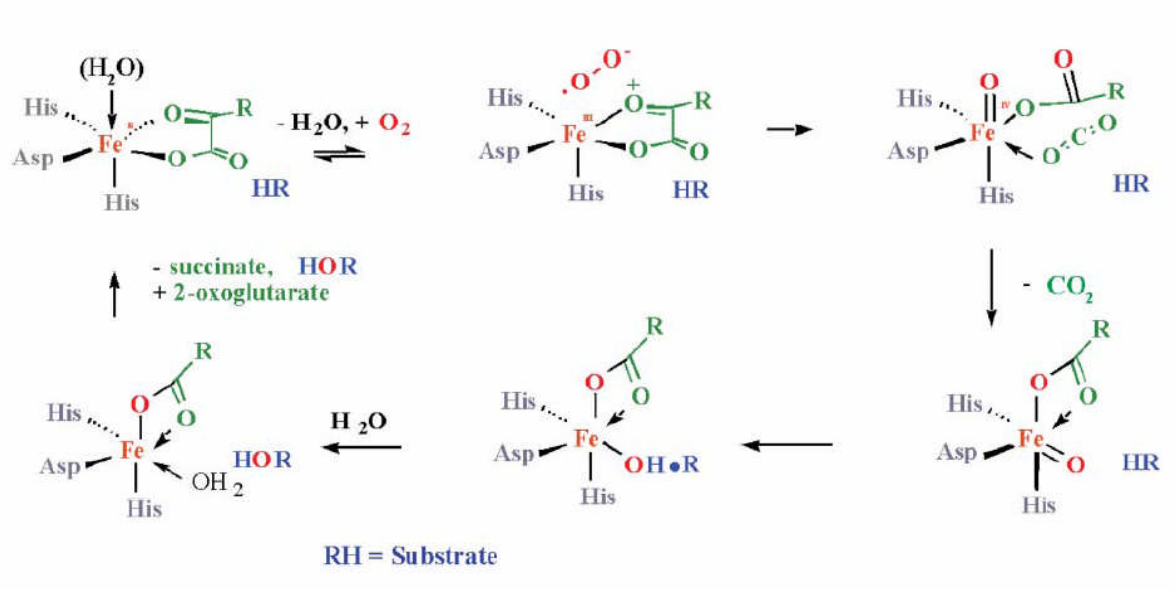

Figure 3: Proposed mechanism of prolyl hydroxylation by PHDs *(McNeill et al. 2005)*
It is suggested that an enzyme-Fe(II) complex binds co-substrate 2-OG. Binding of 2-OG releases a water molecule and thereby triggers the reaction with O_2. After binding of oxygen an oxidative decarboxylation of 2-oxoglutarate to succinate releases CO_2 and generates a ferryl species (Fe^{IV}=O) at the iron centre. The generated highly reactive intermediate is then able to oxidize the prime substrate RH.

2.4 Substrate specificity

All three PHDs are able to hydroxylate proline residues in a conserved LXXLAP (Leu-X-X-Leu-Ala-Pro) sequence motif *in vitro*, but their relative activity seems to be different. Whereas PHD2 and PHD3 show similar specific activity, PHD1 has a lower activity (Tuckerman *et al.* 2004). Concerning proline specificity, all three PHDs can hydroxylate HIF-1α Pro564, but PHD1 and PHD2 preferentially hydroxylate HIF-1α Pro402 (Chan *et al.* 2005). Although all PHDs seem to contribute to HIF-1α regulation, the extent of the contribution of each PHD enzyme might be dependent on its relative abundance (Appelhoff *et al.* 2004).

Li *et al.* recently showed that amino acid substitutions in a HIF-1α peptide caused only minor changes in PHD hydroxylation activity. The hydroxylation activity was measured by an *in vitro* method based on the hydroxylation-coupled decarboxylation of 2-oxoglutarate and mass spectrometry to analyse peptide hydroxylation (Hirsilä *et al.* 2003; Li *et al.* 2004). They reported that the two leucines in the LXXLAP motif of a 20-residue peptide can be replaced by many other amino acids, resulting in no or only a slight decrease in hydroxylation activity. Also the two amino acids glutamate and methionine (indicated here as X-X residues) could be substituted by almost any residue with no change compared to the wild-type peptide. Alanine showed the strictest requirement for hydroxylation and no other amino acid was able to fully substitute for it in case of PHD2, whereas in case of PHD1 and PHD3 it could be substituted by only serine, isoleucine, valine or serine. Additionally, Huang *et al.* showed that Leucine 574 in HIF-1α is required for VHL binding and VHL-mediated degradation. When Leucine 574 was mutated the degradation process of HIF-1α was prevented (Huang *et al.* 2002).

2.5 Regulation of PHD expression and degradation

PHD2 and PHD3 are oxygen-dependently regulated by HIF (Epstein *et al.* 2001; Metzen *et al.* 2005; Pescador *et al.* 2005). Whereas the induction of PHD3 is HIF-1α and HIF-2α dependent, PHD2 is not affected by overexpression or downregulation of HIF-2α (Aprelikova *et al.* 2004). In contrast, PHD1 shows no upregulation under hypoxia and is not a HIF target gene (Appelhoff *et al.* 2004). PHD1 and PHD3 are proteasomally degraded by Siah1a/2 (Nakayama *et al.* 2004). Siah are specific ring finger E3-ubiquitin ligases catalyzing polyubiquitination. Nakayama *et al.* showed that overexpression of Siah2 and Siah1a resulted in decreased levels of PHD1 and PHD3 in human embryonic kidney (HEK293T) cells and that PHD3 is stabilized under normoxic (20% O_2) as well as hypoxic (1% O_2) conditions in Siah2$^{-/-}$ and Siah1a$^{-/-}$ mouse embryonic fibroblasts (MEFs). They also observed an increase of Siah1 and Siah2 mRNA by hypoxia and impaired hypoxic HIF-1α induction in *Siah2*$^{-/-}$ cells (Nakayama *et al.* 2004).

In addition, several other stimuli are known to regulate PHD expression. PHD1 mRNA was shown to be upregulated by estrogen in the breast cancer cell line

ZR75-1 (Seth *et al.* 2002) and the rat orthologue of human PHD3, SM20, was induced in response to p53 activation (Madden *et al.* 1996) as well as nerve growth factor withdrawal in PC-12 cells (Lipscomb *et al.* 2001).

2.6 Regulation of prolyl-4-hydroxylation activity

2.6.1 Molecular oxygen

In 2003, Hirsilä *et al.* determined K_m values for oxygen of the PHDs using insect cell lysates overexpressing PHDs and a synthetic 19-residue peptide with a sequence identical to the C-terminal hydroxylation site of HIF-1α. The *in vitro* hydroxylation activity assay was based on the determination of [^{14}C]CO_2 formed during the hydroxylation-coupled decarboxylation of [1-^{14}C]2-oxoglutarate (Kivirikko and Myllyla 1982). The measured K_m values for oxygen were between 230 - 250 μM close to the oxygen partial pressure (pO_2) in air (Hirsilä *et al.* 2003). These data confirmed already existing data from 2001 showing that PHD enzyme activity was indeed highly sensitive to hypoxia (Epstein *et al.* 2001). Epstein *et al. in vitro* hydroxylated HIF-1α-derived peptides and used a VHL capture assay and showed a progressive reduction of hydroxylation activity by decreasing pO_2 levels. However, these *in vitro* values are of somewhat limited relevance, since the length of peptide substrates showed a marked effect on the K_m values for oxygen (Koivunen *et al.* 2006). When determined with recombinant HIF-1α ODDD (amino acid 356-603) as substrate, K_m values of 100 μM were obtained, corresponding to 40% of the values determined with 19-residue peptides. Nevertheless, the K_m values for oxygen are clearly above physiological pO_2 values in the body (Hirsilä *et al.* 2003). This suggests that PHDs work with maximal sensitivity in the range of physiological tissue pO_2 and therefore act as cellular oxygen sensors. An important aspect is the mechanism by which PHDs are able to adapt to different physiological oxygen concentrations. Whereas Schofield and Ratcliffe assumed that oxygen is the limited factor for PHD hydroxylation capacity (Schofield and Ratcliffe 2005), Stiehl *et al.* recently showed that increased PHD protein abundance can compensate for a decrease in oxygen levels (Stiehl *et al.* 2006). Upregulation of PHD2 and PHD3 mRNA levels under 2% oxygen in cell culture reached a transient maximum after 64 to 112 hours and remaining upregulated for more than 10 days. Co-transfection of *Hif-1*$\alpha^{-/-}$ MEFs with a one-hybrid reporter gene

containing the HIF-1α ODDD and PHD expression plasmids showed that increased PHDs levels are able to compensate for reduced oxygen availability (Stiehl *et al.* 2006).

2.6.2 Iron and divalent metal ions

PHDs are non-heme Fe-binding dioxygenases and able to bind divalent iron directly. Inhibition of the PHD activity by iron chelators induces HIF target genes (Epstein *et al.* 2001). Other divalent ions such as Co^{2+}, Ni^{2+} and Mn^{2+} were able to mimic hypoxia and induce HIF target genes *in vivo* (Goldberg *et al.* 1988). Interestingly, Hirsilä *et al.* recently showed that recombinant PHDs purified from insect cells exert considerable *in vitro* hydroxylation activity without addition of iron. It was shown that Fe^{2+} is tightly bound to the PHDs with a remarkably low K_m value, 0.03 μM for PHD1 and 2 and 0.1 μM for PHD3 (Hirsilä *et al.* 2005). These data were confirmed by the fact that the enzyme preparations were only partially inhibited by various divalent metal ions, such as Co^{2+}, Ni^{2+} and Mn^{2+} as well as up to 1 mM DFX. Recently, Martin *et al.* found that Cu^{2+} can increase HIF-1-dependent reporter gene induction and $CuCl_2$ is able to inhibit HIF-1α prolyl-4-hydroxylation independent of the Fe^{2+} concentration (Martin *et al.* 2005). Based on spectroscopic and structural studies, it was assumed that metals would be effective competitive inhibitors of the PHDs. However, this could not be confirmed by *in vitro* assays (Schofield and Ratcliffe 2004). Therefore, other mechanisms might exist by which metals inhibit the PHD enzymes or stabilize HIF-1α *in vivo.* Salnikow *et al.* reported that intracellular ascorbate, previously shown to be necessary for PHD activity, might be depleted by Co^{2+} and Ni^{2+} (Salnikow *et al.* 2004).

2.6.3 Ascorbate

Ascorbate oxidation is known to be necessary for the reduction of oxidized Fe^{IV} (Myllyla *et al.* 1984) and it is thought to be necessary for the protection of the PHDs from uncoupled reactions by which no substrate hydroxylation takes place but damaging ROS are generated (Myllyharju and Kivirikko 1997). Two independent studies showed that ascorbate promotes PHD activity and HIF hydroxylation, one in rapidly growing tissue culture cells and another one in *junD*-deficient cells which contain reduced anti-oxidant defense systems. These

studies suggest that ascorbate might act as a mediator between antioxidant and hypoxia pathways (Knowles *et al.* 2003; Gerald *et al.* 2004).

2.6.4 2-oxoglutarate

2-oxoglutarate is a tricarboxylic acid (TCA) cycle intermediate and necessary as co-substrate for PHDs, thereby linking oxygen sensing and glucose metabolism. Hereditary cancer syndromes, associated with mutations in the succinate dehydrogenase gene, lead to succinate accumulation which inhibits the HIF prolyl hydroxylases and thereby increases stabilization of HIF (Selak *et al.* 2005). Another study additionally showed that endogenous 2-oxoacids, such as pyruvate and oxaloacetate, are both able to act as competitive inhibitors of the 2-OG-dependent PHDs (Dalgard *et al.* 2004).

Fumarate hydratase catalyzes the conversion of fumarate to malate in the TCA cycle. Individuals with hemizygous germline mutations in the fumarate hydratase gene have elevated intracellular fumarate levels and are predisposed to renal cancer. Isaacs and co-workers recently demonstrated that fumarate hydratase inhibition leads to elevated HIF levels by PHD inhibition. They demonstrated that fumarate inhibits PHD activity by competing with its co-substrate 2-OG (Isaacs *et al.* 2005).

2.6.5 Nitric oxide (NO)

NO is an *in vitro* inhibitor of the 2-oxoglutarate-dependent dioxygenases. Several studies showed inhibition of hydroxylation of HIF-1α by different NO donors (Sogawa *et al.* 1998; Metzen *et al.* 2003). The mechanism believed to influence PHD hydroxylation activity might be competition of NO with O_2 for binding to the iron in the active site (Zhang *et al.* 2002). This competition might explain activation of HIF by NO donors under normoxia (Metzen *et al.* 2003). In contrast another study suggested that NO inhibits complex IV of the mitochondrial electron transport chain in hypoxia and thereby oxygen is redistributed towards the PHDs (Hagen *et al.* 2003).

2.6.6 Reactive oxygen species (ROS)

The role of ROS on HIF and PHD activity is discussed controversially. It has been suggested that PHDs are highly susceptible to oxidative damage, either via active site oxidation (Hausinger 2004) or inactivation via conversion of Fe^{2+}

to Fe^{3+}. Evidence for oxidative damage of PHDs by ROS could be recently demonstrated using junD-deficient cells. JunD is responsible for the reduction of ROS levels as part of a defence against oxidative stress. Gerald *et al*. observed that *junD*$^{-/-}$ cells show reduced PHD2 activity and elevated HIF-1α stabilization which could be rescued by ascorbate. In addition, electron paramagnetic resonance (EPR) measurements showed an increase of oxidized iron (Fe^{3+}) in the catalytic site of PHD2 (Gerald *et al.* 2004). This observation of oxidative inactivation of PHDs might also represent an explanation why HIF-1α can be stabilized by substances such as hydrogen peroxide (Guzy *et al.* 2005). Another postulation is that ROS species produced by mitochondria might be involved in hypoxia signaling (Chandel *et al.* 1998). Chandel *et al.* suggested that ROS production at complex III of the respiratory chain is elevated in hypoxia and that this signal is linked to HIF stabilization. Inhibitors of the respiratory chain which reduced ROS production also reduced hypoxic stabilization of HIF-1α. However, this hypothesis is controversial and it is not even clear whether ROS levels are elevated or reduced in hypoxia.

2.7 Known interactors of the PHDs

Ring finger E3-ubiquitin ligases Siah1 and Siah2 were described in 2004 as PHD1 and PHD3 interactors (Nakayama *et al.* 2004). They catalyze the polyubiquitination of PHD1 and PHD3 and thereby mediate proteasomal degradation. Overexpression of these E3-ubiquitin ligases resulted in decreased levels of PHD1 and PHD3 in human 293T cells. Nakayama *et al.* also reported an increase of Siah1 and Siah2 mRNA by hypoxia, and that *Siah2*$^{-/-}$ cells exhibit impaired induction of HIF-1α under hypoxia (Nakayama *et al.* 2004).

Several yeast two-hybrid screenings were performed and revealed novel interactors of the PHD isoforms. A protein termed human amplified in osteosarcoma nine (OS-9) was identified as HIF-1α, PHD2 and PHD3 interacting protein (Baek *et al.* 2005). Several experiments suggested the formation of a complex consisting of HIF-1α, OS-9 and PHD2 or PHD3. OS-9 and PHD2 were binding independently of HIF-1α at non-overlapping sites. Whereas HIF-1α was promoting the interaction between OS-9 and PHD2, OS-9

overexpression enhanced HIF-1α and PHD2 or PHD3 interaction and thereby promoted HIF-1α hydroxylation, VHL binding and proteasomal degradation.

The tumor suppressor inhibitor of growth family member 4 (ING4) was identified in a yeast two-hybrid screening as PHD2 interacting protein (Ozer *et al.* 2005). No evidence was found that ING4 is a substrate for PHD2 or that it influences PHD2 activity. Surprisingly, ING4 suppresses HIF transcriptional activity. Suppression of ING4 via siRNA increased the expression of a stably transfected HIF-dependent luciferase reporter gene in HeLa cells. ING family members have been shown to promote chromatin remodeling through the recruitment of factors that promote or suppress transcriptional activation. Ozer *et al.* suggested that under normoxic conditions, ING4 might be responsible for recruitment of chromatin-remodeling factors to the promoter regions of HIF target genes and thereby suppress their transcription. It has been proposed that ING4 retains PHD2 in the nucleus in order to degrade HIF upon reoxygenation. However, recent data showed predominant cytoplasmic localization of PHD2 (Soilleux *et al.* 2005).

PHD3 was identified to interact specifically with the cytosolic chaperonin TCP-1 Ring Complex (TRiC), when co-purified in extracts from several cell types (Masson *et al.* 2004). The function of this interaction is still not clear, but additionally it has also been shown that TriC interacts with VHL in mammalian cells. Feldman *et al*. further showed that TriC is required to assemble VHL into the VHL-Elongin B-Elongin C (VBC) complex. When Feldman and co-workers used *in vitro* translated VHL in a lysate of immune-depleted TRiC they failed to produce correctly folded VBC complex (Feldman *et al.* 1999).

Hopfer *et al.* identified the WD-repeat protein MAPK organizer 1 (Morg1) as an *in vitro* and *in vivo* interactor of PHD3 (Hopfer *et al.* 2006). The two proteins displayed similar tissue expression patterns and co-localized in the cytoplasm as well as in the nucleus. Additionally, Hopfer and co-workers showed that HIF-mediated reporter gene activity was decreased by Morg1 and even further reduced to basal levels when Morg1 was co-expressed with PHD3. RNAi-mediated downregulation of Morg1 or PHD3 resulted in strong upregulation of HIF-1 activity. Morg1 was described as molecular scaffold for components of the ERK signaling cascade (Vomastek *et al.* 2004) and the authors suggested that

Morg1 might interact specifically with PHD3 by acting as a molecular scaffold, thereby influencing HIF-1 activity (Hopfer *et al.* 2006).

We recently found that FKBP38, a peptidyl-prolyl *cis/trans* isomerase is an interactor of PHD2. HeLa cells in which FKBP38 was stably downregulated via siRNA showed an increase of PHD2 protein levels in comparison to the wild-type cell line (Barth *et al*., under revision), suggesting that FKBP38 influences PHD2 protein stability.

A novel PHD3 interactor, the activating transcription factor-4 (ATF-4) was as well identified. ATF-4 is stabilized under hypoxia and seems to be a specific hydroxylation target of PHD3 (Koeditz *et al.*, under revision).

3 The HIF prolyl-4-hydroxylase 1 – PHD1

3.1 Cloning of PHD1

Bruick and McKnight searched the GenBank database for sequences related to the catalytic α subunit of the collagen-modifying prolyl-4-hydroxylases and found five human homologs (Bruick and McKnight 2001). All five homologs contained conserved amino acid residues predicted to bind Fe^{2+} and 2-oxoglutarate. They cloned each of these homologs into an expression vector and *in vitro* transcribed/translated them in a rabbit reticulocyte lysate system. Subsequently, the three HIF prolyl hydroxylases were identified in an *in vitro* hydroxylation assay. In parallel, Epstein *et al.* cloned the three human Egl-9 gene homologs, PHD1, PHD2 and PHD3 and amplified them from cDNA banks and a human colonic cDNA library, respectively (Epstein *et al.* 2001).

In 2002, Seth *et al.* utilized Serial Analysis of Gene Expression (SAGE) technology for the identification of estrogen- and tamoxifen-regulated genes in the estrogen-dependent breast cancer cell line ZR75-1. They identified EIT-6 as a direct transcriptional target of the estrogen receptor and showed that constitutive expression of EIT-6 promoted colony growth in human breast cancer cells. Analysis of the EIT-6 sequence revealed that EIT-6 is a human homolog of the rat SM-20 and *C. elegans* Egl-9 gene and sequence alignment showed highest similarity to PHD1 (Seth *et al.* 2002).

In 2002, a novel cell growth regulator, named Falkor, was identified (Erez *et al.* 2002). The Genetic Supressor Elements (GSE) method was used to screen genes critical for cellular DNA-damage response in MEFs. Falkor is expressed

at different levels in various tissues and seems to be localized in the nuclei of cells. Further database blasts showed that Falkor is the mouse orthologue of PHD1. Cobb *et al.* finally cloned the PHD1 rat homolog from a rat liver cDNA library and showed that the PHD1 sequence is highly conserved in human, mouse and rat (Fig. 4) (Cobb *et al.* 2005).

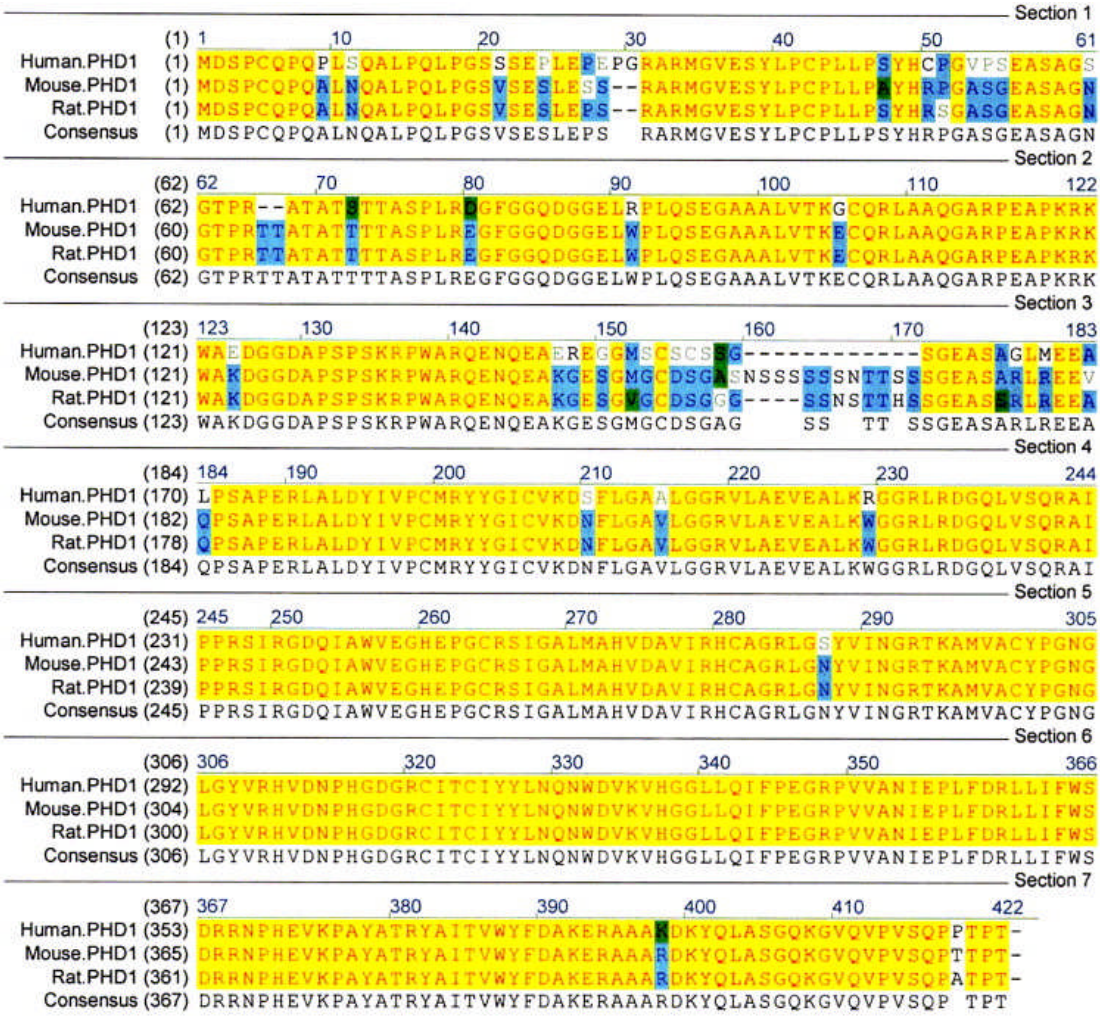

Figure 4: Alignment of human, mouse and rat PHD1 *(Cobb et al. 2005)*

3.2 Transcriptional regulation of PHD1

In contrast to PHD2 and PHD3, PHD1 mRNA is not upregulated under hypoxia (Epstein *et al.* 2001; Appelhoff *et al.* 2004). Erez *et al.* showed a decrease of PHD1 mRNA levels under hypoxic conditions and in response to DFX (Erez *et al.* 2004). A study of the human PHD1 promoter revealed an ARNT binding site and ChIP analysis showed indeed association of ARNT with the PHD1 promoter in hypoxia and after DFX treatment. ARNT is known to form transcriptionally

active heterodimers with different bHLH-PAS proteins, such as HIF-1α, aryl hydrocarbon receptor or SIM and to regulate gene expression in response to hypoxia and xenobiotics. Erez *et al.* suggested that ARNT may be involved in induction and repression of genes under hypoxia, depending on its heterodimerization partner (Erez *et al.* 2004).

The fact that PHD1 was found as an estrogen-induced gene, EIT-6, was recently confirmed in a study, showing that PHD1 mRNA is induced by estrogen in the breast cancer cell line ZR751 and BT474 (Appelhoff *et al.* 2004; Tian *et al.* 2006).

3.3 Alternative initiation of translation and proteolytic regulation of PHD1

In previous experiments, Tian *et al*. observed in a wide variety of cell lines two species of PHD1, termed PHD1p43 and PHD1p40 due to their molecular weight (Tian *et al.* 2006). Both species were present in cancer cells derived from a variety of different tissues. When specific PHD1 siRNA oligonucleotides were used, they observed a downregulation of expression of both forms, indicating that both species were the product of PHD1 mRNA. Studies of the PHD1 mRNA revealed an alternative initiation codon corresponding to methionine 34, also found in rat and mouse PHD1 cDNA sequences. Initiation at this start codon produced a 40.2 kDa protein in comparison to 43.7 kDa for a PHD1 species generated by initiation at the upstream ATG codon. PHD1 is proteolyticaly regulated by the specific ring finger E3-ubiquitin ligases Siah1/2 (Nakayama *et al.* 2004). Tian *et al*. showed that both PHD1 species are subject to proteolytic regulation, but that they differ significantly in their protein stability. PHD1p40 has a shorter half-life than the longer species PHD1p43, approximately 50 versus 100 minutes. Overexpression of either Siah1 or Siah2 reduced protein levels of the two species. However, PHD1 protein levels of both isoforms were identical in wild-type and *Siah1a*$^{-/-}$ / *Siah2*$^{-/-}$ MEFs suggesting that other proteolytic pathways might be responsible for the difference in protein stability of the two isoforms (Tian *et al.* 2006). Both PHD1 isoforms showed similar hydroxylation activity of HIF-1α-derived peptides in a VHL capture assay, suggesting that differential isoform regulation could influences activity on another, non-HIF-α, substrate. This would also explain the functional relevance of the two PHD1 species which are highly conserved in mammals (Tian *et al.* 2006).

3.4 Possible function of PHD1

When Erez *et al.* isolated PHD1 mRNA from cisplatin-treated MEFs, they showed that the C-terminal domain of PHD1 enhances cell growth under stress conditions such as cisplatin treatment but also under normal conditions (Erez *et al.* 2002). In contrast, co-expression of full length PHD1 or its C-terminal fragment abolished the growth enhancing effect. EIT-6 was found to promote colony growth in a human breast cancer cell line (Seth *et al.* 2002). To clarify these contradictive data, Erez *et al.* further investigated the role of PHD1 in cell and tumor growth and showed that PHD1 is able to inhibit HIF-1α accumulation and transcriptional activity under normoxic conditions and DFX treatment (Erez *et al.* 2003). To exclude p53 dependency of this effect, they performed the same assay in wild-type p53 or *p53*$^{-/-}$ HCT116 colon cancer carcinoma cells. No difference was observed in the PHD1-mediated transcriptional inhibition between the wild-type and the knock-out cell line. Furthermore, they compared survival of HCT116 cells stably transfected with PHD1, with a control cell line after DFX treatment. Erez and co-worker observed reduced cell survival after DFX treatment in HCT116 PHD1 transfected cells compared to the control cell line. No difference in cell growth between the two cell lines was observed in the absence of hypoxia-mimetic treatment. These results led to an *in vivo* experiment in which HCT116 PHD1 transfected cells were injected into CD1-nude mice. The result was a significantly reduced average tumor volume in HCT116 PHD1 treated mice compared to the control group. Histological analysis of the tumors indicated that tumors from HCT116 PHD1 mice showed more necrosis than those derived from control mice. When capillary density analysis of the tumors was examined, it was remarkable that PHD1 overexpressing cells showed a 50% reduced microvessel density compared with control tumor cells. Based on these data, Erez *et al.* proposed that PHD1 is able to inhibit tumor growth in hypoxia via inhibition of HIF-1α accumulation and transactivation activity. Resulting inhibition of HIF target gene activation, such as VEGF, reduced tumor neovascularization (Erez *et al.* 2003). Recently, a PHD1$^{-/-}$ knock out mouse strain was generated. These mice are viable and show no phenotype except a reduced fertility of male mice (Takeda *et al.* 2006; Ratcliffe *et al.* unpublished). These data would confirm a suggested PHD1 function in spermatogenesis and is consistent to the high expression of PHD1 in testis.

4 Working hypothesis

The fact that three different HIF prolyl-4-hydroxylases are known and that these isoforms differ in their response to hypoxia, in their expression pattern and their subcellular localization suggests that in addition to HIF, other substrates of each specific PHD enzyme may exist.

The goal of my PhD thesis was to identify and characterize new interactors of PHD1. Human and mouse testis cDNA libraries were independently screened by yeast two-hybrid methodology and more than 300 potential interactors were identified. Fourty of each screening were confirmed by re-testing in yeast and eight interactors finally tested for *in vitro* interaction. Among others the cerebellar degeneration-related protein 2 (Cdr2) was identified as an interactor of PHD1 in both independent yeast two-hybrid screenings. Subsequently, I investigated the interaction of PHD1 and Cdr2 *in vitro*, analyzed Cdr2 mRNA levels under normoxic and hypoxic conditions as well as its expression pattern in tissues and cell lines. Additionally, the degradation pathway of Cdr2 was examined, poly- and monoclonal antibodies generated and ongoing studies include now the analysis of a possible Cdr2 prolyl hydroxylation by PHD1.

Yeast two-hybrid screening of human and mouse testis cDNA libraries using PHD1 as bait

Verena S. Hofmann[1], Jutta Nesper[2], Dörthe Katschinski[3], Roland H. Wenger[1] and Gieri Camenisch[1]

[1]Institute of Physiology and Zürich Center for Integrative Human Physiology, University of Zürich, CH-8057 Zürich, Switzerland
[2]Department of Biology, University of Konstanz, D-78457 Konstanz, Germany
[3]Department of Heart and Circulatory Physiology, University of Göttingen, D-37073 Göttingen, Germany

Material and Methods

The principle of a yeast two-hybrid system

The yeast two-hybrid system is an *in vivo* system that identifies the interaction between two proteins. Therefore a bait (here PHD1) forms a fusion protein with a Gal4 **D**NA **B**inding domain and the second protein, the prey (here a protein of a testis cDNA library) is fused to a Gal4 **A**ctivation **D**omain.

In case of an interaction between PHD1 and a testis cDNA protein, a functional transcription factor is build and is able to activate chromosomally-integrated reporter genes in the yeast, such as his3, uracil and β-galactosidase. This interaction can be monitored by growth of cells on plates lacking histidine or uracil, respectively. Furthermore the yeast cells stain blue in a β-galactosidase assay. The combination of three different reporter genes reduces the risk of false positive interaction. Figure 5 shows the principle of a yeast two-hybrid system.

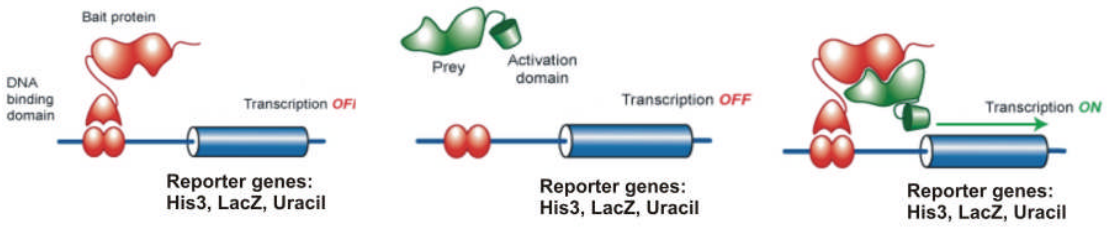

Figure 5: The principle of a yeast two-hybrid system
In two different yeast expression vectors a bait protein is fused to a Gal4 DNA Binding domain and a prey protein forms a fusion protein with a Gal4 Activation Domain. Interaction of bait and prey reconstitutes a functional transcription factor which activates chromosomally-integrated reporter genes.

Gateway Cloning System

The Gateway Cloning System (Invitrogen) is a lambda phage-based site-specific recombination system, which facilitates the cloning and subcloning between different vectors. This recombination system was found to be used by lambda during the switch between the lytic and the lysogenic pathways. The recombination sites termed att (attachment sites), incorporate the DNA sequence of interest and thereby allow the switch between different vectors. Most Gateway vectors contain the *ccdB* gene cassette flanked by two att sites.

The CcdB protein interferes with *E. coli* DNA gyrase and thereby is able to inhibit growth of most *E. coli* strains. In case of recombination, the *ccdB* gene is replaced by the gene of interest and allows negative selection of the donor and destination vectors in *E. coli*. Two different types of reactions can be distinguished:

1. The **BP Reaction**, a recombination reaction between an expression vector and a Donor vector to create an Entry Clone.

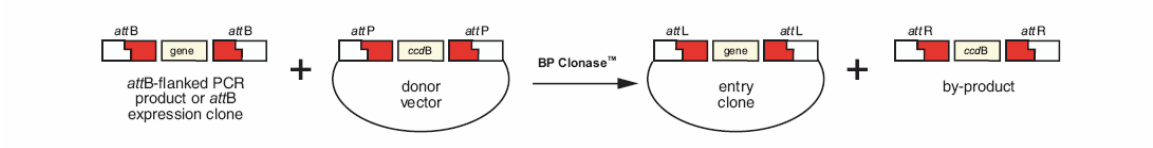

2. The **LR Reaction**, a recombination reaction between an Entry Clone and a Destination Vector generates an expression clone through added recombination proteins/enzymes.

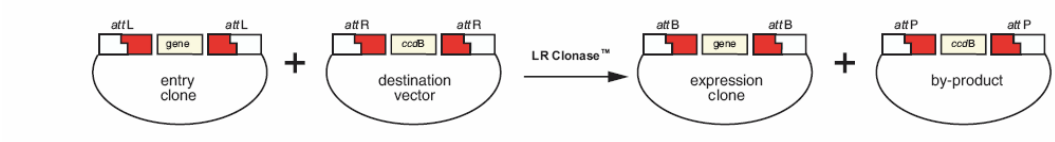

Figure 6: BP and LR reaction of the Gateway Cloning System

The following recombination reactions were used:

BP Recombination Reaction:

attB expression clone (150 ng/μl)	1-2	μl
pDONR vector (supercoiled, 150 ng/μl)	1	μl
5 × BP Clonase reaction buffer	2	μl
TE Buffer, pH 8.0	to 8	μl

2 μl BP Clonase enzyme is added to the components above and mixed well by vortexing briefly twice and the reaction is incubated at 25°C overnight

LR Recombination Reaction:

Entry clone (supercoiled, 100 – 300 ng)	1-2	μl
Destination vector (150 ng/μl)	1	μl
5 × LR Clonase reaction buffer	2	μl
TE Buffer, pH 8.0	to 8	μl

2 μl LR Clonase enzyme is added to the components above and mixed well by vortexing briefly twice and the reaction is incubated at 25°C overnight

After overnight incubation 2 μl of 2 μg/μl Proteinase K solution was added to the mixture and incubated at 37°C for 10 minutes. 1 - 3 μl of reaction mix was transformed into competent *E. coli* Top10 and selected for the appropriate antibiotic-resistant entry or expression clones.

The Invitrogen Gateway ProQuest Yeast-Two-Hybrid System

Vectors

The Gateway-based ProQuest Yeast Two-Hybrid System is an *in vivo* screening method allowing a rapid switch of genes of interest found in the screening to different expression vectors for analysis and expression. The mouse testis cDNA library is provided in the pEXP-AD502 vector fusing the gene of interest to a GAL4-activation domain (GAL4AD). The bait is fused to the GAL4-DNA-binding domain (GAL4DB). Both proteins of interest are incorporated in the specific recombination site att1 and att2.

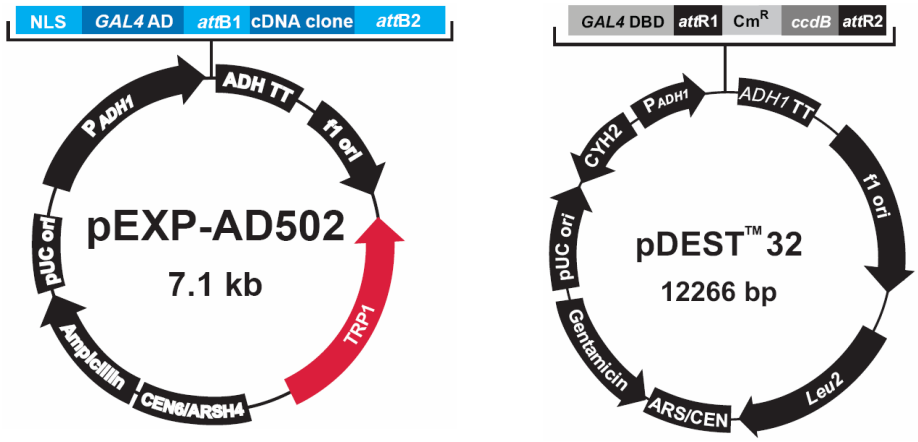

Figure 7: Yeast expression vectors used in yeast two-hybrid screening
pEXP-AD502 contains a protein encoded by a cDNA in fusion library and pDEST32 contains a protein of interest (bait).

Vector features

pEXP-AD502 generates a fusion of the GAL4AD and a protein of interest (or protein encoded by a cDNA in fusion library) cloned into the MCS in the correct orientation and reading frame.

GAL4AD	GAL4 activation domain
ADH1	Truncated 410 bp *S. cerevisiae* ADH1 promoter
ADH TT	*S. cerevisiae* ADH1 terminator
TRP1	*S. cerevisiae* TRP1 gene for auxotrophic selection in yeast
pUC origin	Bacterial origin of replication which allows propagation of the plasmid in *E. coli* at low copy numbers
Amp	Ampicillin resistance gene
attB1	Recombination site
attB2	Recombination site
ARS4/CEN6	Yeast origin

pDEST32 generates a fusion of the GAL4BD and a protein of interest (bait) cloned into the MCS in the correct orientation and reading frame.

GAL4 BD	GAL4 DNA binding domain
ADH1	Truncated 410 bp *S. cerevisiae* ADH1 promoter
ADH TT	*S. cerevisiae* ADH1 terminator
LEU2	*S. cerevisiae* LEU2 gene for auxotrophic selection in yeast
pUC origin	Bacterial origin of replication which allows propagation of the plasmid in *E. coli* at low copy numbers
Gen	Gentamicin resistance gene
attR1	Recombination site

attR2	Recombination site
ccdB	ccdB gene for gateway-compatible selection
ARS4/CEN6	Yeast origin

Additional vectors used in ProQuest yeast two-hybrid screening

pDEST22 generates a fusion of the GAL4AD and a protein of interest cloned into the MCS in the correct orientation and reading frame. pDEST22 represents the pEXPAD502 analog used for confirmation of protein:protein interaction in further yeast two-hybrid assays.

pDBLeu expresses GAL4BD and is used as control vector for bait dependent self-activity.

Yeast strain

The Yeast strain MaV203 with the following genotype was used:

MaV203 (MATα, leu2-3,221, trp1-901, his3Δ200, ade2-101, gal4Δ, gal80Δ, SPAL10::URA3, GAL1::lacZ, $HIS3_{UAS\ GAL1}$::HIS3@LYS2, $can1^R$, $cyh2^R$)

All used control strains were derived from MaV203 and have the same genotype.

The strains used in this system contain:

- A set of non-reverting auxotrophic mutations: leu2 and trp1 to allow selection for the DB-X and AD-Y fusion vectors, and his3 for growth dependent upon induction of the reporter gene GAL1::HIS3
- Deletions of the GAL4 and GAL80 genes encoding GAL4 and its repressor GAL80, respectively. In the absence of GAL80, galactose is not required for activation of GAL4-inducible promoters.
- Three stably integrated single-copy GAL4-inducible reporter genes: SPAL10::URA3 integrated at URA3; $HIS3_{UAS\ GAL1}$::HIS3 integrate at LYS2; and GAL1::lacZ integrated at unknown loci
- The recessive drug resistance marker $cyh2^R$ for curing the control vector pDBLeu for plasmid shuffling

Yeast Control Strain A – E

Reporter gene expression within the yeast two-hybrid screening can vary from strong to weak, which might not reflect the affinity of protein:protein interaction in the native environment. To facilitate the selection of potential interactors a set of five control strains was used to compare found interactions in its strength to the increasing strength of interaction of the control strains A-E. Table 2 summarizes the control strain A – E and shows their interacting inserts.

Control Strain	Resident Plasmids	cDNA Insert	Interaction Strength
Control A	pPC97	no insert	none
	pPC86	no insert	
Control B	pPC97-RB	human RB Acc# M28419 amino acids 302-928	weak
	pPC86-E2F1	human E2F1 Acc# M96577 amino acids 342-437	
Control C	pPC97-*CYH2*^{S}-dDP	*Drosophila* DP Acc# X79708 amino acids 1-377	moderately strong (also a control for plasmid shuffling)
	pPC86-dE2F	*Drosophila* E2F Acc# U10184 amino acids 225-433	
Control D	pPC97-Fos	rat cFos Acc# X06769 amino acids 132-211	strong
	pPC86-Jun	mouse cJun Acc# X12761 amino acids 250-325	
Control E	pCL1 (encoding full length GAL4)	GAL4 Acc# K10486 amino acids 1-881	very strong
	pPC86	no insert	

Table 2: Control strains A-E of ProQuest yeast two-hybrid screening

Cloning of pENTR4PHD1, -PHD2 and -PHD3

Entry vectors were generated by cloning PCR fragments into *Bam*HI and *Eco*RV-digested pENTR4 or pENTR/D-TOPO vectors. Full-length PHD1 to 3 (accession numbers NM_053046, NM_022051 or NM_022073, respectively) were amplified by PCR from plasmids pcDNA3.1/PHD1, pcDNA3.1/HA-PHD2 and pcDNA3.1/PHD3.

The Clontech Matchmaker/Dualsystems Biotech yeast two-hybrid system

The Clontech/Dualsystem Matchmaker yeast two-hybrid system represents a combination of the Clontech Matchmaker system, which libraries are provided in the pACT2 expression vector, and the Dualsystem Biotech system using the pLexA bait vector.

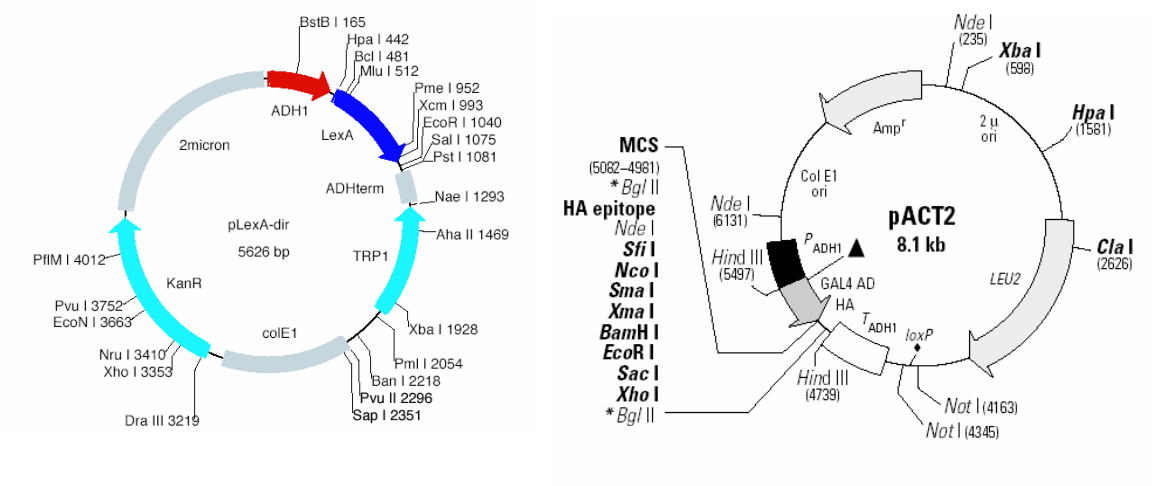

Figure 8: Yeast expression vectors used in yeast two-hybrid screening
pACT2 contains a protein encoded by a cDNA in fusion library and pLexA-dir contains a protein of interest (bait).

Vector features

pACT2 generates a fusion protein between the GAL4AD, an HA epitope tag, and a protein of interest (or protein encoded by a cDNA in fusion library) cloned into the MCS in the correct orientation and reading frame.

GAL4AD	GAL4-DNA activation domain
ADH1	Truncated 410 bp *S. cerevisiae* ADH1 promoter
LEU2	*S. cerevisiae* LEU2 gene for auxotrophic selection in yeast
pBR322	Bacterial origin of replication which allows propagation of the plasmid in *E. coli* at low copy numbers
Amp	Ampicillin resistance gene
2micron	Origin of replication derived from the endogenous yeas 2µ circle.
HA	Hemagglutinin (HA) epitope

pLexA generates a fusion protein between the GAL4BD and a protein of interest cloned into the MCS in the correct orientation and reading frame.

GAL4DB	GAL4-DNA binding domain
LexA	LexA amino acids 1-202
ADH1	Truncated 410 bp *S. cerevisiae* ADH1 promoter
ADHterm	*S. cerevisiae* ADH1 terminator
TRP1	*S. cerevisiae* TRP1 gene for auxotrophic selection in yeast
colE1	Bacterial origin of replication which allows propagation of the plasmid in *E. coli* at low copy numbers
KanR	Kanamycin resistance gene
2micron	Origin of replication derived from the endogenous yeast 2µ circle

Yeast strain

The yeast strain DSY-1 with the following genotype was used:

DSY-1 (MATα, his3Δ200, trp1-901, leu2-3,221 ade2, LYS2::(lexAop)4-HIS3,URA3::(lexAop)8-lacZ, GAL4)

The strains used in this system contain:

- Two integrated reporter genes, HIS3 for auxotrophic selection on minimal medium lacking the amino acid histidine and the colorimetric reporter lacZ endocing β-galactosidase. The two genes are under the control of two different minimal promoters which are fused to 4 or 8 copies of the lexA operator sequence

Cloning of pLexAPHD1, -PHD2 and -PHD3

pLexAPHD1 was obtained by digesting pcDNA3.1PHD1 with *Bam*HI and *Eco*RV, Klenow fill-in and cloned into *Sma*I digested pLexA. **pLexAPHD2** was obtained by digesting pcDNA3.1PHD2 with *Sac*I and 3'5'-exonuclease and cloned into *Sma*I digested pLexA. **pLexAPHD3** was obtained by digesting pcDNA3.1PHD3 with *Kpn*I and 3'5'-exonuclease and cloned into *Sma*I digested pLexA.

Yeast *(S. cerevisiae)* cultivation

S. cerevisiae was cultivated at 30°C in liquid culture or on solid agar plates. Yeast cells have different stages of growth divided into early-log phase, mid log-phase, late log-phase and stationary phase. These phases are based on cell density and how quickly the cells are able to grow and divide based on nutrient use. Table 3 gives relation of the absorbance of the sample at 600 nm and its corresponding cell density.

Phase of growth	**OD_{600}**	**Cells/ml**
Early log-phase	< 0.4	< 10^7
Mid log-phase	0.4 – 1.7	1 – 5 x 10^7
Late log-phase	1.7 – 6.6	5 x 10^7 - 2 x 10^8
Stationary phase	> 6.6	2 x 10^8

Table 3: Growth stages of yeast and corresponding OD_{600}

Yeast Transformation

Small scale transformation

For small scale yeast transformation, 25 ml culture in YPAD (Yeast extract - Peptone - Dextrose plus Adenine medium) or selection medium were inoculated with several yeast colonies from a fresh plate and grown overnight at 30°C on a rotary shaker up to a density of OD_{600} > 1.3. Overnight culture was diluted to receive a starting culture with an OD_{600} of 0.2. Cells were grown at 30°C up to OD_{600} 0.6. Afterwards the culture was pelleted at 2 500 rpm for 5 minutes and washed with distilled water. Per small scale transformation 1.5 ml culture was centrifuged at 2 500 rpm for 5 minutes and the supernatant was removed. 100 ng DNA was added to a fresh tube and mixed with 300 µl of freshly prepared PEG/LiAc mix. PEG/LiAc mix was prepared per transformation of 240 µl 50% PEG, 36 µl of 1 M LiAc and 25 µl of denaturated single stranded DNA (2 mg/ml stock solution). To keep the DNA single strand it was boiled in advance for 5 minutes at 100°C and chilled on ice immediately. 300 µl of the whole mixture was then added to the yeast pellet, gently vortexed and incubated for 45 minutes on 42°C. Afterwards the cells were pelleted and resuspended in 100 µl 0.9% NaCl, finally plated on selection medium and incubated at 30°C for 48 – 72 hours. This method should yield a transformation efficiency of approximately 10^4-10^5 cfu/µg.

YPAD liquid (1 l)

10 g	Bacto yeast extract
20 g	Bacto peptone
100 mg	Adenine sulfate

Dissolve in 950 ml H_2O, adjusted pH with HCl to 6.0 and autoclave. Afterwards add 50 ml 40% Glucose

YPAD plates (500 ml)

5 g	Bacto yeast extract
10 g	Bacto peptone
50 mg	Adenine sulfate

Dissolve in 225 ml H_2O, adjust pH with HCl to 6.0, autoclave and cool to 50°C. Afterwards add 50 ml 40% Glucose. Separately dissolve 10 g Agar in 250 ml H_2O, autoclave and mix after cool to 50°C with yeast extract, peptone and adenine sulfate solution.

Synthetic complete drop-out media (Sc drop-out) liquid (1 l)

6.7 g Yeast nitrogen base w/o amino acids

0.65 g Drop-out (DO) Supplement

Dissolve in 950 ml H_2O, adjusted pH with 10 M NaOH to 5.9 and autoclave. Afterwards add 50 ml 40% Glucose.

Sc plates (500 ml)

3.35 g Yeast nitrogen base w/o amino acids

0.32 g DO Supplement

Dissolve in 225 ml H_2O, adjust pH with 10 M NaOH to 5.9 and autoclave. Afterwards add 25 ml 40% Glucose; Dissolve 10 g Agar in 250 ml H_2O, autoclaved separately and add after cooling to 50°C to yeast nitrogen base and DO supplement mix.

Nutrients

Tryptophan	stock conc.: 10 g/l	add 2 ml/l medium (final conc.: 0.02 g/l)
Histidine	stock conc.: 10 g/l	add 2 ml/l medium (final conc.: 0.02 g/l)
Leucine	stock conc.: 10 g/l	add 10 ml/l medium (final conc.: 0.1 g/l)
Adenine	stock conc.: 10 g/l	add 2 ml/l medium (final conc.: 0.02 g/l)

Filter sterile solutions and store dark at 4°C.

PLATE transformation

The abbreviation PLATE stands for PEG, Lithium acetate, Tris and EDTA. A single yeast colony was inoculated as starter culture in 2 – 3 ml media and grown overnight at 30°C on a rotary shaker. Per transformation, 0.5 ml of the culture was centrifuged at 12 200 rpm for 30 seconds. To the remaining yeast pellet 50 µl of denatured single stranded DNA (2 mg/ml stock solution) was added. 1 – 2 µg of plasmid DNA were added and mixed by pipetting. Finally, 0.5 ml of PLATE solution was mixed gently by pipetting with the yeast pellet and the single stranded DNA. The PLATE solution consists of 40% PEG3350 (w/v), 100 mM Lithium acetate, 10 mM Tris, pH 7.5 and 1 mM EDTA. The cultures were incubated at 30°C without shaking for 24 – 48 hours. After collecting by centrifugation and resuspension in 200 µl in 0.9% NaCl yeast culture was spread on solid selection media and incubated at 30°C for 48 – 72 hours.

Yeast plasmid DNA preparation

A single yeast colony was inoculated in appropriate medium and incubated on a rotary shaker overnight at 30°C. 8 ml of yeast cultures were centrifuged at 2 500 rpm for 5 minutes and the pellet was resuspended in 500 µl sorbitol buffer. The resuspension was incubated gently shaking at 30°C for 30 minutes. After centrifugation the remaining spheroblasts were resuspended in 300 µl buffer 1, afterwards 300 µl buffer 2 was added and the gently mixed suspension was incubated for 5 minutes at room temperature. Furthermore, 300 µl buffer 3 were added, the tubes mixed by inverting and again incubated 5 minutes at room temperature. The cloudy suspension was centrifuged at 13 krpm for 10 minutes and the supernatant was transfered to a fresh tube and precipitate with 600 µl isopropanol. After centrifugation at 13 krpm for 30 minutes the remaining DNA pellet was washed with 70% ethanol and finally vacuum dried and resuspended in 50 µl H_2O. For transformation of yeast plasmid into bacteria (*E. coli*) via electroporation 5 µl were used.

Sorbitol Buffer

5 ml	3 M Sorbitol
2.5 ml	0.5 M EDTA pH 8.0
15 µl	β-Mercaptoethanol
10 mg	Lyticase (733 units/mg)
	Add H_2O to 15 ml

Buffer 1		**Buffer 2**		**Buffer 3**	
50 mM	TrisCl, pH 8.0	200 mM	NaOH	3 M	KAc, pH 5.5
10 mM	EDTA	1%	SDS (w/v)		
100 µg/ml	RNase A				

X-gal Assay

The yeast culture was grown on two layers of filter paper on agar plates. The filter paper was shortly deep frozen in liquid nitrogen for few seconds and added to a new plate with 8 ml freshly prepared X-gal solution. Excess solution was removed and the membrane soaked with the X-gal solution incubated at 37°C. The incubation duration varied between few minutes and several hours depending on the strength of interaction.

Z-Buffer	
60 mM	Na_2HPO_4
40 mM	NaH_2PO_4
10 mM	KCl
1 mM	$MgSO_4$
50 mM	2-Mercaptoethanol
	pH 7.0, sterile filtered

X-gal solution	
100 µl	X-gal (100 mg/ml DMF)
60 µl	2-Mercaptoethanol
10 ml	Z-Buffer

Coupled *in vitro* transcription/translation reaction (Promega)

The TNT quick coupled transcription/translation system enables in a single tube coupled transcription/translation reaction for eukaryotic *in vitro* translation. The system consists of a rabbit reticulocyte lysate, RNA polymerase, nucleotides and recombinant RNase inhibitor. The system is available for either T7 or SP6 RNA polymerase promoters and can be used to synthesize proteins with or without radioactive labeling. The following table represents the standard reaction protocol used in radioactive GST pull-downs.

Standard Reaction using [^{35}S] methionine	**Volume**
TNT Quick Master Mix	20 µl
[^{35}S] methionine	1 µl
Plasmid DNA template (0.5 µg)	1 µl
Nuclease-free water to final volume Σ 25 µl	x µl

The reaction mix was incubated at 30°C for 90 minutes and used for protein expression analysis or GST pull-down assay.

Bacterial expression of recombinant proteins

Recombinant proteins were fused to Glutathione-S-transferase (GST). The plasmids were transformed into the BL-21-AI *E. coli*. An overnight culture containing the corresponding antibiotic and 0.1% glucose for repression of expression was inoculated with a single colony. On the next day, the overnight culture was diluted 1:40 and grown at 37°C to an OD_{600} of 0.4. Expression was induced by arabinose. The bacteria were induced for 3 - 4 hours at 37°C. Afterwards, the bacterial culture was centrifuged at 8 000 rpm for 15 minutes at 4°C and pellets were stored at -20°C until purification.

Lysis of bacteria

Bacterial pellets of a 2 l culture were resuspended in 8 ml PBS with EDTA-free protease inhibitors (Roche). Bacterial lysis was carried out by disruption of bacteria in a French press at 2.7 kbar. In case of FPLC purification, the lysate was centrifuged at 40 000 rpm for 1 hour at 4°C.

Purification of recombinant proteins with Biologic Duo Flow fast performance liquid chromatography (FPLC)

GST-fusion proteins

After centrifugation the supernatant of the lysate was loaded on a GSTrap FF column (Amersham) with a flow rate of 0.2 ml/minute to bind the fusion protein to the glutathione sepharose matrix. The 2-buffer system consisted of a buffer A (1× PBS) as washing buffer and a buffer B (32.5 mM glutathione/50 mM Tris/Cl pH 8.0) used as elution buffer.

Step Number	Step
1	Isocratic flow with 100% buffer A at 1.00 ml/min for 10.0 ml
2	Dynamic loop: Inject x ml sample at 0.2 ml/min
3	Isocratic flow with 100% buffer A at 1.00 ml/min for 10.0 ml
4	Elution with 100% buffer B at 1.00 ml/min for 10.0 ml
5	Isocratic flow with 100% buffer A at 1.00 ml/min for 10.0 ml

GST-fusion protein pull-down with IVTT proteins

GST pull-down assays were used to test protein-protein interaction *in vitro*. Glutathione sepharose beads were washed three times with bead binding buffer and centrifuged at 1000 rpm for 30 seconds at 4°C. To bind the recombinant protein to beads, 10 – 20 μg protein were diluted in 500 μl bead binding buffer and 30 μl glutathione sepharose beads were added. The beads were rotated either overnight or for a minimum of 2 hours at 4°C. Afterwards the beads were washed three times with 500 μl Co-IP buffer and 20 μl of the IVTT reaction were added to the corresponding sample and rotated again for 2 hours at 4°C. Beads were pellet at 1 000 rpm for 30 seconds at 4°C and washed 3 – 5 times with 1 ml Co-IP buffer. The supernatant was removed completely after centrifugation

and the pellet was boiled for 5 minutes at 95°C with 20 µl 2 × SDS sample buffer. 18 µl of the supernatant were load to a SDS-PAGE, avoiding spill-over across lanes. After run, the gel was stained with coomassie staining solution for 15 minutes and 30 minutes fixed in a fixation solution consisting of 50% methanol and 10% acetic acid. Using a washing solution with 7% methanol, 7% acetic acid and 1% glycerol the gel was destained completely and vacuum dried at 80°C for 2 hours and exposed to an autoradiography screen overnight. To reduce unspecific binding, beads were blocked with 1% BSA and up to 0.5% Triton-X-100 was added to the Co-IP buffer to increase the stringency.

Bead Binding Buffer (GST-fusion protein)		**Co-IP Buffer**	
50 mM	K-phosphate pH 7.5	50 mM	Tris-Cl pH 7.6
150 mM	KCl	100 mM	NaCl
1 mM	$MgCl_2$	0.1%	Triton X-100
10%	Glycerol	2 mM	EDTA
1%	Triton X-100		

Database search and analysis of identified interactors

The following databases were used to identify and characterize found interactors of PHD1:

BLAST/Protein search

http://www.ncbi.nlm.nih.gov/BLAST/
http://au.expasy.org/
http://www.ncbi.nlm.nih.gov/entrez/query.fcgi?db=Protein&itool=toolbar
http://www.ebi.ac.uk/interpro/databases.html
http://genome-www5.stanford.edu/cgi-bin/source/sourceSearch

Protein domain search:

http://www.ncbi.nlm.nih.gov/entrez/query.fcgi?db=cdd
http://elm.eu.org/
http://www.sanger.ac.uk/Software/Pfam/search.shtml
http://scansite.mit.edu/motifscan_seq.phtml

Homology search

http://www.wormbase.org/
http://flybase.bio.indiana.edu/

Results

ProQuest yeast two-hybrid screening

Figure 9 represents the process flow of both yeast two-hybrid screenings.

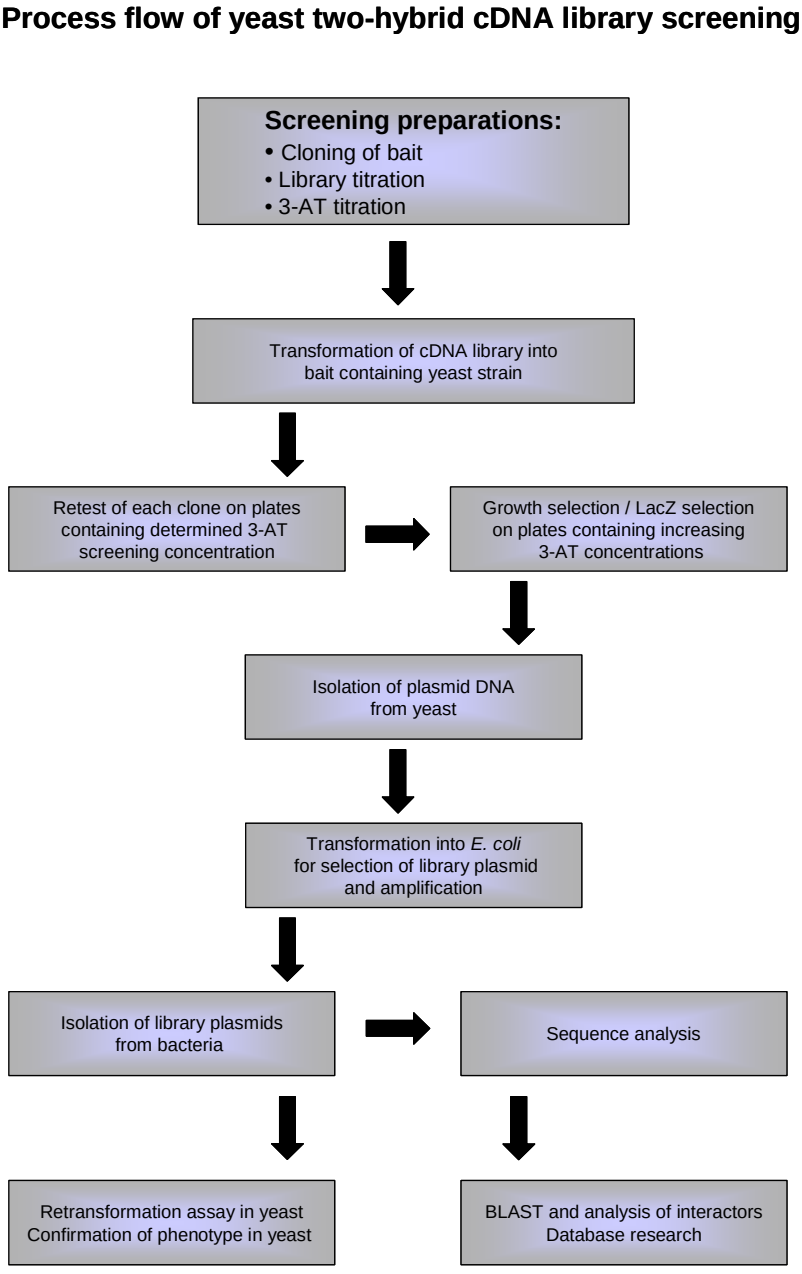

Figure 9: Process flow of yeast two-hybrid screening

Titration of mouse testis cDNA library (Invitrogen)

The mouse testis cDNA library (Invitrogen) (1.6 μg/μl) contained an expected amount of 3.38×10^7 number of independent clones. To screen a total number of clones in the 10^5 - 10^6 range several small scale transformations with different amounts of cDNA library from 0.5 μg up to 10 μg were tested. The use of 5 μg cDNA library in a 10 × transformation scale achieved only 3.2×10^4 clones. In the corresponding yeast two-hybrid screening the number of independent clones was increased by transformation of 50 μg cDNA library using a 250 ml yeast culture scale.

Self-activation and transformation control

The following combinations of plasmids were tested in a small scale transformation to exclude self-activation of bait and mouse testis cDNA library (Table 4). Additional pDBLeu was used as transformation control.

Plasmid 1	Plasmid 2	Selection	Purpose
pDBLeu	-	SC -leu	Transformation control
-	-	SC –leu -trp	Transformation control
pDBLeu	pEXP-AD502	SC –leu -trp	Self activation control
pDEST32PHD1	pEXP-AD502	SC –leu -trp	Self activation control of pDEST32PHD1
pDBLeu	mtestis cDNA	SC –leu -trp	Self activation control of mouse testis cDNA
pDEST32PHD1	pEXP-AD502-HIF2α 73-870	SC –leu -trp	Positive interaction control

Table 4: Self activity and transformation controls

Titration of the 3-aminotriazol (3-AT) concentration

To determine the 3-AT concentration necessary to suppress basal levels of HIS3 expression, four clones of Mav203 containing the following plasmids were plated on selection plates with different 3-AT concentrations ranging from 5 mM – 50 mM.

1. Control strains A - E
2. pDBLeu
3. pDBLeu + pEXPAD502
4. pDEST32-PHD1 + pEXP-AD502
5. pDEST32-PHD1

The titration resulted in an optimal 3-AT concentration of 10 mM, where no growth of yeast cells except the interaction controls B – E was observed. To avoid false positive growth due to basal histidine expression, the screening was carried out at 12.5 mM 3-AT.

ProQuest mouse testis cDNA library screening

Selection medium (250 ml Sc –trp) was inoculated with Mav203 pDEST32PHD1 overnight and diluted the next day in 500 ml YPDA to achieve a starting OD_{600} of 0.3. The culture was grown up to a density of 0.6 and then distributed over 10 tubes and centrifuged at 2 500 rpm for 5 minutes. Each pellet was washed with 30 ml sterile H_2O and all pellets resuspended and pooled in 6 ml H_2O. In total, 4 transformations were carried out in parallel as follows:

32 µl mouse testis cDNA library (= 50 µg)
\+ 400 µl ssDNA (herring sperm DNA)
\+ 1.5 ml yeast suspension Mav203 transformed with pDEST32PHD1
\+ 6 ml 40% PEG/1 × TE/1 × LiAc

Yeast cells were incubated for 45 minutes at 30°C in a water bath, then 700 µl DMSO were added. Cells were heat shocked for 20 minutes at 42°C, the culture was regularly gently mixed in between and immediately after the heat shock cells were put on ice for exactly 2 minutes and centrifuged for 5 minutes at 2 500 rpm. All 4 pellets were resuspended in 24 ml 0.9% NaCl and 200 µl culture was plated per 15-cm Sc –leu-trp-his 12.5 mM 3-AT plate. In addition dilutions of 1:10, 1:100, 1:1000 and 1:10000 were plated on Sc–leu-trp plates to determine the transformation efficiency. As positive interaction control, the pellet of 10 ml Mav203 culture transformed with pDEST32PHD1 was resuspended in 120 µl H_2O and transformed with 1 µg pEXP-AD502HIF-2α73-870 and plated on

screening plates. After incubation of 48 – 72 h clones were picked and retested on 12.5 mM 3-AT plates and glycerol stocks were generated from potential interactors. In total, 3×10^6 independent clones were screened.

Determination of phenotype

To further characterize positive interactions, clones were plated in triplicates on plates with an increasing concentration of 3-AT ranging from 12.5 mM up to 50 mM 3-AT. In addition, control strains A – E as well as a positive control (pDEST32PHD1 + pEXPAD502HIF-2α73-870) and a negative control (pDEST32PHD1 + pEXPAD502) were added. Figure 10 shows the determination of phenotype on different concentration of 3-AT as well as an X-gal assay of the first 70 potential interactors.

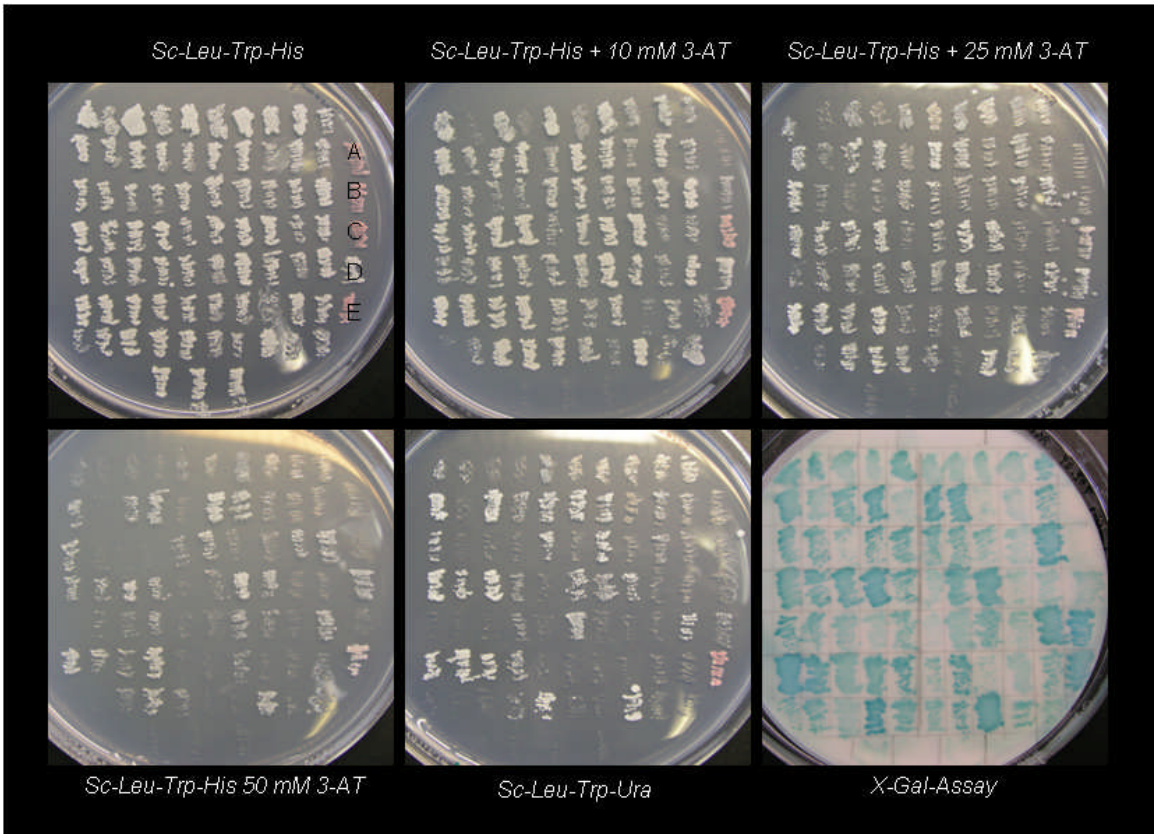

Figure 10: Determination of phenotype. *Clones were plated on different concentrations of 3-AT to determine the strength of interaction and a X-gal assay was carried out.*

All growth differences on 3-AT plates as well as the intensity of the blue staining in the X-gal assay were reported. Plasmid DNA was isolated from 40 interactors

that formed the first clones. Isolated yeast plasmid DNA was transferred by electroporation in XL-1-Blue *E. coli* bacteria, plasmids were isolated and sequenced. The sequencing results are summarized in table 12 and table 13.

Retransformation assay

All sequenced interactors were retested by transformation of the isolated plasmids into Mav203 pDEST32PHD1. The phenotype was assessed by plating on plates with increasing concentrations of 3-AT and in X-gal assays.

In the following tables 5 – 11 the phenotype of potential interactors of PHD1 are shown.

#	Glycerol stock	Phenotype			DNA isolated from yeast	E.coli transformation	DNA conc. approx. ng/µl	Yeast re-transformation	Phenotype retransformation			activates itself	Sequencing
		+ 3-AT	- ura	β-Gal					+ 3-AT	- ura	β-Gal		
1	✓	25 mM	+	++	✓	✓	300 ng /µl	✓	25 mM		++	–	✓
2	✓	–	–	++	✓	✓	300 ng /µl	✓	–	–	++	–	✓
3	✓	25 mM	–	+	✓	✓	300 ng /µl	✓	25 mM	–	+	–	✓
4	✓	10 mM	–	+	✓	✓	300 ng /µl	✓	10 mM	–	+	–	✓
5	✓	50 mM	+	++	✓	✓	300 ng /µl	✓	10 mM	–	++	–	✓
6	✓	10 mM	–	+	✓	✓	300 ng /µl	✓	25 mM	–	+	–	✓
7	✓	50 mM	–	+	✓	✓	300 ng /µl	no growth	–	–	–	–	✓
8	✓	25 mM	–	+	✓	✓	300 ng /µl	✓	50 mM	–	+	–	✓
9	✓	25 mM	–	+	✓	✓	300 ng /µl	✓	25 mM	–	+	–	✓
10	✓	10 mM	–	++	✓	✓	300 ng /µl	✓	10 mM	–	++	–	✓
11	✓	50 mM	+++	++	✓	✓	300 ng /µl	✓	25 mM	+	++	–	✓
12	✓	25 mM	–	+	✓	✓	300 ng /µl	✓	10 mM	–	+	–	✓
13	✓	50 mM	+++	++	✓	✓	300 ng /µl	✓	25 mM	++	+	–	✓
14	✓	50 mM	+	+++	✓	✓	300 ng /µl	✓	25 mM	–	+++	–	✓
15	✓	25 mM	++	+	✓	✓	300 ng /µl	✓	10 mM	+	+	–	✓
16	✓	50 mM	++	+++	✓	✓	300 ng /µl	✓	50 mM	+	+++	–	✓
17	✓	50 mM	++	+++	✓	✓	300 ng /µl	✓	50 mM	+	+++	–	✓
18	✓	25 mM	–	–	✓	✓	300 ng /µl	✓	25 mM	–	+	–	✓
19	✓	25 mM	+	+	✓	✓	300 ng /µl	no growth	–	–	–	–	✓
20	✓	25 mM	–	++	✓	✓	300 ng /µl	✓	25 mM	–	++	–	✓
21	✓	50 mM	+	++	✓	✓	300 ng /µl	✓	50 mM	++	+++	–	✓
22	✓	25 mM	–	++	✓	✓	300 ng /µl	✓	25 mM	–	+++	–	✓
23	✓	10 mM	–	–	✓	✓	300 ng /µl	✓	25 mM	–	+	–	✓
24	✓	10 mM	–	++	✓	✓	300 ng /µl	✓	25 mM	–	++	–	✓
25	✓	50 mM	+	++	✓	✓	300 ng /µl	✓	25 mM	+	+++	–	✓
26	✓	50 mM	–	++	✓	✓	300 ng /µl	✓	25 mM	–	++	–	✓
27	✓	25 mM	++	++	✓	✓	300 ng /µl	✓	–	–	–	–	✓
28	✓	25 mM	–	+	✓	✓	300 ng /µl	✓	25 mM	–	++	–	✓
29	✓	50 mM	+	+	✓	✓	300 ng /µl	✓	25 mM	–	+	–	✓
30	✓	50 mM	–	+++	✓	✓	300 ng /µl	✓	50 mM	–	+++	–	✓
31	✓	50 mM	+++	++	✓	✓	300 ng /µl	✓	50 mM	++	++	–	✓
32	✓	50 mM	++	++	✓	✓	300 ng /µl	✓	50 mM	++	++	–	✓
33	✓	50 mM	+++	++	✓	✓	300 ng /µl	✓	50 mM	+++	+++	–	✓
34	✓	50 mM	–	+++	✓	✓	300 ng /µl	no growth	–	–	–	–	✓
35	✓	25 mM	–	++	✓	✓	300 ng /µl	✓	50 mM	–	+++	–	✓
36	✓	25 mM	++	–	✓	✓	300 ng /µl	no growth	–	–	–	–	✓
37	✓	50 mM	++	++	✓	✓	300 ng /µl	✓	50 mM	–	++	–	✓
38	✓	50 mM	+	+++	✓	✓	300 ng /µl	✓	50 mM	+	++	–	✓
39	✓	10 mM	–	–	✓	✓	300 ng /µl	✓	10 mM	–	–	–	✓
40	✓	25 mM	–	+	✓	✓	300 ng /µl	✓	25 mM	–	+	–	✓

Table 5: Phenotype of the first 40 potential interactors of PHD1 in yeast two-hybrid screening

#	Glycerol stock	Phenotype		
		+ 3-AT	- ura	β-Gal
41	✓	25 mM	–	+
42	✓	25 mM	–	+
43	✓	50 mM	–	+
44	✓	50 mM	+	–
45	✓	25 mM	–	+
46	✓	25 mM	++	–
47	✓	50 mM	–	+
48	✓	50 mM	–	++
49	✓	10 mM	–	+
50	✓	50 mM	++	+++
51	✓	50 mM	+++	+++
52	✓	50 mM	+++	+++
53	✓	50 mM	+++	++
54	✓	50 mM	+	++
55	✓	25 mM	–	++
56	✓	25 mM	–	+
57	✓	50 mM	–	+++
58	✓	10 mM	–	–
59	✓	10 mM	–	–
60	✓	10 mM	–	+
61	✓	–	–	+
62	✓	10 mM	–	++
63	✓	50 mM	–	+
64	✓	50 mM	–	+++
65	✓	50 mM	+++	++
66	✓	25 mM	–	+
67	✓	10 mM	–	++
68	✓	50 mM	+++	+++
69	✓	25 mM	–	+
70	✓	25 mM	–	+
71	✓	10 mM	–	+
72	✓	25 mM	+++	+
73	✓	10 mM	–	+
74	✓	25 mM	–	+
75	✓	25 mM	–	+
76	✓	25 mM	–	+
77	✓	25 mM	+++	+++
78	✓	50 mM	+++	+++
79	✓	50 mM	–	+
80	✓	25 mM	–	+

Table 6: Phenotype of potential PHD1 interactors in yeast two-hybrid assay I

#	Glycerol stock	Phenotype		
		+ 3-AT	- ura	β-Gal
81	✓	25 mM	–	+
82	✓	50 mM	+++	++
83	✓	50 mM	++	+++
84	✓	50 mM	+	+
85	✓	25 mM	+	++
86	✓	50 mM	+	++
87	✓	50 mM	+++	+
88	✓	25 mM	++	+
89	✓	50 mM	–	+
90	✓	50 mM	–	+
91	✓	50 mM	+++	++
92	✓	50 mM	–	+
93	✓	50 mM	+++	+
94	✓	50 mM	+	++
95	✓	25 mM	++	+
96	✓	10 mM	–	+
97	✓	10 mM	–	–
98	✓	50 mM	+++	+
99	✓	25 mM	–	+
100	✓	10 mM	–	–
101	✓	25 mM	–	+
102	✓	50 mM	++	+++
103	✓	50 mM	–	+
104	✓	50 mM	++	+++
105	✓	50 mM	+++	+++
106	✓	50 mM	+++	+++
107	✓	25 mM	–	++
108	✓	50 mM	–	+
109	✓	50 mM	+++	+
110	✓	50 mM	+++	+
111	✓	25 mM	+	+
112	✓	25 mM	–	+
113	✓	50 mM	+	++
114	✓	25 mM	–	+
115	✓	–	–	+
116	✓	50 mM	+++	+
117	✓	25 mM	–	+
118	✓	25 mM	–	+
119	✓	50 mM	–	+
120	✓	50 mM	–	+

Table 7: Phenotype of potential PHD1 interactors in yeast two-hybrid assay II

#	Glycerol stock	Phenotype		
		+ 3-AT	- ura	β-Gal
121	✓	25 mM	–	+
122	✓	25 mM	–	+
123	✓	50 mM	–	++
124	✓	50 mM	–	+
125	✓	50 mM	++	+
126	✓	10 mM	–	+
127	✓	25 mM	–	++
128	✓	25 mM	+	++
129	✓	50 mM	++	+
130	✓	50 mM	–	++
131	✓	50 mM	–	++
132	✓	25 mM	–	+
133	✓	25 mM	–	–
134	✓	25 mM	++	+
135	✓	50 mM	–	+
136	✓	50 mM	++	+
137	✓	50 mM	–	+
138	✓	50 mM	+	+++
139	✓	25 mM	–	+
140	✓	25 mM	–	+++
141	✓	10 mM	–	++
142	✓	10 mM	–	++
143	✓	10 mM	–	+
144	✓	10 mM	+	++
145	✓	25 mM	–	+
146	✓	10 mM	–	++
147	✓	50 mM	++	++
148	✓	50 mM	+	+++
149	✓	10 mM	–	+
150	✓	50 mM	+	+++
151	✓	25 mM	++	+++
152	✓	10 mM	–	–
153	✓	10 mM	–	+++
154	✓	50 mM	++	+++
155	✓	50 mM	–	++
156	✓	50 mM	+	+++
157	✓	50 mM	–	++
158	✓	10 mM	–	–
159	✓	25 mM	+	+
160	✓	10 mM	–	–

Table 8: Phenotype of potential PHD1 interactors in yeast two-hybrid assay III

#	Glycerol stock	Phenotype		
		+ 3-AT	- ura	β-Gal
201	✓	50 mM	++	++
202	✓	10 mM	–	–
203	✓	25 mM	–	+
204	✓	25 mM	+	+++
205	✓	50 mM	++	++
206	✓	25 mM	+	++
207	✓	25 mM	–	+++
208	✓	10 mM	+	+
209	✓	25 mM	–	+
210	✓	10 mM	–	+
211	✓	25 mM	–	++
212	✓	50 mM	–	+++
213	✓	25 mM	–	+
214	✓	50 mM	–	++
215	✓	10 mM	–	+
216	✓	50 mM	++	+++
217	✓	10 mM	–	+
218	✓	10 mM	–	+
219	✓	10 mM	+	+
220	✓	50 mM	–	++
221	✓	–	–	–
222	✓	25 mM	–	+++
223	✓	10 mM	–	++
224	✓	25 mM	–	+
225	✓	10 mM	–	–
226	✓	50 mM	–	+
227	✓	25 mM	+	+
228	✓	50 mM	+++	+++
229	✓	50 mM	–	+++
230	✓	10 mM	–	–
231	✓	25 mM	+	+
232	✓	25 mM	++	–
233	✓	25 mM	–	–
234	✓	10 mM	–	–
235	✓	25 mM	–	+
236	✓	10 mM	–	–
237	✓	25 mM	+	+
238	✓	25 mM	–	+++
239	✓	10 mM	–	–
240	✓	50 mM	–	+

Table 9: Phenotype of potential PHD1 interactors in yeast two-hybrid assay IV

#	Glycerol stock	Phenotype		
		+ 3-AT	- ura	β-Gal
241	✓	50 mM	–	++
242	✓	25 mM	–	+
243	✓	25 mM	–	+
244	✓	25 mM	++	++
245	✓	25 mM	+++	++
246	✓	50 mM	+	+++
247	✓	50 mM	–	+
248	✓	25 mM	–	+++
249	✓	25 mM	–	+
250	✓	50 mM	–	+++
251	✓	50 mM	–	+
252	✓	25 mM	–	–
253	✓	10 mM	–	+
254	✓	10 mM	–	–
255	✓	25 mM	–	–
256	✓	50 mM	+	–
257	✓	50 mM	+++	++
258	✓	25 mM	++	++
259	✓	25 mM	–	++
260	✓	50 mM	+++	++
261	✓	50 mM	++	+
262	✓	25 mM	+	+
263	✓	50 mM	++	+++
264	✓	25 mM	–	+
265	✓	50 mM	–	–
266	✓	50 mM	+	–
267	✓	50 mM	–	+
268	✓	25 mM	–	–
269	✓	25 mM	–	–
270	✓	25 mM	–	+
271	✓	–	–	–
272	✓	50 mM	–	+
273	✓	50 mM	–	–
274	✓	–	–	–
275	✓	10 mM	–	–
276	✓	50 mM	–	+
277	✓	–	–	–
278	✓	25 mM	–	+
279	✓	50 mM	++	+
280	✓	50 mM	–	++

Table 10: Phenotype of potential PHD1 interactors in yeast two-hybrid assay V

#	Glycerol stock	Phenotype		
		+ 3-AT	- ura	β-Gal
281	✓	10 mM	–	+
282	✓	25 mM	+	+
283	✓	10 mM	–	+
284	✓	10 mM	–	+
285	✓	10 mM	+	+
286	✓	50 mM	+++	+++
287	✓	50 mM	–	+++
288	✓	25 mM	+++	++
289	✓	50 mM	–	+++
290	✓	10 mM	–	+
291	✓	10 mM	–	+
292	✓	50 mM	+++	++
293	✓	10 mM	–	+
294	✓	25 mM	–	+
295	✓	–	–	+
296	✓	–	–	–
297	✓	50 mM	+	+++
298	✓	10 mM	–	+
299	✓	25 mM	–	+
300	✓	25 mM	–	+
301	✓	10 mM	–	++
302	✓	10 mM	–	+
303	✓	–	–	–
304	✓	50 mM	+	+++
305	✓	25 mM	–	+
306	✓	25 mM	–	+
307	✓	10 mM	–	–
308	✓	25 mM	+	++
309	✓	50 mM	++	++
310	✓	50 mM	–	+++
311	✓	10 mM	–	+
312	✓	25 mM	–	+++
313	✓	10 mM	–	+
314	✓	50 mM	+	+
315	✓	10 mM	–	+
316	✓	–	–	–
317	✓	10 mM	–	+
318	✓	10 mM	–	+
319	✓	25 mM	–	–
320	✓	10 mM	–	+

Table 11: Phenotype of potential PHD1 interactors in yeast two-hybrid assay VI

Yeast two-hybrid assay with PHD 2, 3 and PH-4

The sequenced interactors were additionally tested in interaction assays with PHD2, PHD3, and PH-4 (amino acid 83-502). 27 interactors showed also a positive phenotype for PHD3, which was mainly weaker compared to the PHD1 phenotype. No interaction was observed with PHD2 and PH-4. Tables 12 and 13 represent the observed phenotypes of interaction showing the maximum concentration of 3-AT on which the clones were still growing, growth on uracil lacking plates and the strength of X-gal-Blue staining ranging from + (weak blue staining) to +++ (strong blue staining).

Interaction of HIF prolyl hydroxylases with potential PHD1-Interactors in a Yeast Two Hybrid Assay

PHD1-Interactor No.	Protein	Accession Nucleotide	Phenotype PHD1			*Phenotype PHD2*			Phenotype PHD3			*Phenotype PH-4 (83-502)*		
			3-AT	Uracil	ß-Gal	*3-AT*	*Uracil*	*ß-Gal*	3-AT	Uracil	β-Gal	*3-AT*	*Uracil*	*β-Gal*
1 (A1)	Laminin, beta 2	BC026051	25 mM	_	+	*No interaction*			*No interaction*			*No interaction*		
2 (A2)	Adult male testis cDNA, hypothetical protein	AK005628	25 mM	_	++	*No interaction*			50 mM	++	++	*No interaction*		
3 (A3)	Adult male hypothalamus cDNA, hypothetical C2 domain (Calcium / lipid-binding domain, CaB) structure containing protein	AK038916	50 mM	+++	+++	*No interaction*			*No interaction*			*No interaction*		
6 (B1)	Similar to hypothetical protein MGC24975	XM_148801	25 mM	_	++	*No interaction*			25 mM	_	+	*No interaction*		
8 (B2)	Mouse DNA sequence from clone RP23-184G6	AL645861	50 mM	_	+++	*No interaction*			25 mM	_	+	*No interaction*		
10 (B3)	RIKEN cDNA 4930404K22 gene	XM_136025	25 mM	_	+	*No interaction*			25 mM	_	_	*No interaction*		
12 (B4)	Cerebellar degeneration-related 2 (Cdr2)	NM_007672	50 mM	++	+	*No interaction*			10 mM	_	_	*No interaction*		
14 (B5)	LIM-only protein ACT	AF083394	25 mM	_	++	*No interaction*			*No interaction*			*No interaction*		
15 (C1)	Spr mRNA for speriolin	AB032199	25 mM	+	+	*No interaction*			10 mM	_	_	*No interaction*		
16 (C2)	Similar to nuclear protein with a coiled coil-4 domain of bilateral origin like	XM_196054	10 mM	+	+	*No interaction*			25 mM	_	+	*No interaction*		
18 (C4)	Tripartite motif-containing 45 (Trim45)	BC057358	25 mM	_	+	*No interaction*			25 mM	_	+	*No interaction*		
19 (C5)	Mus musculus RIKEN cDNA 4930404K22 gene	XM_136025	50 mM	_	+	*No interaction*			50 mM	_	_	*No interaction*		
22 (D1)	Similar to hypothetical protein MGC5356	BC051628	25 mM	_	++	*No interaction*			*No interaction*			*No interaction*		
23 (D2)	Rattus norvegicus similar to RelA-associated inhibitor	XM 230882	50 mM	+	+++	*No interaction*			25 mM	_	+	*No interaction*		
25 (D4)	Zinc finger protein 212 (Zfp212)	BC006693	50 mM	+++	++	*No interaction*			10 mM	_	_	*No interaction*		
26 (D5)	Mouse DNA sequence from clone RP23-422L16	AL603707	50 mM	+++	+++	*No interaction*			25 mM	_	+	*No interaction*		
28 (E2)	RIKEN cDNA clone 4921524L21: hypothetical protein	AK014961	25 mM	_	+	*No interaction*			10 mM	_	+	*No interaction*		
29 (E3)	Mouse adult male testis cDNA: hypothetical Retroviral-type aspartic protease containing protein	AK005882	10 mM	_	+	*No interaction*			*No interaction*			*No interaction*		
31 (E4)	TPA: Adam38 gene for testase-8	BN000119	25 mM	_	+	*No interaction*			*No interaction*			*No interaction*		
32 (E5)	Tankyrase, TRF-1interacting ankyrin-related ADP-ribose polymerase	BC057370	50 mM	+	++	*No interaction*			*No interaction*			*No interaction*		
33 (F1)	RIKEN cDNA clone 1700010L19: Weakly similar to Tektin A1	AK005842	10 mM	_	++	*No interaction*			*No interaction*			*No interaction*		

Table 12: Interaction of HIF prolyl hydroxylases with potential PHD1 interactors in yeast two-hybrid assay I

Interaction of HIF prolyl hydroxylases with potential PHD1-Interactors in a Yeast Two Hybrid Assay

PHD1-Interactor No.	Protein	Accession Nucleotide	Phenotype PHD1			*Phenotype PHD2*			Phenotype PHD3			*Phenotype PH-4 (83-502)*		
			3-AT	Uracil	ß-Gal	*3-AT*	*Uracil*	*ß-Gal*	3-AT	Uracil	β-Gal	*3-AT*	*Uracil*	*β-Gal*
34 (F2)	Latent transforming growth factor beta binding protein 4	BC032073	10 mM	_	_	*No interaction*			*No interaction*			*No interaction*		
35 (F3)	Procollagen, type VIII, alpha 1	BC011061	10 mM	_	++	*No interaction*			*No interaction*			*No interaction*		
37 (F5) / (C1)	RFX2 regulatory factor X, 2 (Regulatory factor trans acting) 2)	BX648130	50 mM	_	+	*No interaction*			50 mM	_	_	*No interaction*		
39 (G2)	Similar to hypothetical protein (LOC385766)	XM_358937	10 mM	_	+	*No interaction*			25 mM	_	++	*No interaction*		
40 (G3)	Arsenate resistance protein 2	BC066831	10 mM	+	+	*No interaction*			50 mM	_	++	*No interaction*		
41 (G4)	Nidogen 2 (Entactin	BC057016	25 mM	_	+	*No interaction*			10 mM	_	_	*No interaction*		
44 (H1) / A4	Testis specific serine kinase substrate / Serine / Threonine kinase 22 substrate (Stk22s1)	AF025310	10 mM	_	+	*No interaction*			*No interaction*			*No interaction*		
45 (H2)	Hypothetical Laminin-type EGF-like domain / Cytochrome c family heme-binding site / G-protein beta WD-40 repeats containing protein	AK040807	50 mM	+	++	*No interaction*			10 mM	_	_	*No interaction*		
A6	RIKEN cDNA 2310038K02 gene	BC057041	25 mM	_	+	*No interaction*			50 mM	_	+	*No interaction*		
A7	RIKEN clone 4932411P22 similar to PROXI (fragment)	AK029978	50 mM	_	+	*No interaction*			50 mM	++	+++	*No interaction*		
B3	Clone IMAGE:5036118	BC025923	10 mM	_	+	*No interaction*			10 mM	_	_	*No interaction*		
B4 / D6	Eukaryotic translation initiation factor 4E nuclear import factor 1 (Eif4enif1)	BC033410	25 mM	++	+	*No interaction*			50 mM	++	+	*No interaction*		
B7 / C4	Mouse DNA sequence from clone RP23-193K14	AC091548	50 mM	+	+++	*No interaction*			10 mM	_	_	*No interaction*		
B8 / C3 / E2	Mouse DNA sequence from clone RP23-49C8	AL805980	50 mM	+	+++	*No interaction*			50 mM	_	++	*No interaction*		
C2	Tubby super-family protein (Tusp) / tubby like protein 4	AF219945	25 mM	_	++	*No interaction*			10 mM	_	+	*No interaction*		
C5/E4	Granulin (Grn) / Progranulin, Acrogranulin	NM_008175	25 mM	_	+	*No interaction*			*No interaction*			*No interaction*		
D3	Similar to RelA-associated inhibitor (Inhibitor of ASPP protein)	XM_145419	25 mM	_	+	*No interaction*			10 mM	_	+	*No interaction*		
D7	RIKEN clone:A630023020: CLAST4 Protein homolog	AK041598	50 mM	+++	+++	*No interaction*			50 mM	_	++	*No interaction*		

Table 13: Interaction of HIF prolyl hydroxylases with potential PHD1 interactors in a yeast two-hybrid assay II

Recombination of potential interactors in pDONR221 and expression vectors

Eight preys were chosen to proceed with further analysis. The choice was made based on database search, known protein function, expression pattern and strength of interaction in yeast. These interactors were recombined into the pDONR221, enabling recombination into various expression vectors and were tested for *in vitro* interaction in a GST pull-down assay. Table 14 shows the 8 potential PHD1 interactors chosen for *in vitro* interaction testing:

PHD1 interactors tested for *in vitro* interaction in GST pull down assay									
PHD1-Interactor No.	**Protein**	**Possible function**	**Accession Nucleotide**	**Accession Protein**	**cDNA found x-fold in screening**	**Phenotype yeast retransformation**			**cDNA source / expression**
						3-AT	**Uracil**	**ß-Gal**	
10 (B3)	RIKEN cDNA 4930404K22 gene	Similar to Spermidine / spermine N(1)-acetyltransferase (Rattus norvegicus)	XM_136025	P21673	3	25 mM	_	X	Testis
12 (B4)	Cerebellar degeneration-related 2 (Cdr2)	Unknown, cdr2 gene expressed in paraneoplastic cerebrellar degeneration (PCD)	NM_007672	Q01850	3	50 mM	✓	X	ubiquitous
15 (C1)	Speriolin	Spermatogenic cell-specific centrosomal protein	AB032199	Q76KD6	3	25 mM	✓	X	Testis, mammary gland
18 (C4)	Tripartite motif-containing 45 (Trim45)	unknown	BC057358	Q6PFY8	1	25 mM	_	X	ubiquitous
45 (H2)	Wdr59 protein: Hypothetical Laminin-type EGF-like domain / Cytochrome c family heme-binding site / G-protein beta WD-40 repeats containing protein	unknown	BC066082	Q6NZK7	1	50 mM	✓	XX	
A3	Tripartite motif protein 37 (Trim 37)	RING-B-box-coiled-coil protein	BC059070	Q6PCX9	1	25 mM	_	X	ubiquitous
B4 / D6	Eukaryotic translation initiation factor 4E nuclear import factor 1 (Eif4enif1)	Translation initiation factor: Binds to the mRNA 5' cap structure m7GpppN and promotes ribosome binding to the mRNA in the cytoplasm	BC033410	Q8CFW0	2	25 mM	✓	X	ubiquitous
C2	Tubby super-family protein (Tusp) / tubby like protein 4 (Tulp4)	Tubby gene family: All proteins share a highly conserved carboxyl terminus but the N-terminal is poorly conserved.	AF219945	Q9JIL5	1	25 mM	_	XX	ubiquitous

Table 14: Summary of PHD1 interactors tested for in vitro interaction in a GST-pull down assay

In vitro interaction of PHD1 interactors in a GST pull-down assay

The pDEST17-prey plasmids containing the potential interactors were transcribed and translated using a coupled *in vitro* transcription and translation system. GST-PHD1 was bacterial expressed in BL-21AI *E. coli* and purified by fast performance liquid chromatography using a GSTrap FF column. A strong *in vitro* interaction with GST-PHD1 was observed for an unknown Riken cDNA4930404K22 clone, the testis-specific Speriolin protein and a hypothetical laminin-type EGF-like homolog termed Wdr59. Cdr2, Trim37 as well as Tulp4 showed a weak interaction with GST-PHD1 *in vitro.* No interaction was observed between GST-PHD1 and Trim45 and Eif4enif1, respectively (Fig. 11).

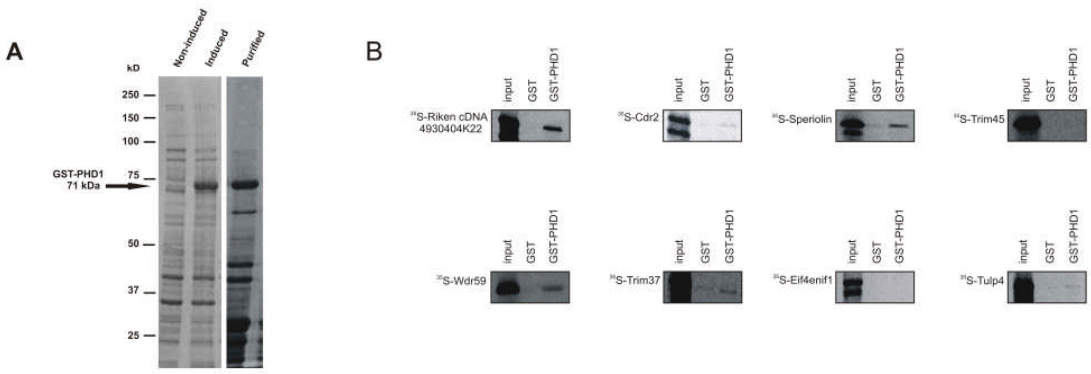

Figure 11: In vitro interaction of potential PHD1 interactors in a GST pull down assay
(A) Purification of recombinant GST-PHD1 expressed in BL21AI E.coli (B) Protein-protein interaction of in vitro transcribed and translated (IVTT) ^{35}S-labeled potential PHD1 interactors and recombinant GST-PHD1 fusion proteins, or GST alone were analyzed by GST pull-down with glutathione sepharose. Bound proteins and input controls (5%) were separated by SDS-PAGE and visualized by autoradiography.

Matchmaker/Dualsystems yeast two-hybrid screening

Library amplification

The human testis cDNA library (Clontech) was obtained as bacterial glycerol stock with an expected number of 3.5×10^6 independent clones. A screening number of twice the size of the original library, meaning 7×10^6 clones and 30 000 colonies per 15-cm plate was aimed. This corresponded to a scale of 233 dishes each 150 µl culture volume (total volume of 34.5 ml LB media). The cDNA library was obtained with a volume titer of 3.37×10^9 cfu/ml. The quotient of the number of clones to screen (7×10^6 clones) and the library titer (3.37×10^9 cfu/ml) resulted in 2.07 µl library volume. An overnight culture of 2.5 µl library volume (bacteria culture) in 36 ml LB medium including ampicillin for selection was plated on the next day on 234 plates and cultivated for 48 hours at 30°C. In total, 6.68×10^6 clones were scraped and pooled in medium, incubated with shaking for 1 hour at 37°C and finally centrifuged for 15 minutes at 4°C at 8 000 rpm. Library plasmids were isolate by DNA plasmid preparation.

Self-activation and transformation control

The following combinations of plasmids were tested in a small scale transformation to exclude self-activation of the bait. The vector pLexA was used as an additional transformation control (Table 15).

Plasmid 1	Plasmid 2	Selection	Purpose
pLexA	-	SC -leu	Transformation control
-	-	SC –leu -trp	Transformation control
pLexA	pACT2	SC –leu -trp	Self activation control
pLexAPHD1	pACT2	SC –leu -trp	Self activation control of pLexAPHD1
pLexALaminC	pACT2-largeT	SC –leu -trp	Interaction negative control
pLexAp53	pACT2-largeT	SC –leu -trp	Interaction positive control

Table 15: Self activity and transformation controls

Titration of the 3-AT concentration

To determine the 3-AT concentration necessary to suppress basal levels of HIS3 expression, four clones of DSY-1α containing the following plasmids were plated on selection plates with different concentration of 3-AT ranging from 1 mM to 15 mM 3-AT.

1. pLexA-LaminC + pACT2-largeT
2. pLexA-p53 + pACT2-largeT
3. pLexA
4. pLexA + pACT2
5. pLexAPHD1 + pACT2
6. pLexAPHD1

The titration resulted in an optimal 3-AT concentration of 2.5 mM 3-AT, where no growth of yeast except the positive interaction control pLexA-p53 + pACT2-largeT was observed.

Matchmaker human testis cDNA library screening

In total, 50 μg of the human testis cDNA library were screened with a transformation efficiency of 1.2×10^4 clones/μg library. The protocol followed the Gateway screening conditions and in total 280 potential interactors were retested and confirmed on 2.5 mM 3-AT dishes and later the phenotype on plates containing increasing concentrations of 3-AT was determined (Table 16 – 22). 40 clones were chosen, plasmid DNA was isolated, transformed for amplification and selection into XL-1-Blue *E. coli.* These 40 clones were confirmed in a retransformation assay and sequenced for further analysis (Table 16).

#	Glycerol stock	Phenotype		DNA isolated from yeast	E.coli transformation	DNA conc. approx. ng/µl	Yeast re-transformation	Phenotype re-transformation		activates itself	Sequencing
		+ 3-AT	β-Gal					+ 3-AT	β-Gal		
1	✓	5 mM	+++	✓	✓	50 ng/µl	✓	5 mM	+++	–	✓
2	✓	7.5 mM	+	✓	✓	200 ng/µl	✓	10 mM	++	–	✓
3	✓	10 mM	+++	✓	✓	100 ng/µl	✓	15 mM	+++	–	✓
4	✓	25 mM	+++	✓	✓	100 ng/µl	✓	25 mM	+++	–	✓
5	✓	15 mM	++	✓	✓	100 ng/µl	✓	15 mM	++	–	✓
6	✓	15 mM	+++	✓	✓	400 ng/µl	✓	15 mM	+++	–	✓
7	✓	15 mM	+++	✓	✓	50 ng/µl	✓	25 mM	+++	–	✓
8	✓	25 mM	++	✓	✓	300 ng/µl	✓	25 mM	+++	–	✓
9	✓	10 mM	++	✓	✓	300 ng/µl	✓	10 mM	+++	–	✓
10	✓	2.5 m	+	✓	✓	200 ng/µl	✓	2.5 mM	+	–	✓
11	✓	2.5 m	+	✓	✓	300 ng/µl	✓	2.5 mM	–	–	✓
12	✓	2.5 m	+	✓	✓	300 ng/µl	✓	2.5 mM	–	–	✓
13	✓	10 mM	+++	✓	✓	300 ng/µl	✓	10 mM	+++	–	✓
14	✓	15 mM	+++	✓	✓	50 ng/µl	✓	25 mM	+++	–	✓
15	✓	15 mM	+++	✓	✓	300 ng/µl	✓	25 mM	+++	–	✓
16	✓	25 mM	+++	✓	✓	100 ng/µl	✓	2.5 mM	+	–	✓
17	✓	10 mM	++	✓	✓	200 ng/µl	✓	15 mM	++	–	✓
18	✓	25 mM	+++	✓	✓	200 ng/µl	✓	25 mM	+++	–	✓
19	✓	15 mM	+++	✓	✓	300 ng/µl	✓	15 mM	++	–	✓
20	✓	10 mM	+++	✓	✓	100 ng/µl	✓	25 mM	+++	–	✓
21	✓	15 mM	+++	✓	✓	200 ng/µl	✓	15 mM	++	–	✓
22	✓	2.5 m	+	✓	✓	100 ng/µl	✓	2.5 mM	+	–	✓
23	✓	2.5 m	+	✓	✓	50 ng/µl	✓	2.5 mM	+	–	✓
24	✓	2.5 m	+	✓	✓	200 ng/µl	✓	2.5 mM	–	–	✓
25	✓	25 mM	+++	✓	✓	200 ng/µl	✓	25 mM	+++	–	✓
26	✓	2.5 m	/	✓	✓	50 ng/µl	✓	2.5 mM	–	–	✓
27	✓	7.5 mM	++	✓	✓	200 ng/µl	✓	10 mM	++	–	✓
28	✓	5 mM	++	✓	✓	50 ng/µl	✓	7.5 mM	++	–	✓
29	✓	15 mM	+++	✓	✓	100 ng/µl	✓	15 mM	+++	–	✓
30	✓	25 mM	+++	✓	✓	200 ng/µl	✓	25 mM	+++	–	✓
31	✓	10 mM	+++	✓	✓	50 ng/µl	✓	15 mM	+++	–	✓
32	✓	7.5 mM	++	✓	✓	100 ng/µl	–	–	–	–	✓
33	✓	15 mM	+++	✓	✓	50 ng/µl	✓	15 mM	++	–	✓
34	✓	2.5 mM	++	✓	✓	50 ng/µl	✓	–	–	–	✓
35	✓	2.5 mM	/	✓	✓	50 ng/µl	✓	2.5 mM	–	–	✓
36	✓	5 mM	+	✓	✓	50 ng/µl	✓	2.5 mM	+	–	✓
37	✓	25 mM	+++	✓	✓	50 ng/µl	✓	25 mM	+++	–	✓
38	✓	25 mM	+++	✓	✓	50 ng/µl	✓	15 mM	++	–	✓
39	✓	10 mM	++	✓	✓	50 ng/µl	✓	15 mM	+++	–	✓
40	✓	10 mM	+	✓	✓	50 ng/µl	✓	10 mM	+++	–	✓

Table 16: Phenotype of the first 40 potential interactors of PHD1 in pLexA yeast two-hybrid screening

#	Glycerol stock	Phenotype	
		+ 3-AT	β-Gal
41	✓	7.5 mM	—
42	✓	15 mM	+
43	✓	2.5 mM	++
44	✓	10 mM	+++
45	✓	10 mM	++
46	✓	7.5 mM	+
47	✓	2.5 mM	—
48	✓	5 mM	—
49	✓	25 mM	+++
50	✓	5 mM	++
51	✓	2.5 mM	—
52	✓	5 mM	+++
53	✓	10 mM	+++
54	✓	15 mM	+++
55	✓	25 mM	++
56	✓	5 mM	++
57	✓	7.5 mM	++
58	✓	5 mM	+
59	✓	2.5 mM	—
60	✓	2.5 mM	+
61	✓	15 mM	++
62	✓	2.5 mM	—
63	✓	2.5 mM	++
64	✓	2.5 mM	++
65	✓	10 mM	++
66	✓	15 mM	++
67	✓	10 mM	++
68	✓	7.5 mM	++
69	✓	10 mM	+
70	✓	10 mM	+
71	✓	2.5 mM	+
72	✓	2.5 mM	+
73	✓	2.5 mM	+
74	✓	15 mM	+++
75	✓	10 mM	+
76	✓	25 mM	++
77	✓	2.5 mM	++
78	✓	5 mM	+
79	✓	15 mM	+
80	✓	5 mM	+++

Table 17: Phenotype of potential PHD1 interactors in pLexA yeast two-hybrid assay I

#	Glycerol stock	Phenotype	
		+ 3-AT	β-Gal
81	✓	5 mM	+
82	✓	15 mM	+++
83	✓	7.5 mM	—
84	✓	15 mM	+++
85	✓	25 mM	+++
86	✓	25 mM	++
87	✓	5 mM	+
88	✓	15 mM	++
89	✓	5 mM	++
90	✓	7.5 mM	++
91	✓	5 mM	+
92	✓	10 mM	+
93	✓	10 mM	+
94	✓	10 mM	+
95	✓	5 mM	+
96	✓	5 mM	++
97	✓	7.5 mM	++
98	✓	5 mM	++
99	✓	7.5 mM	+
100	✓	5 mM	—
101	✓	25 mM	+++
102	✓	2.5 mM	+
103	✓	2.5 mM	+
104	✓	5 mM	+
105	✓	15 mM	+++
106	✓	25 mM	+++
107	✓	15 mM	+++
108	✓	10 mM	+
109	✓	15 mM	++
110	✓	10 mM	++
111	✓	5 mM	+
112	✓	5 mM	++
113	✓	5 mM	+
114	✓	10 mM	+++
115	✓	10 mM	+++
116	✓	25 mM	++
117	✓	10 mM	++
118	✓	10 mM	++
119	✓	15 mM	++
120	✓	25 mM	+++

Table 18: Phenotype of potential PHD1 interactors in pLexA yeast two-hybrid assay II

#	Glycerol stock	Phenotype	
		+ 3-AT	β-Gal
121	✓	25 mM	+++
122	✓	10 mM	++
123	✓	5 mM	++
124	✓	2.5 mM	+
125	✓	2.5 mM	+
126	✓	5 mM	+
127	✓	2.5 mM	+
128	✓	2.5 mM	+
129	✓	25 mM	+++
130	✓	5 mM	++
131	✓	5 mM	++
132	✓	7.5 mM	++
133	✓	2.5 mM	+
134	✓	25 mM	+++
135	✓	10 mM	+++
136	✓	10 mM	+++
137	✓	15 mM	++
138	✓	15 mM	++
139	✓	5 mM	+
140	✓	5 mM	+
141	✓	15 mM	+++
142	✓	5 mM	++
143	✓	5 mM	+
144	✓	25 mM	++
145	✓	15 mM	+++
146	✓	10 mM	+++
147	✓	2.5 mM	++
148	✓	10 mM	+++
149	✓	15 mM	+++
150	✓	5 mM	++
151	✓	2.5 mM	++
152	✓	2.5 mM	+
153	✓	10 mM	+++
154	✓	5 mM	++
155	✓	10 mM	++
156	✓	25 mM	++
157	✓	5 mM	++
158	✓	10 mM	+++
159	✓	7.5 mM	+++
160	✓	7.5 mM	+

Table 19: Phenotype of potential PHD1 interactors in pLexA yeast two-hybrid assay III

#	Glycerol stock	Phenotype	
		+ 3-AT	β-Gal
160	✓	7.5 mM	+
161	✓	5 mM	+
163	✓	7.5 mM	++
164	✓	10 mM	++
165	✓	25 mM	+++
166	✓	15 mM	+++
167	✓	2.5 mM	+
168	✓	2.5 mM	+
169	✓	25 mM	+++
170	✓	15 mM	+++
171	✓	15 mM	++
172	✓	15 mM	+++
173	✓	15 mM	+++
174	✓	7.5 mM	+++
175	✓	2.5 mM	++
176	✓	5 mM	+
177	✓	5 mM	+
178	✓	25 mM	+++
179	✓	10 mM	++
180	✓	5 mM	+
181	✓	10 mM	+++
182	✓	10 mM	++
183	✓	10 mM	++
184	✓	10 mM	++
185	✓	5 mM	+
186	✓	10 mM	+++
187	✓	15 mM	+
188	✓	5 mM	+
189	✓	5 mM	+
190	✓	10 mM	++
191	✓	10 mM	++
192	✓	15 mM	+++
193	✓	15 mM	++
194	✓	25 mM	+++
195	✓	15 mM	++
196	✓	10 mM	++
197	✓	15 mM	++
198	✓	15 mM	+++
199	✓	2.5 mM	+
200	✓	15 mM	+++

Table 20: Phenotype of potential PHD1 interactors in pLexA yeast two-hybrid assay IV

#	Glycerol stock	Phenotype	
		+ 3-AT	β-Gal
201	✓	5 mM	++
202	✓	7.5 mM	+++
203	✓	2.5 mM	+++
204	✓	7.5 mM	+
205	✓	7.5 mM	++
206	✓	5 mM	+
207	✓	7.5 mM	—
208	✓	5 mM	+
209	✓	25 mM	+++
210	✓	2.5 mM	+
211	✓	2.5 mM	+
212	✓	5 mM	+
213	✓	10 mM	++
214	✓	5 mM	+
215	✓	25 mM	+++
216	✓	25 mM	+++
217	✓	10 mM	++
218	✓	25 mM	+++
219	✓	5 mM	+
220	✓	5 mM	+
221	✓	10 mM	+++
222	✓	7.5 mM	+
223	✓	5 mM	++
224	✓	2.5 mM	++
225	✓	10 mM	+++
226	✓	15 mM	+++
227	✓	10 mM	+
228	✓	15 mM	++
229	✓	2.5 mM	++
230	✓	5 mM	++
231	✓	7.5 mM	++
232	✓	7.5 mM	+++
233	✓	2.5 mM	+
234	✓	15 mM	—
235	✓	5 mM	+
236	✓	7.5 mM	+++
237	✓	5 mM	—
238	✓	5 mM	+++
239	✓	5 mM	+++
240	✓	7.5 mM	—

Table 21: Phenotype of potential PHD1 interactors in pLexA yeast two-hybrid assay V

#	Glycerol stock	Phenotype	
		+ 3-AT	β-Gal
241	✓	5 mM	++
242	✓	15 mM	++
243	✓	10 mM	—
244	✓	2.5 mM	+
245	✓	15 mM	+++
246	✓	5 mM	+
247	✓	10 mM	++
248	✓	25 mM	+++
249	✓	15 mM	+++
250	✓	5 mM	++
251	✓	5 mM	++
252	✓	5 mM	+
253	✓	10 mM	++
254	✓	7.5 mM	+
255	✓	5 mM	+
256	✓	10 mM	+++
257	✓	7.5 mM	+++
258	✓	5 mM	—
259	✓	10 mM	+++
260	✓	7.5 mM	++
261	✓	7.5 mM	+
262	✓	15 mM	+++
263	✓	2.5 m	++
264	✓	15 mM	+++
265	✓	5 mM	++
266	✓	—	—
267	✓	10 mM	++
268	✓	25 mM	+++
269	✓	10 mM	++
270	✓	10 mM	+++
271	✓	25 mM	+++
272	✓	15 mM	+
273	✓	2.5 mM	+
274	✓	5 mM	++
275	✓	5 mM	++
276	✓	25 mM	+++
277	✓	10 mM	++
278	✓	2.5 mM	+
279	✓	15 mM	++
280	✓	10 mM	++

Table 22: Phenotype of potential PHD1 interactors in pLexA yeast two-hybrid assay VI

Table 23 represents the sequencing results of potential interactor of pLexAPHD1.

Potential interactors of pLexAPHD1 in hTestis cDNA-Library Screening (Matchmaker/Dualsystems)								
PHD1-Interactor No.	**Protein**	**Possible function**	**Accession Nucleotide**	**Accession Protein**	**cDNA x-fold in screening**	**Phenotype yeast retransformation**		**cDNA source / expression**
						3-AT	**ß-Gal**	
2	DEAD box polypeptide 5 (DDX5)	DEAD box proteins, characterized by the conserved motif Asp-Glu-Ala-Asp (DEAD) are putative RNA helicases.	NM_004396	AAP36310	1	10 mM	++	ubiquitous
4	Karyopherin (importin) beta 3	Play a central role in nucleocytoplamic transport	BC045640	AAC51317	3	25 mM	+++	ubiquitous
5	TCP10L t-complex 10 (mouse)-like	Seems to be a leucin zipper transcription factor which is involved in cell proliferation and differentation in the liver and testis.	AF115967	NP_653260	1	15 mM	++	Liver, testis
6	Hypothetical protein FLJ25351	unknown	BC030659	BAB71654	1	15 mM	+++	testis, germ cell tumors
8	Testis-development related NYD-SP20D	unknown	AY035868	AAH29483	1	25 mM	+++	testis, germ cell tumors
10	Clone CS0DF015YB17 / Clusterin isoform	unknown	CR625885	NP_001822	1	2.5 mM	+	
13	Bromodomain adjacent to zinc finger domain, 2A	unknown	BC008965	Q9UIF9	1	10 mM	+++	ubiquitous
15	Clone FLJ35821 fis	unknown	AK093140	NP_689802	1	25 mM	+++	testis, stem cells
16	KIAA0090 protein	unknown	BC016303	NP_055862	1	2.5 mM	+	ubiquitous
17	Thyroid hormone receptor interactor 6 (Trip6)	Trip6 functions at a point of convergence between the activated LPA(2) receptor and downstream signals involved in cell adhesion and migration	NM_003302	AAK21007	1	15 mM	++	ubiquitous
19	Cerebellar degeneration-related protein 2 (Cdr2)	Unknown, cdr2 gene expressed in paraneoplastic cerebrellar degeneration (PCD), in contrast to other cdr genes	BC017503	NM_007672	Found in ProQuest / Gateway Screening	15 mM	++	ubiquitous
21	Zinc finger protein 198	unknown	BC036372	AAH36372.	1	15 mM	++	ubiquitous
22	General transcription factor IIIC, polypeptide 4 (notice: weak similarity)	unknown	BC060821	NP_036336	1	2.5 mM	+	ubiquitous
25	RAR-related orphan receptor C	DNA-binding transcription factor and it is a member of a subfamily of nuclear hormone receptors. The specific of this protein are not known;	BC031554	NP_001001523	1	25 mM	+++	ubiquitous
27	Histone-lysine N-methyltransferase (SET domain bifurcated (ERG-associated protein with SET domain)	The set domain is a highly conserved, approximately 150 aa implicating modulation of chromatin structure.	BC028671	Q15047	1	10 mM	++	ubiquitous
28	cDNA clone MGC: 72082	unknown	BC062735	AAH54871	1	7.5 m	++	testis, germ cell tumors
30	DnaJ (Hsp40) homolog, subfamily A, member 3	Belongs to the conserved HSP40 family of proteins	BC011855	AAL35323	1	25 mM	+++	ubiquitous
38	Hypothetical protein MGC33948	unknown	BC029536	AAH29536	1	15 mM	++	testis
40	Acrosin binding protein	Protein is located in the sperm acrosome and is thought to function as a binding protein to proacrosin for packaging and condensation of the acrosin zymogen.	BC033010	BAB39388	1	10 mM	+++	testis, prostate, ubiquitous

Table 23: Potential interactors of pLexAPHD1 in htestis cDNA library screening

18 clones were further tested for pLexAPHD3 interaction (Table 24). Even though pLexAPHD3 showed no self-activity on 3-AT plates, it showed self-activity in X-gal assays. No determination of the X-gal phenotype therefore took place.

Interaction of potential PHD1 interactor with HIF prolyl hydroxylase 3		
PHD1 Interactor-No.	**Protein**	**Phenotype**
		+ 3-AT
2	DEAD box polypeptide 5 (DDX5)	10 mM
4	Karyopherin (importin) beta 3	25 mM
6	Hypothetical protein FLJ25351	25 mM
8	Testis-development related NYD-SP20D	25 mM
10	Clone CS0DF015YB17	10 mM
13	Bromodomain adjacent to zinc finger domain, 2A	25 mM
15	Clone FLJ35821 fis	15 mM
16	KIAA0090 protein	none
17	Thyroid hormone receptor interactor 6 (Trip9)	none
19	Cerebellar degeneration-related protein 2 (Cdr2)	10 mM
21	Zinc finger protein 198	25 mM
22	General transcription factor IIIC, polypeptide 4	10 mM
25	RAR-related orphan receptor C	15 mM
27	Histone-lysine N-methyltransferase	15 mM
28	Clone MGC: 72082	15 mM
30	DnaJ (Hsp40) homolog, subfamily A	15 mM
38	Hypothetical protein MGC33948	15 mM
40	Acrosin binding protein	15 mM

Table 24: Interaction of potential PHD1 interactors with HIF prolyl hydroxylase 3

Summary

To identify new potential interactors of the HIF prolyl-4-hydroxylase 1 (PHD1) human and mouse testis cDNA libraries were screened independently by yeast two-hybrid methodology. In total, more than 400 potential interactors of PHD1 were found, 10% of them were further investigated and *in vitro* interaction tests were carried out with 8 interactors. Additional 40 interactors were tested for interaction with PHD2, 3 and PH-4. Clones of interest were cloned or recombined into bacterial and mammalian expression vectors. The cerebellar degeneration-related protein 2 (Cdr2) was found in both independent screenings, twice as full length mouse sequence and once as human C-terminal fragment. Previous studies reported that Cdr2 mRNA is ubiquitously expressed whereas the protein is limited to the brain and to the testis, both organs with low oxygen partial pressure. Cdr2 was originally termed due to its antibodies in a rare autoimmune disease called paraneoplastic cerebellar degeneration (PCD). PCD appears when ovarian and breast tumors start to express Cdr2. The consequence is that a $CD8^+$ cytotoxic T-cells mediated immune response is initiated which leads to tumor immunity and cerebellar degeneration. PCD is one of the rare cases where naturally occurring tumor immunity becomes visible. As an interactor of PHD1 in yeast, we assumed that Cdr2 might be a substrate of PHD1 and thereby is regulated on a posttranscriptional level. We decided to choose Cdr2 for further analysis to investigate this postulated mechanism and to understand more about Cdr2 ectopic expression in tumors and tumor immunity.

Protein stability of the onconeuronal antigen Cdr2 is regulated by PHD1

Verena S. Hofmann, Balamurugan Kuppusamy, Daniel P. Stiehl, Roland H. Wenger and Gieri Camenisch

Institute of Physiology and Zürich Center for Integrative Human Physiology (ZIHP), University of Zürich (UZH), CH-8057 Zürich, Switzerland

Abstract

The heterodimeric transcription factor HIF is a key regulator of the hypoxic response, regulating the expression of a variety of genes, involved in the maintenance of the oxygen homeostasis. Under normoxic conditions, two proline residues within the HIF-α subunit are hydroxylated by HIF prolyl-4-hydroxylase domain-containing enzymes (PHDs), which target HIF-α for degradation by the ubiquitin-proteasome pathway. This is due to the dependency of PHDs on molecular oxygen as a co-substrate. In contrast, HIF-α hydroxylation is inhibited in hypoxia, leading to the stabilization and activation of HIF.

We recently discovered the onconeural protein Cerebellar degeneration-related protein 2 (Cdr2) as an interactor of the HIF prolyl hydroxylase 1 (PHD1) found in two independent yeast two-hybrid screenings. The physiological function of Cdr2 is unknown, but the protein got its name because of the presence of its antibodies in a disease called paraneoplastic cerebellar degeneration (PCD). In PCD breast or ovarian tumors express the onconeural antigen Cdr2 which leads to an immune response to Cdr2 associated with tumor immunity and an autoimmune cerebellar degeneration. Whereas Cdr2 transcripts are found in most tissues, protein expression is restricted to the brain and testis as well as to ovarian and breast cancer tumors - all known tissues with a low oxygen partial pressure. We confirmed the interaction of PHD1 and Cdr2 *in vitro* and showed that Cdr2 is not regulated on the mRNA level but the protein levels are significantly elevated under hypoxic conditions, as well as upon PHD and proteasome inhibition in transiently transfected cells. Mapping of the hCdr2 protein sequence revealed two conserved proline clusters, which might be hydroxylated under normoxia. Our data suggest that Cdr2 protein is limited to the brain and the testis due to hypoxic conditions in these organs. Furthermore it is known that solid tumors show low oxygen partial pressure in comparison to their tissue of origin. We generated polyclonal and monoclonal antibodies against Cdr2 were able to detect endogenous Cdr2 in several breast and ovarian cancer cell lines. Unfortunately, we could not confirm the observed stabilization of Cdr2 under hypoxia and PHD inhibition for endogenous Cdr2.

Introduction

1 The onconeural antigen Cdr2

The onconeural antigen Cdr2 was first identified in context with a human neurodegenerative disease that is associated with cancer and with anti-tumor immunity. This paraneoplastic cerebellar degeneration (PCD) syndrome occurs in patients with gynecological tumors including breast or ovarian tumors. PCD is characterized by the presence of specific autoantibodies named anti-Yo (Anderson *et al.* 1988). Sera of these patients identified in total three cerebellar degeneration related antigens (Cdr1-3). Cdr1 has a molecular weight of 34 kDa and is composed of nearly identical hexapeptide repeats, making more than 90% of the protein (Dropcho *et al.* 1987). Cdr2 was cloned independently from HeLa cells and from a human cerebellar cDNA library and encodes a protein which contains a coiled coil and leucine zipper domain in the N-terminus. Cdr3 shares around 45% amino acid homology with Cdr2 and was also cloned from a HeLa expression library (Corradi *et al.* 1997). To investigate the expression pattern of these different genes and to address which gene encodes the PCD tumor antigen, Corradi *et al*. carried out a RT-PCR analysis of PCD tumors. They showed that although all three Cdr transcripts could be detected in the cerebellum, only Cdr2 mRNA was detected in the PCD ovarian tumors (Corradi *et al.* 1997). Figure 12 shows an alignment of human Cdr1, Cdr2 and Cdr3 protein sequences. Whereas Cdr2 and Cdr3 show 44 % protein homology, Cdr2 and Cdr1 have only 13 % matching aminoacids.

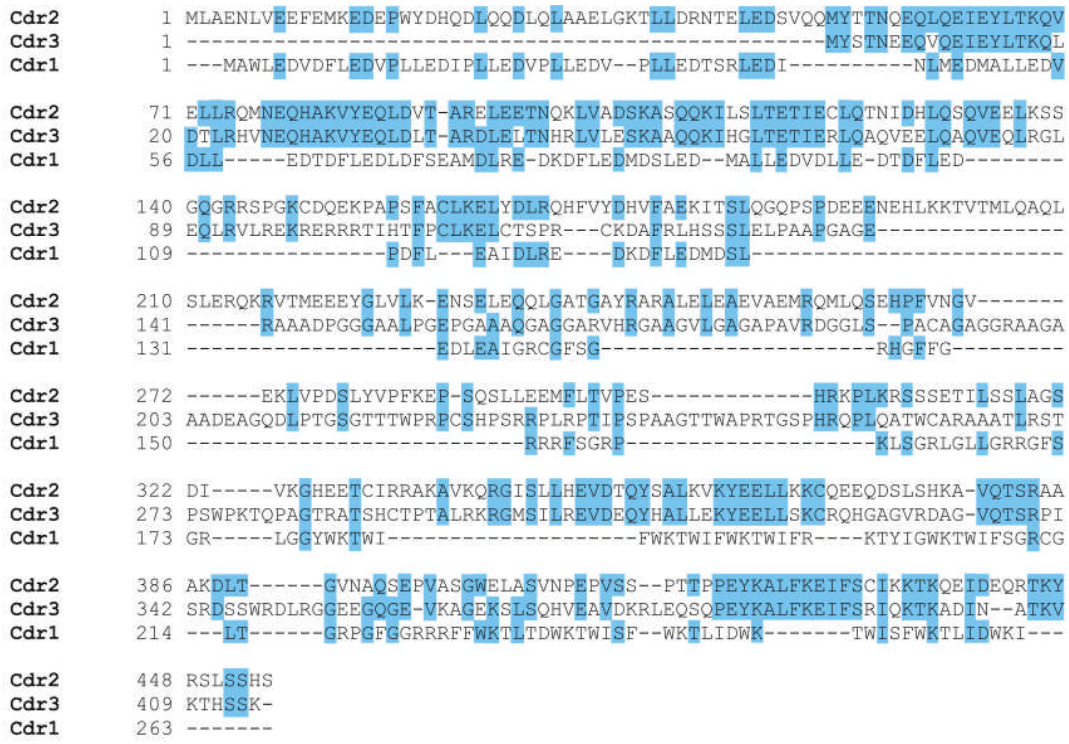

Figure 12: Alignment of hCdr1, hCdr2 and hCdr3 *Cdr2 and Cdr3 show 44 % matching amino acids (blue) whereas Cdr2 and Cdr1 show only 13 % matching aminoacids (blue)*

1.1 Cdr2 mRNA and protein expression pattern

Corradi *et al.* analyzed the Cdr2 expression pattern in mice and showed that Cdr2 mRNA is ubiquitously expressed (Fig. 13A), whereas the protein is absolutely restricted to the brain and to the testis (Fig. 13B) (Corradi *et al.* 1997).

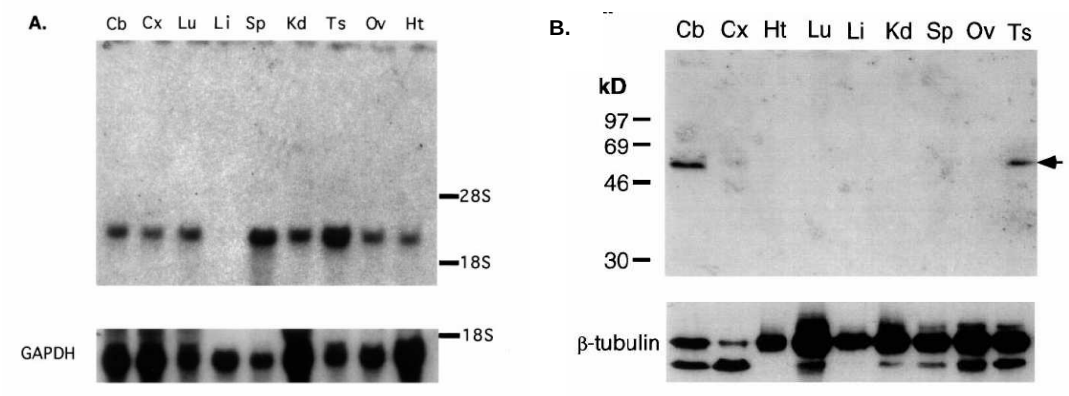

Figure 13: A. Expression pattern of mouse Cdr2 mRNA in different tissues; B. Tissue distribution of mouse Cdr2 protein *(Corradi et al. 1997)(Cb: Cerebellum, Cx: Cortex, Lu: Lung, Li: Liver, Sp: Spleen, Kd: Kidney, Ts: Testis, Ov: Ovary, Ht: Heart;*

Sequence analysis of the brain and spleen Cdr2 cDNAs showed 100% identity suggesting a tissue-specific post-transcriptional regulatory mechanism. Analysis

of Cdr2 expression by *in situ* hybridization localized Cdr2 mRNA in cerebellar Purkinje neurons as well as in cells of the outermost layers of the seminiferous tubules of the testis (Corradi *et al.* 1997). Immunohistochemical analysis detected Cdr2 protein in cerebellar Purkinje neurons, brainstem neurons and spermatogonia (Corradi *et al.* 1997). Analysis of Cdr2 protein expression in gynecological tumors obtained from neurologically normal cancer patients revealed that five out of nine representative ovary tumors expressed a 52 kDa protein, migrating at the same position as Cdr2 from Purkinje cells, loaded as a positive control. In addition, analysis of breast tumors from patients without PCD showed in some of the tumors an expression of Cdr2. These findings suggest an ectopic expression of Cdr2 in a large number of gynecological tumors independent of the presence of paraneoplastic neurological degeneration (Darnell *et al.* 2000).

1.2 What is the physiological function of Cdr2 ?

So far, the physiological function of Cdr2 has not been revealed. Some reports described Cdr2 interaction partners that could lead to assumptions about the physiological function. Okano *et al.* used the Cdr2 leucine zipper dimerization domain in a yeast two-hybrid screen to identify potential interactors (Okano *et al.* 1999). They showed that Cdr2 interacted specifically with c-Myc in yeast and *in vitro.* Although c-Myc is known as a nuclear transcription factor, its localization can vary between the cytoplasm and nucleus in relation to cellular proliferation and differentiation in cell lines (Vriz *et al.* 1992), *in vivo* (Bai *et al.* 1994) and in human tumors (Royds *et al.* 1992). Immunohistochemical examination of rat brain sections showed a significant co-localization of Cdr2 and c-Myc in the cytoplasm of Purkinje neurons. This finding was confirmed by additional confocal microscopy in rat cerebellar sections (Okano *et al.* 1999). Overexpression of Cdr2 in mouse neuroblastoma cells (N2A) revealed a striking redistribution of c-Myc into the cytoplasm, where co-localization with Cdr2 was observed. Cdr2 interacted with c-Myc and changed the subcellular localization of c-Myc to the cytoplasm. Functionally, the interaction of Cdr2:c-Myc attenuated c-Myc-dependent reporter gene expression. PCD disease antisera inhibited the interaction of Cdr2 with c-Myc which led to the following hypothesis: the PCD immune response might be able to block the ability of Cdr2 to down-regulate c-

Myc regulated gene expression which could lead to excess signaling along a pathway involved in neuronal apoptosis. Dysregulation of cell cycle pathways in Purkinje neuronal apoptosis has been implicated in cerebellar degeneration (Feddersen *et al.* 1992). Furthermore, it has been shown that nerve growth factor (NGF) is able to prevent c-Myc-induced apoptosis in fibroblasts supporting the suggestion that the transcription factor c-Myc can mediate neuronal apoptosis (Ulrich *et al.* 1998).

It has previously been shown that c-Myc modulates cell cycle pathways or apoptosis. For instance, c-Myc is an activator of cdc25A (Galaktionov *et al.* 1996). Cdc25 family members are proteins that act on several downstream targets which lead to the phosphorylation of the retinoblastoma gene product (pRb) and the release of the transcription factor E2F, a common final step in S-phase entry. Additionally, c-Myc is able to induce ARF (Zindy *et al.* 1998) an inducer of p53-mediated apoptosis (Prives 1998). So, Okano's *et al*. assumption is that abundant c-Myc entry into the nucleus in case of PCD induces inappropriate cell cycle signaling and Purkinje cell apoptosis. Figure 14 represents a model for the role of Cdr2 antibodies in PCD pathogenesis.

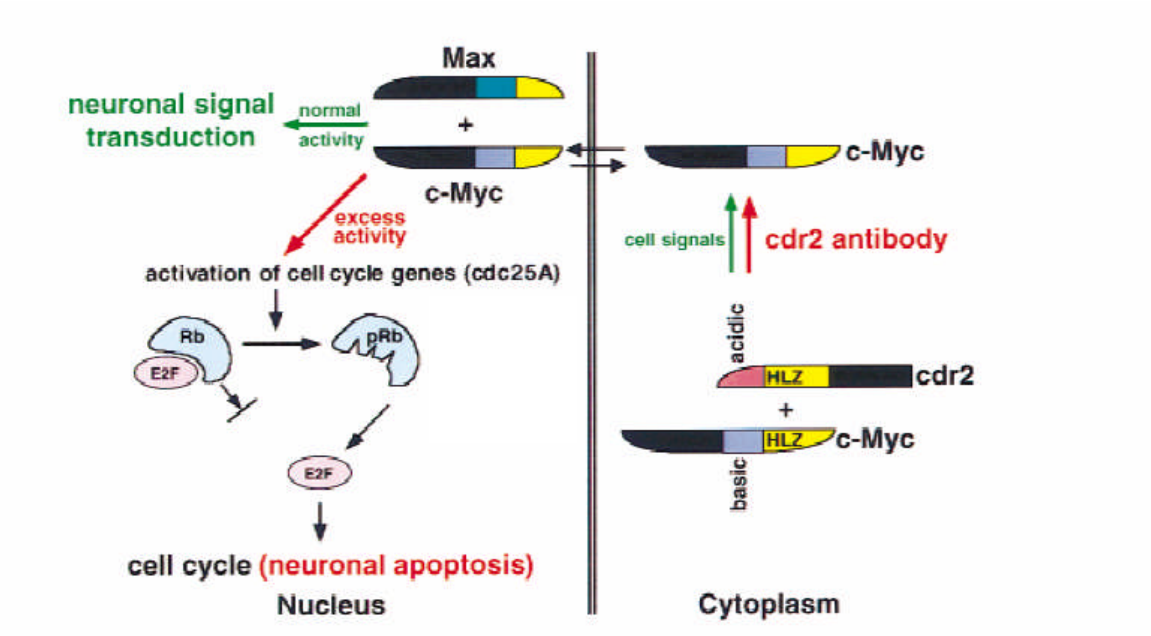

Figure 14: A model for the role of Cdr2 antibodies in PCD pathogenesis *(Okano et al. 1999). Cdr2 interacts with c-Myc in Purkinje cell cytoplasm, and thereby regulates c-Myc entry into the nucleus, where it acts to promote transcription and transduces neuronal signaling.Cdr2 antibodies in PCD patients are able to disrupt this interaction which leads to dysregulated entry of c-Myc into the nucleus. Aberrant c-Myc-induced gene transcription might lead to inappropriate cell cycle signaling and Purkinje cell apoptosis.*

In the case of gynecologic tumors it is still not clear why Cdr2 is co-expressed with c-Myc, whose activity promotes tumor progression. Evan and Littlewood suggested that c-Myc overexpression is a two-edged sword in tumor cells, on one hand promoting tumor progression and under some circumstances inducing tumor cell apoptosis (Evan and Littlewood 1998). They assume that the inhibition of c-Myc-dependent transcription by Cdr2 may attenuate c-Myc function *in vivo*. Therefore, it would be of great interest to investigate if a common function of Cdr2 in tumor cells and neurons might be the inhibition of c-Myc, thereby inhibiting the induction of apoptosis. To emphasize this importance it has to be mentioned that Cdr2 expression is found in more than 60% of ovarian tumors and more than 25% of breast tumors (Darnell *et al*.; unpubl.)

A further publication by Takanaga *et al*. identified a serine/threonine protein kinase (PKN) as interactor of PCD17 and Cdr2 (Takanaga *et al.* 1998). PCD17 and Cdr2 have exactly the same sequence except the 14 amino acids of the C-terminal region, and PCD17 lacks the N-terminal 67 amino acid residues of Cdr2 (Sakai *et al.* 1993). PKN has a catalytic domain which shows homology with protein kinase C (PKC) family members and contains in addition a unique regulatory region harboring repeats of leucine-zipper-like sequence (Takanaga *et al.* 1998). PKN was the first identified serine/threonine protein kinase that can bind to and be activated by the small GTPase Rho and in addition PKN can also be activated by fatty acids such as arachidonic acid *in vitro (Kitagawa et al. 1995; Amano et al. 1996)*. Upon arachidonic acid activation, PKN was able to phosphorylate the C-terminal part of PCD17. The presence of two putative DNA binding motifs as well as the leucine zipper-like motif in the N-terminal domain of PCD17 suggests that PCD17 might act as transcription factor. Some transcription factors are using leucine zipper motifs as homo- or heteromdimerization and Takanaga *et al.* therefore tested whether PCD17 could dimerize. *In vitro* translated PCD17 bound to GST-PCD_{1-316} and GST-PCD_{1-134} but not to GST-$PCD_{136-316}$, suggesting that PCD17 can form a homodimer in the N-terminal region. Furthermore a chloramphenicol acetyl transferase (CAT) activity reporter assay revealed a transcriptional activity of PCD17 in mammalian cells, comparable to that of CREBα induced by cAMP as a positive control. Taken together, Takanaga *et al*. suggest that the binding of anti-Cdr2 antibodies in PND patients to the leucine zipper region of PCD17, which was shown before

as the epitope, might repress gene transcription by inhibiting the homodimerization or the interaction with PKN (Takanaga *et al.* 1998). However, Darnell's group has not been able to show Cdr2 phosphorylation (Okano et al. 1999).

Furthermore, Sakai *et al.* identified the nuclear factor-kappa B (NF-κB) as an additional interactor of PCD17 (Sakai *et al.* 2001). NF-κB is known as a widely expressed transcription factor and involved mainly in regulating the immune response to infection. It is activated through cytokines, free radicals and bacterial or viral antigens. Target genes of NF-κB include among others the cytokines TNF-α, IL-2, IL-6 and interferon and the cell surface molecules VCAM-1, ICAM-1 and MHC class I and II. Sakai *et al.* investigated the effect of PCD17 on the transcriptional activity of NF-κB. Therefore they used a luciferase reporter assay and showed that the PCD17 can suppress basal or activated NF-κB-dependent transcriptional activity. Additionally, DNA binding of constitutive NF-κB complexes was decreased in the nucleus of TNF-α-stimulated neuroblastoma cells. Because PCD17 is a cytoplasmic protein and does not bind to classical NF-κB consensus site, indirect influence on the nuclear translocation of NF-κB in response to TNF-α was proposed. Corresponding to the interaction study of Cdr2 and c-Myc it has been suggested that the anti-apoptotic activity of NF-κB might be decreased in neurons expressing abundant PCD17 and thereby rendering these cells susceptible to c-Myc-induced apoptosis.

2 The role of Cdr2 in paraneoplastic neurological disorders (PNDs)

2.1 Definition of PNDs

PNDs are defined as diverse group of human neurodegenerative diseases that are associated with cancer and with anti-tumor immunity. Patients with breast, ovarian or lung tumors start to express proteins that are under physiological conditions exclusively found in neuronal cells. The neoplastic expression of these so-called onconeural antigens elicits an immune response which suppresses tumor growth. However, immune cells can by an unknown mechanism overcome the blood-brain-barrier and recognize the endogenous proteins in neuronal cells. This autoimmune response leads to neurodegenerative syndromes associated with symptoms such as progressive gait ataxia, dysarthria or nystagmus (Albert and Darnell 2004). When neurological symptoms start, most patients have not yet been diagnosed with cancer (de Beukelaar and Sillevis Smitt 2006).

2.2 Classification of PNDs

PND syndromes

Traditionally, PNDs are classified according to the neurological symptoms by which they were identified in the clinics. However, it has to be emphasized that many patients do not fit into this scheme because their symptoms are apparent in more than one defined syndrome. Therefore, all paraneoplastic disorders can be seen as a subset of diffuse and multifocal “paraneoplastic encephalomyelitis” or “paraneoplastic encephalomeyloneuritis” (Dropcho 2005). A paraneoplastic encephalomyelitis is characterized by the involvement of several areas of the nervous system, for example the limbic system, brainstem, cerebellum, spinal cord (myelitis) or autonomous nervous system.

PND antigens

The antigens of a large number of antibodies associated with paraneoplastic syndromes have been identified and the corresponding genes have been cloned and sequenced. The classification is based on this information and serves as an alternative possibility of classification of these disorders. Table 25 represents an

overview about the so far identified antineuronal antibody-associated paraneoplastic disorders.

Antibody	Neuronal Reactivity	Protein Antigens	Cloned Genes	Tumor	Paraneoplastic Symptoms	References
Anti-Hu (ANNA-1)	Nucleus more than cytoplasm (all neurons)	35–40 kD	*HuD, HuC, Hel-N1*	Small-cell lung cancer, neuroblastoma, prostate cancer	Paraneoplastic encephalomyelitis, paraneoplastic sensory neuronopathy, paraneoplastic cerebellar degeneration, autonomic dysfunction	Graus et al.,[22] Dalmau et al.,[44] Szabo et al.,[45] Levine et al.,[46] Sakai et al.[47]
Anti-Yo (PCA-1)	Cytoplasm, Purkinje cells	34 and 62 kD	*CDR34, CDR62*	Ovarian, breast, and lung cancers	Paraneoplastic cerebellar degeneration	Peterson et al.,[8] Fathallah-Shaykh et al.,[48] Darnell et al.[49]
Anti-Ri	Nucleus more than cytoplasm (central nervous system neurons)	55 and 80 kD	*Nova*	Breast, gynecologic, lung, and bladder cancers	Ataxia with or without opsoclonus–myoclonus	Jensen et al.,[50] Yang et al.,[51] Luque et al.,[52] Buckanovich et al.[53]
Anti-Tr	Cytoplasm, Purkinje cells	?	—	Hodgkin's lymphoma	Paraneoplastic cerebellar degeneration	Peltola et al.[54]
Anti-VGCC	Presynaptic neuromuscular junction	64 kD	P/Q type VGCC, *MysB*	Small-cell lung cancer	Lambert–Eaton myasthenic syndrome	Carpentier and Delattre[30]
Antiretinal	Photoreceptors, ganglion cells	23, 65, 145, and 205 kD	Recoverin	Small-cell lung cancer, melanoma, gynecologic cancers	Cancer-associated retinopathy, melanoma-associated retinopathy	Maeda et al.,[55] Polans et al.,[56] Thirkill et al.[57]
Anti-amphiphysin	Presynaptic nerve terminals	128 kD	Amphiphysin	Breast cancer, small-cell lung cancer	Stiff-person syndrome, paraneoplastic encephalomyelitis	Saiz et al.,[58] De Camilli et al.,[59] Folli et al.[60]
Anti-CRMP5 (Anti-CV2)	Oligodendrocytes, neurons, cytoplasm	66 kD	*CRMP5* (*POP66*)	Small-cell lung cancer, thymoma	Encephalomyelitis, cerebellar degeneration, chorea, sensory neuropathy	Yu et al.[61]
Anti-PCA-2	Purkinje cytoplasm and other neurons	280 kD	—	Small-cell lung cancer	Encephalomyelitis, cerebellar degeneration, Lambert–Eaton myasthenic syndrome	Bataller et al.[10]
Anti-Ma1	Neurons (subnucleus)	40 kD	*Ma1*	Lung cancer, other cancers	Brain-stem encephalitis, cerebellar degeneration	Rosenfeld et al.[62]
Anti-Ma2	Neurons (subnucleus)	41.5 kD	*Ma2*	Testicular cancer	Limbic brain-stem encephalitis	Rosenfeld et al.[62]
ANNA-3	Nuclei, Purkinje cells	170 kD	—	Lung cancer	Sensory neuronopathy, encephalomyelitis	Chan et al.[63]
Anti-mGluR1	Purkinje cells, olfactory neurons, hippocampus	Metabotropic glutamate receptor	Glu receptor	Hodgkin's lymphoma	Paraneoplastic cerebellar degeneration	Smitt et al.[64]
Anti-VGKC	Peripheral nerve	VGKC	Potassium channels	Thymoma, small-cell lung cancer	Neuromyotonia	Vernino and Lennon,[65] Hart et al.[66]
Anti-MAG	Peripheral nerve	MAG	*MAG*	Waldenström's macroglobulinemia	Peripheral neuropathy	Vital[67]

* There is no uniform nomenclature for some of the antibodies.[42,43] In this article, we use the nomenclature developed in our laboratory. Where differences exist, they are indicated in parentheses. VGCC denotes voltage-gated calcium channel, VGKC voltage-gated potassium channel, and MAG myelin-associated glycoprotein.

Table 25: Anti-neuronal antibody-associated paraneoplastic disorders *(Darnell and Posner 2003)*

The physiological functions of the neuronal antigens are manifold. PND antigens include nerve-terminal vesicle-associated proteins such as the breast cancer/stiff-person PND antigen amphiphysin and RNA-binding proteins such as the Nova antigen that regulates alternative splicing in neurons (Darnell 2004).

2.3 Proposed pathogenesis of PNDs

It is believed that PNDs are initiated when tumor cells start to synthesize proteins which are normally limited to neurons. The expression of these onconeural antigens, such as Cdr2, has the potential to trigger an anti-tumor immune response. Some of these onconeural antigens are also expressed in normal testis, an organ that is like the brain, known as an immunologically privileged tissue. Although the tumor antigen is identical to the neural antigen it causes for unknown reasons an immune response. Apoptotic tumor cells can be

phagocytosed by dendritic cells that migrate to lymph nodes and activate antigen-specific $CD4^+$, $CD8^+$ and B cells by cross-presentation of the antigen to immune cells. It is believed that the cytotoxic $CD8^+$ T cells are mostly responsible for the suppression of tumor growth by inducing apoptotic death via granzyme-mediated pathways. The antibodies and the $CD8^+$ T cells overcome the blood-brain-barrier and attack neurons that express the antigens under physiological conditions (Darnell and Posner 2003; Albert and Darnell 2004). Figure 15 summarizes the proposed pathogenesis of PNDs.

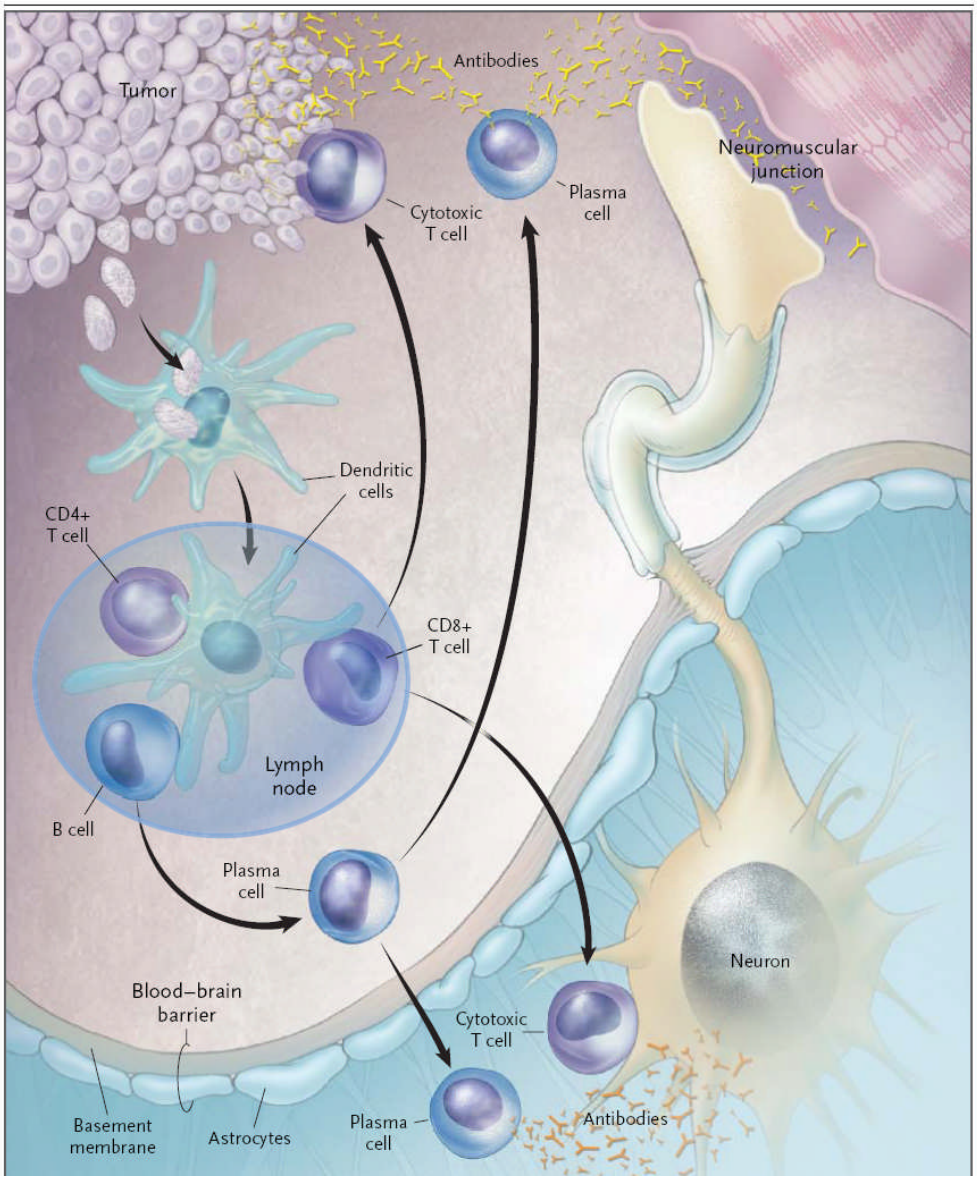

Figure 15: Proposed pathogenesis of paraneoplastic neurological disorders *(Darnell and Posner 2003)*

2.4 Characteristics of PND-associated tumors

PND-associated tumors are classically diagnosed when patients ask medical advice due to neurological symptoms. Tumors in paraneoplastic neurologic disorders show histologically no difference from other tumors except a heavy infiltration of inflammatory cells (Darnell and Posner 2003; Darnell and Posner 2003). Several reports show a more benign cancer course in PND patients compared to control groups with non-PND-associated tumors (Albert and Darnell 2004). PND-associated tumors are often limited in growth and the metastatic potential seems to be decreased compared to non-PND tumors. This leads to a better prognosis for PND patients relative to patients with histologically identical tumors without PND association. However, anti-tumor immune response is not very efficient in PNDs. A study of Rojas *et al*. showed that around 50% of PND patients die from their cancer and the other half die from neurological degeneration (Rojas *et al.* 2000). These data indicate that the PND associated anti-tumor immunity is incomplete.

2.5 Immunology of PNDs

In 2003, Posner *et al.* defined the following characteristics of autoimmunity in CNS paraneoplastic syndromes (Table 26) (Posner 2003).

- High titer antibodies that react only with tumor(s) and the nervous system are present
- The antibodies are synthesized within the CNS
- Antigen-specific T cells are found in blood, CSF, and brain
- Intraneuronal deposits of antibody have been described
- The tumor often grows more slowly

Table 26: Evidence for autoimmunity in CNS paraneoplastic syndromes *(Posner 2003)*

The role of antibodies and immune cells in PNDs will be introduced in the following chapters.

2.5.1 Antibodies in PND

High titers of antibodies against onconeural antigens are present in all PND patients in the blood and the cerebrospinal fluid and are used as diagnostic markers for PND. However, there is no clear role for antibodies in the

pathogenesis of the disease. PND antigens are found intracellularly in neuronal cells and a variety of studies in patients showed that plasmapheresis, the removal of these antibodies from the blood, had no influence on disease progression (Furneaux *et al.* 1990; Graus 1992). Additionally, mouse models for PND in which recombinant proteins of onconeural antigens were injected or PND antibodies passively transferred into mice did not lead to the onset of the disease (Sakai *et al.* 1995; Sillevis Smitt *et al.* 1996; Sakai *et al.* 2001). Based on these data, the role for a cellular immune response in the pathogenesis of the disorder was investigated (Roberts and Darnell 2004). Indeed, clear evidence for a cellular immune response has been found in paraneoplastic cerebellar degeneration (PCD) patients. Antigen-specific cytotoxic T lymphocytes (CTL) isolated from these patients were able to recognize peptides derived from the antigen Cdr2 without additional *in vitro* stimulation (Albert *et al.* 1998; Albert *et al.* 2000; Tanaka *et al.* 2001).

2.5.2 Cytotoxic T cells mediate the PND tumor immune response

One important characteristic of PND antigens is the fact that they are typically intracellular proteins. Antibodies generally mediate immune responses against extracellular proteins, whereas immunity against intracellular antigens is mediated by T cells. This led to the conclusion that tumor reactive T cells were finally responsible for mediating the anti-tumor immune responses to intracellular PND antigens. Studies using peripheral blood obtained from PND patients showed the presence of PND-antigen-specific $CD8^+$ cytotoxic T lymphocytes. These T cells were able to lyse target cells which presented processed Cdr2 peptides on major histocompatibility complex class I (MHC I) molecules (Albert *et al.* 1998). $CD8^+$ T cell immunity is based on the recognition of antigenic peptides in association with MHC I on the surface of host cells by T cell receptors (TCR) present on cytotoxic T cells. T cell receptors bind to a triad of three proteins on the surface of the tumor cells: MHC I molecule, $\beta 2$ microglobulin and a short peptide derived from the proteolytically degraded antigen associated with the MHC I molecule (Fig. 16) (Albert and Darnell 2004).

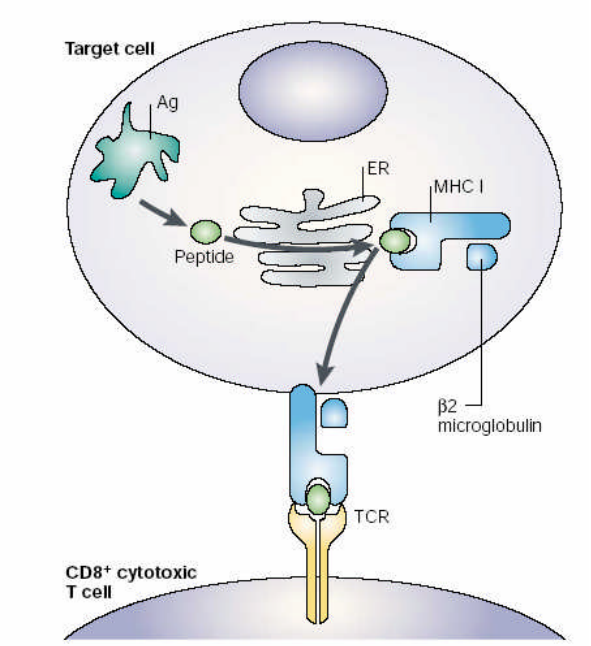

Figure 16: CD8$^+$ T cell immunity *(Albert and Darnell 2004)*
TCR on CD8$^+$ cytotoxic T cells is able to recognize the MHC I associated antigen peptide on the surface of a host cell. TCR binds to a triad of three proteins on the surface of target cell: MHC I molecules, β2 microglobulin and short peptide derived from proteolytically degraded antigen. Association of small antigenic peptides with MHC I molecules takes place in the endoplasmatic reticulum (ER) before displayed on the surface.

2.5.3 Antigen cross-presentation by dendritic cells in PND tumor immunity

Prerequisite for an activation of CD8$^+$ T cells is the antigen presentation via MHC I-peptide complex on antigen-presenting cells (APCs). Classically, only self and viral proteins were thought to have access to the class I pathway of APCs. In PNDs it has been shown that dendritic cells (DCs) are the main acting APCs, but the examination of antigen expression (Cdr2, NOVA and Hu) revealed no endogenous PND antigen expression (Buckanovich *et al.* 1996; Corradi *et al.* 1997; Okano and Darnell 1997). This paradox of necessary induction of the CD8$^+$ T cells by antigen-presenting cells expressing MHC I-peptides complexes and a missing endogenous expression in dendritic cells of these antigens lead to the question, how else dendritic cells can gain access to PND antigens in order to activate a CD8$^+$ T cell response against tumors?

Recent studies revealed that antigens derived from apoptotic tumor cells can be cross-presented by dendritic cells for the generation of MHC I-peptide complexes (Albert *et al.* 1998). Cross-presentation is defined as the ability of certain APCs to phagocytose, process and present extracellular antigens with MHC I molecules to CD8$^+$ T cells. This capability is necessary for antigen

presentation of tumor antigens from non APCs. APCs like dendritic cells and in some cases macrophages are specially equipped for cross-presentation which is linked to the cell's capacity to phagocytose (Guermonprez *et al.* 2002).Recent generation of a mouse model to investigate activation of T cells to antigens derived from apoptotic cells showed that dendritic cells process antigens from cells that contain fully or partially processed proteins (Blachere *et al.* 2005).

A study of the autoimmune disease systemic lupus erythematosus (SLE) showed that keratinocytes exposed to ultraviolet irradiation undergo apoptosis which allows the lupus antigen Ro to be extruded from the dying cell in membranous bodies (Casciola-Rosen *et al.* 1994). This led to the hypothesis that antigens that are derived from apoptotic cells could be internalized by DCs which finally leads to the activation of antigen-specific T cells. In a recent study dendritic cells lacking the transporter associated with antigen processing (TAP) were used (Blachere *et al.* 2005). TAP is necessary for peptide delivery from the cytosol into the lumen of the endoplasmatic reticulum (ER). In the ER, these peptides are loaded on MHC I molecules for presentation on the cell surface. Blachere *et al.* showed that $TAP^{-/-}$ dendritic cells had still access to the MHC I pathway when phagocytosed by apoptotic cells. They observed that apoptotic cells are able to process the antigen within the dendritic cell using their own proteasome and TAP. When TAP was missing in apoptotic cells and dendritic cells the capability of cross presentation was completely lost. In conclusion, these data suggest two distinct pathways for the processing of exogenous epitopes. In the first pathway processing of exogenous antigens is dependent on the expression of a functional TAP by the DC. The internalized antigen undergoes the phagosome-to-cytosol pathway in which the protein is cleaved proteasomally into peptides and released into the cytosol. Peptide translocation from the cytosol into the lumen of the ER is accomplished by the DC's TAP. The MHC class I molecules are then loaded with the peptide in the lumen of the ER and reach the cell surface through the secretory pathway. The second pathway is called retrograde transport pathway**.** This antigen cross-presentation pathway utilizes the proteasome and transporter activity present in the dying cell for the generation of MHC I-peptide complexes. Apoptotic cells are phagocytosed by dendritic cells and ER chaperones within the apoptotic cell facilitate the delivery of peptide epitopes to dendritic cells. Both pathways finally lead to the

presentation of the tumor antigen on the dendritic cells which activates an antigen-specific $CD8^+$ T cell immune response and may support the $CD8^+$ T cell mediated anti-tumor immunity in PNDs (Blachere *et al.* 2005).

2.5.4 $CD4^+$ T cells determine $CD8^+$ T cell activation or tolerance

The cross-presentation pathway in dendritic cells is not automatically linked to T cell activation but can also lead to T cell tolerance (Heath and Carbone 2001; Guermonprez *et al.* 2002). A cell-based system using model antigens revealed that T cell activation is dependent on the presence of $CD4^+$ T helper cells. In the absence of $CD4^+$ T helper cells, DCs were found to cross-present antigens to $CD8^+$ T cells and trigger a tolerance pathway in which $CD8^+$ T cells divide several times, but finally die an apoptotic cell death (Albert *et al.* 2001). Studies on transgenic mice confirmed these data and indicate that the presence versus the absence of antigen-reactive $CD4^+$ T cells determines $CD8^+$ T cell activation or tolerance (Albert *et al.* 2001).

2.6 Paraneoplastic neurological degenerations: keys to tumor immunity

In 1909 Paul Ehrlich was the first who described the concept of immune surveillance suggesting that the immune system could repress a potentially “overwhelming frequency” of carcinomas.

Thomas and Burnet adopted this idea in the mid 1950s and proposed that immune mechanisms could act as natural defense against tumor cells (Burnet 1957). This assumption was based on considerations of graft rejection and the newly recognized ability of T cells to survey the body for virally infected cells and kill them. The dilemma of this insight was and still is that if cellular immunity recognizes and eliminates tumor cells, the phenomenon would not be apparent through clinical signs or symptoms and therefore difficult to study. PNDs may provide the best known examples for naturally occurring human tumor immunity. Most PND patients are unaware that they have a latent malignancy. In some rare cases even neoplasms have been documented to vanish without treatment after the onset of the neurological disease (Darnell and DeAngelis 1993). However, most cases show an incomplete anti-tumor immune response and patients still die to 50% due to their cancer (Rojas *et al.* 2000). Dalmau *et al.* showed 1992 that the expression of PND-associated antigens is not limited to a few tumors. The PND-associated antigen Hu was shown to be expressed in

100% of small lung cancer samples (Dalmau *et al.* 1992), but it is rarely targeted by the immune system in patients with PND. The Cdr2 antigen is detectable in 60% of ovarian tumors and approximately 25% of breast tumors, but is only rarely targeted in patients, leading to cerebellar degeneration (Peterson *et al.* 1992). When Dalmau *et al.* examined a group of small lung cancer patients who developed no PNDs they showed that 85% of these patients fail to mount an antitumor response. About 15 – 20% of patients developed an antitumor immune response, which was at least partially effective, but no PND symptoms (Dalmau *et al.* 1990). These data are contradictive to the idea that anti-tumor responses are a very rare phenomenon or that they have to be associated with autoimmunity. However, they stay invisible when not associated with PNDs. Another study of different cancer populations that develop PND immune responses is necessary to understand how anti-tumor immunity develops and what is required to tip the balance toward autoimmunity (Albert and Darnell 2004).

Material and Methods

Multiple amino acid deletion by PCR

Multiple amino acid deletions of constructs were carried out by PCR using the following primer, reaction mixture and cycling parameters.

- pENTR4-hCdr2 1-454 Δ265-314 was generated using the template pENTR4-hCdr2 1-454 and primer pc_1_del_forward and pc_1_del_reverse.
- pENTR4-hCdr2 216-454 Δ265-314 was generated using the template pENTR4-hCdr2 216-454 and primer pc-1_del_forward and pc_1_del_reverse.
- pENTR4-hCdr2 216-397 was generated using template pENTR4-hCdr2 216-454 and primer pc_2_del_forward and pc_2_del_reverse.

Primer	**Sequence (5′ → 3′)**
pc_1_del_forward pc_1_del_reverse	CGA CAG ATG TTG CAG TCA GAG CTC AGC AGC TTG GCA GGG AGT ACT CCC TGC CAA GCT GCT GAG CTC TGA CTG CAA CAT CTG TCG
pc_2_del_forward pc_2_del_reverse	GAG TGA ACT CCC AGT CTG AGT AAG CCT ATT GCC TAT CGC CTC GAG GCG ATA GGC AAT AGG CTT ACT CAG ACT GGG CGT TCA CTC

PCR Reaction Mixture	**Volume**
Plasmid (50 – 100 ng)	x µl
Pfu-Turbo-Buffer 10 × (Stratagene)	5 µl
Deletion Primer forward (10 µM)	1.25 µl
Deletion Primer reverse (10 µM)	1.25 µl
dNTP mix (50 µM each nucleotide)	1 µl
ddH_2O up to 50 µl	x µl
Turbo-Pfu-DNA polymerase (2.5 U/µl) (Stratagene)	1 µl

Number of Cycles	**Temperature**	**Time**
1	95°C	1 min
	95°C	30 sec
20	55°C	1 min
	72°C	1 min/kb of plasmid length
1	72°C	7 min

The reaction mixture was digested with *Dpn*I for 2 h at 37°C and 5 μl of the PCR product were transformed into *E. coli* Top10 bacteria. Purified plasmids were sequenced.

RNA isolation and purification

Up to 3 x 10^7 cells were lysed by scraping in 3 ml solution D in 12 ml tubes. For RNA extraction the following solutions were added sequentially on ice and the suspension was vortexed thoroughly in between: 0.3 ml of 2 M NaAc pH 4.0, 3.0 ml of water-saturated phenol and 0.6 ml chloroform-isoamyl alcohol mixture (49:1). The well-mixed suspension was cooled on ice for 20 minutes and centrifuged at 10 800 rpm for 20 minutes at 4°C. The aqueous phase was precipitated in a fresh 12 ml tube with 3 ml isopropanol at -20°C for 1 hour. Afterwards, the RNA was pelleted by centrifugation (10 800 rpm, 20 minutes at 4°C) and the supernatant was removed completely. The RNA pellet was dissolved in 0.3 ml solution D, transferred into a fresh Eppendorf tube and again precipitated with 0.3 ml isopropanol at -20°C for 1 hour. The solution was centrifuged again for 20 minutes at 10 800 rpm at 4°C and the pellet washed by vortexing in 75% ethanol (-20°C). After repeated centrifugation, the RNA pellet was air dried for up to 1 hour and dissolved in 50 μl DEPC-treated water. The resuspended RNA was heated for 15 minutes at 56°C to assist solubilization and finally stored at -80°C.

Solution D

4 M	Guanidine thiocyanate
25 mM	Sodium citrate (pH 7.0)
0.5%	Sarcosyl

RNA quantification

RNA concentration was measured at OD_{260}. Additionally, 5 μg RNA were loaded on an agarose gel. Therefore 2.5 g agarose were diluted in 185 g DEPC-H_2O, melted in the microwave and cooled down briefly to about 75°C under tap water. 25 ml 10 × MOPS and 40 ml 37% formaldehyde were added and the gel was

poured into a gel chamber. 1 volume RNA was mixed with 3 volumes sample buffer containing additionally 1/100 volume ethidium bromide, heated at 56°C for 15 minutes, 1/10 volume of bluemix was added and the samples were loaded immediately on the gel. The gel was run for 30 minutes at 40 V and RNA was detected by UV light.

10 x MOPS

0.4 M	Morpholinopropanesulfonic acid (pH 7.0)
0.1 M	Sodium acetate x 3 H_2O
10 mM	Na_2EDTA x 2 H_2O
	Fill up to 1 l with DEPC-H_2O

Sample Buffer

192 µl	37% formaldehyde
600 µl	100% formamide
120 µl	10 x MOPS

Bluemix

50%	Glycerol
1 mM	EDTA
0.1%	Bromphenolblue
0.1%	Xylene cyanol ff

First-strand cDNA synthesis

The following components were added to a nuclease-free Eppendorf tube:

- 1.5 µl oligo$(dT)_{12-18}$ (0.2 µg/µl) (Stratagene)
- 5 µg of total RNA
- x µl of DEPC-treated H_2O for a total reaction volume of 50 µl

The mixture was heated for 5 minutes at 65°C and slowly cooled down to room temperature for 10 minutes allowing the primers to anneal to the RNA. The following components were added to the mixture:

- 2 µl of 10 mM dNTP mix (Sigma)
- 1 µl Ribonuclease Inhibitor (40 U/µl) (Fermentas)
- 0.5-1 µl of StrataScript reverse transcriptase (200 U/µl) (Stratagene)

The reaction was mixed gently and incubated at 42°C for 1 hour. To inactivate the reaction, the mixture was heated to 90°C for 5 minutes, kept on ice and diluted 1:2 with sterile H_2O and stored at -20°C until quantitative PCR analysis.

Quantitative PCR (qPCR)

2 µl cDNA of each sample were distributed in a 96-well-qPCR plate (Abgene). 1 $\times 10^2$ – 1 $\times 10^8$ copies of a corresponding plasmid were pipetted as standard into additional wells. According to the manufacture's manual, a master mix including the following components per well was added:

Syber Green Mixture (Sigma)	12.5 µl
ROX Dye (Sigma)	0.1 µl
10 µM forward primer	1 µl
10 µM reverse primer	1 µl
H_2O	8.5 µl
Final volume/well	23 µl

qPCR thermal profile

Number of Cycles	Temperature	Time
1	95°C	10 min
40	95°C	30 sec
	60°C	1 min
	72°C	1 min
1	55°C	30 sec
	95°C	1 min

q-PCR-Primer	Sequence (5′ → 3′)
hCdr2 forward hCdr2 reverse	GTA TGA CCT CCG CCA ACA CT CTG CAA CAT CTG TCG CAT CT
hPHD1 forward hPHD1 reverse	CTG GGC AGC TAT GTC ATC AA AAA TGA GCA ACC GGT CAA AG
hPHD2 forward hPHD2 reverse	GAA AGC CAT GGT TGC TTG TT TTG CCT TCT GGA AAA ATT CG
hPHD3 forward hPHD3 reverse	ATC GAC AGG CTG GTC CTC TA CTT GGC ATC CCA ATT CTT GT
hL28 forward hL28 reverse	GCA TCT GCA ATG GAT GGT C ACA AGA ACT CCT AGT ACA CA
mCdr2 forward mCdr2 reverse	CTG AAG TCT TCC AGC CAA GG GCT CCA GCT CAC TGT TCT CC
mPHD1 reverse mPHD1 forward	TTG CCT GGG TAG AAG GTC AC GCT CGA TGT TGG CTA CCA CT
mPHD2 forward mPHD2 reverse	GCA ACG GAA CAG GCT ATG TC CTC GCT CAT CTG GCA TCA AAA
mPHD3 forward mPHD3 reverse	CAA CTT CCT CCT GTC CCT CA GGC TGG ACT TCA TGT GGA TT
mS12 forward mS12 reverse	GAA GCT GCC AAA GCC TTA GA AAC TGC AAC CAA CCA CCT TC

Bacterial expression of recombinant proteins

Three different expression systems were used for bacterial expression of recombinant proteins. Recombinant proteins were either fused to Glutathione-S-transferase (GST), hexa-histidine $(HIS)_6$ or maltose-binding protein (MBP). The plasmids were transformed into the corresponding bacterial strain as describe in the following table, an overnight culture containing the corresponding antibiotic and if necessary 0.1% glucose was inoculated with a single colony. On the next day, the overnight culture was diluted 1:40 and grown at 37°C to an OD_{600} of 0.4. Expression was induced either by arabinose or isopropyl β-D-1-thiogalactopyranoside (IPTG) depending on the expression system. The bacteria were induced for 3 - 4 hours at 37°C. Afterwards, the bacterial culture was centrifuged at 8 000 rpm for 15 minutes at 4°C and pellets were stored at -20°C until purification.

The following table 27 shows an overview of the used expression systems:

	GST-fusion system (Invitrogen)	**$(HIS)_6$-fusion system (Invitrogen)**	**MBP-fusion system (NewEnglandBiolabs)**
Bacterial strain	BL21-AI	BL21-AI	TB1
Genotype Bacteria strain	*F^- ompT hsdS$_B$ (r_B^- m_B^-) gal dcm araB::T7RNAP-tetA*	*F^- ompT hsdS$_B$ ($r_B^-m_B^-$) gal dcm araB::T7RNAP-tetA*	*F^- ara Δ(lac-proAB) [Φ80dlacΔ(lacZ)M15] rpsL(Str^R) thi hsdR*
Induction by	Arabinose	Arabinose	IPTG
Repression of expression	0.1% Glucose	0.1% Glucose	-

Table 27: Bacterial expression systems

LB Medium	
1%	Tryptone
0.5%	Yeast extract
0.5%	NaCl

Lysis of bacteria

Bacterial pellets of a 2 l culture were resuspended either in 8 ml PBS (GST-fusion and HIS_6-fusion proteins) or 8 ml column buffer (MBP-fusion protein) with EDTA-free protease inhibitors (Roche). Bacterial lysis was carried out by

disruption of bacteria in a French press at 2.7 kbar or chemical lysis using 0.5% NP-40 added to the resuspension or column buffer. After chemical lysis, the bacterial suspension was rotated on ice for 30 minutes and afterwards sonicated for 3 × 30 pulses. In case of FPLC purification, the lysate was centrifuged at 40 000 rpm for 1 hour at 4°C whereas for batch purification a centrifugation step at 12 000 rpm for 1 hour at 4°C was carried out.

Purification of recombinant proteins

Biologic Duo Flow fast performance liquid chromatography (FPLC)

GST-fusion proteins

After centrifugation, the supernatant of the lysate was loaded on a GSTrap FF column (Amersham) with a flowrate of 0.2 ml/min to bind the fusion protein to the glutathione sepharose matrix. The 2-buffer system consisted of a buffer A (1 × PBS) as washing buffer and a buffer B (32.5 mM glutathione/50 mM Tris/Cl pH 8.0) used as elution buffer.

$(HIS)_6$-fusion proteins

After centrifugation the supernatant was loaded on a HiTrap chelating HP column (Amersham) with a flowrate of 0.2 ml/min. The column was manually prepared in advance by loading 0.1 M $NiSO_4$. The 2-buffer system consisted of a buffer A (His_6) binding buffer and a buffer B $(His)_6$ elution buffer including 0.5 M imidazole.The following program run represents the general protein purification steps used for GST-and $(HIS)_6$–fusion protein purification by FPLC.

Step Number	Step
1	Isocratic flow with 100% buffer A at 1.00 ml/min for 10.0 ml
2	Dynamic loop: Inject x ml sample at 0.2 ml/min
3	Isocratic flow with 100% buffer A at 1.00 ml/min for 10.0 ml
4	Elution with 100% buffer B at 1.00 ml/min for 10.0 ml
5	Isocratic flow with 100% buffer A at 1.00 ml/min for 10.0 ml

Batch purification

$(HIS)_6$-fusion proteins

0.5 ml Ni-NTA-agarose beads (Qiagen) were washed three times with bead binding buffer and the lysate was added to the beads and rotated for 2 hours at 4°C. Afterwards, the beads were washed four times with 20 ml/10 ml/1.5 ml/1.5 ml bead binding buffer, each time rotating for 10 minutes at 4°C. $(His)_6$-fusion proteins were eluted with twice 300 µl $(His)_6$ elution buffer.

MBP-fusion proteins

1.5 ml amylose beads (NEB) were washed three times with column buffer and the lysate was added to the beads and rotated for 2 hours at 4°C. Beads were washed afterwards four times with 25 ml column buffer, each time rotating for 10 minutes at 4°C. MBP-fusion proteins were eluted with 3 ml column buffer including 10 mM maltose (MBP elution Buffer). The elution was repeated twice each time with 2 ml MBP elution buffer.

MBP column buffer	
20 mM	TrisCl pH 7.4
200 mM	NaCl
1 mM	EDTA

MBP elution buffer
= MBP-column buffer
+ 10 mM D-Maltose

$(His)_6$ binding buffer	
0.02 M	Na_3PO_4
0.5 M	NaCl

$(His)_6$ elution buffer	
0.02 M	Na_3PO_4
0.5 M	NaCl
0.5 M	Imidazole, pH 7.4

SDS-polyacrylamide gel electrophoresis (SDS-PAGE)

For SDS-PAGE the following volumes dependent on the percentage of the gel were mixed in a 50 ml tube. Polymerization took place within 30 minutes and proteins were separated by gel electrophoresis at 100 – 200 V.

Separating gel			Stacking gel		
1.5 M	Tris/Cl pH 8.7	7.5 ml	1 M	Tris/Cl pH 6.8	1.25 ml
30%	Acrylamide	5-20 ml	30%	Acrylamide	1.67 ml
10%	SDS	300 µl	10%	SDS	100 µl
1%	Bisacrylamide	7.8-2 ml	1%	Bisacrylamide	1.30 ml
	H_2O	ad 30 ml		H_2O	ad 10 ml
10%	APS	200 µl	10%	APS	100 µl
	TEMED	20 µl		TEMED	10 µl

Gel percentage	**5.0%**	**7.5%**	**10.0%**	**12.5%**	**15.0%**	**17.5%**	**20.0%**
30% Acrylamide	5.0	7.5	10.0	12.5	15.0	17.5	20.0 ml
1% Bisacrylamide	7.8	5.8	3.9	3.1	2.6	2.2	2.0 ml

10 x SDS-PAGE Running Buffer (1 l)	
Tris	30 g
Glycine	144 g
1 mM	EDTA
SDS(1%)	10 g

10 x Sample Buffer	
0.4 M	Tris/Cl pH 6.8
10%	SDS
0.5 M	β-ME

Semi-dry electrophoretic transfer/immunoblotting

Proteins were blotted to a nitrocellulose membrane (0.2 µm) (GE Healthcare) between three layers of filter paper soaked in blotting buffer at 10 – 20 V_{const} for 1 – 2 hours. Afterwards, the nitrocellulose membrane was briefly rinsed in PBS and stained for 5 minutes in Ponceau S solution. After complete destaining in PBS the nitrocellulose membrane was blocked in 5% non-fat milk powder in PBS for at least 30 minutes at room temperature. Primary antibodies were added and the blot was rotated either overnight at 4°C or for a maximum of 2 hours at room temperature. The antibody solution was removed and the membrane washed three times 10 minutes with an excess volume of PBS with 0.5% Tween. The membrane was afterwards incubated with the horse-radish-peroxidase- (HRP-) coupled secondary antibodies at the desired dilution for one hour at room temperature. The washing procedure as above was repeated. The detection of the antigen took either place using a commercially available chemiluminescent HRP substrate (Pierce) following the supplier's reference or a self-prepared substrate was used with the following components: 10 ml 100 mM

Tris/Cl pH 8.5, 3 µl 30% H_2O_2, 50 µl 250 mM luminol and 25 µl 90 mM p-coumaric acid. The solution was equally distributed over the nitrocellulose membrane and incubated for 1 minute at room temperature. Excess liquid was removed and the membrane immediately wrapped into saran foil and exposed either to x-ray film or a charge-coupled device (CCD) camera.

Blotting Buffer	
25 mM	Tris
192 mM	Glycine
20%	MeOH
0.04%	SDS

Ponceau S	
0.2%	Ponceau S
3%	Trichloracid
3%	Sulfosalicylic acid

Cell Culture

Transient transfection of eukaryotic cells using polyethylenimine (PEI)

DNA solution used for transient transfections was heated at 68°C for 20 minutes to avoid contamination of the cells. For a 10-cm dish culture the following amount of DNA and PEI were used. Depending on the size of the dish the amounts were adapted according to table 28.

Solution A: 3 µg DNA in 100 µl 150 mM NaCl

Solution B: 15 µl 1 mg/ml PEI plus 85 µl 150 mM NaCl

Both solutions were incubated for 5 minutes at room temperature. Solution B was added to Solution A, briefly vortexed and incubated for 25 – 30 minutes at room temperature. Culture media was replaced with fresh one and PEI-DNA-mix was added dropwise to 50% - 75% confluent cells in a 10-cm dish. The cells were incubated for 16 up to 48 hours before further experiments.

Culture format	Media per well [ml]	DNA [µg]	Final volume of DNA dilution [µl]	PEI [µl] of 1mg/ml	Final volume of PEI dilution [µl]
24-well	0.5	0.5 - 1.0	50	2.5 - 5	50
12-well	1	0.5 - 1.5	50	2.5 - 7.5	50
6-well	2.5	1.0 - 3.0	100	5.0 - 15.0	100
100 mm plate	10	2.0 - 4.0	100	10.0 - 20.0	100
150 mm plate	18	4.5 - 10.0	200	22.5 - 50.0	200

Table 28: PEI transfection in different scales

DMEM high glucose® (Sigma)	
10% (vol/vol)	Fetal calf serum (FCS)
1% (vol/vol)	Penicillin/Streptomycin

McCoy's 5A medium + L-Glutamine	
10% (vol/vol)	Fetal calf serum (FCS)
1%(vol/vol)	Penicillin/Streptomycin

Dual-Luciferase reporter assay system (Promega)

10 µl of whole cell lysates (WCL) were distributed in a 96-well plate and 10 µl of the LANII, a mix of luciferin (luciferase substrate), ATP and magnesium, were added. Firefly luminescence was detected in a 96-well luminometer (Berthold) and 10 µl of the Stop&Glo substrate (1:50) were added to measure renilla luminescence.

Preparation of whole cell extracts

Cells were washed twice with ice-cold PBS, scraped into an ice-cold Eppendorf tube and centrifuged at 14 000 rpm for 30 seconds at 4°C. The supernatant was removed and depending on the size of dish 100 – 200 µl of cell lysis buffer were added. The cells were incubated on ice for 10 minutes with briefly vortexing every 2 minutes. The cell extract was centrifuged for 15 minutes at 14 000 rpm at 4°C and the supernatant was transferred to a fresh Eppendorf tube and stored at –80°C until analysis.

Cell lysis buffer for whole cell extracts	
10 mM	Tris (pH 8.0)
1 mM	EDTA (pH 8.0)
400 mM	NaCl
0.1%	NP-40

10 × PBS (1 l)	
80 g	NaCl
2 g	KCl
14.4 g	Na_2HPO_4
2.4 g	KH_2PO_4

Preparation of mouse tissue extracts

The tissue was dissected from adult C57B6 mice and immediately deep frozen in liquid nitrogen and stored at -80°C or processed by homogenization in a Polytron (Kinematica) in 1 × PBS including EDTA-free protease inhibitors on ice. The volume of PBS was adapted depending on the size of the organ or tissue between 200 – 400 µl. Extracts were incubated on ice for 15 minutes with briefly vortexing every 2 minutes and final centrifugation for 15 minutes at 14 000 rpm

at 4°C. Supernatants were transferred into fresh ice-cold Eppendorf tubes, aliquoted and stored at -80°C until analysis.

Immunofluorescence analysis

Cells were cultivated on coverslides, washed twice with ice-cold PBS and fixed for 30 minutes with 4% paraformaldehyde. Afterwards, the cells were washed three times with PBS and 20 mM glycine in PBS was added twice for 5 minutes each at room temperature to quench free aldehyde groups. Cells were permeabilized by 0.1% saponin-glycine in PBS for 20 minutes at room temperature and washed three times with PBS. Primary antibodies were diluted in 0.1% saponin-PBS and the cover-slide was incubated for 1 hour at 37°C upside down on parafilm in a 150 mm dish in 30 µl antibody solution. A wet tissue was added to the incubation chamber for optimal humidity. The coverslide was transferred back to the 12-well plate and washed three times with PBS. The secondary antibodies, also diluted in saponin-PBS, were added directly into the well (100 µl/well) and the plates were incubated for 30 minutes in the dark to avoid bleaching. To continue with nuclear 4,6-diamidino-2-phenylindol (DAPI) stain, cells were washed three times with PBS and 100 µl DAPI staining solution (1 ng/µl) were added per well and incubated for 30 minutes at room temperature in the dark. The coverslide was washed three times with 5 minutes incubation time in between and finally mounted with 100 µl Mowiol on an object slide, dried overnight at room temperature and stored at 4°C until analysis by confocal laser scanning microscopy (SP1, Leica Microsystems).

4% Paraformaldehyde

4 g	Paraformaldehyde
	Dissolve in 100 ml PBS, stir and warm to 60°C, then add afew drops of 4°C 10 M NaOH until it is completely dissolved, cool to room temperature and adjust pH to 7.4 with 37% HCl

Mowiol

2.4 g	Mowiol 4-88
6 g	Glycerol → stirr to mix add 6 ml H_2O and mix for several hours at room temperature; add 12 ml 0.2 M Tris (pH 8.5), heat to 50°C for 10 minutes, with occasional mixing, after Mowiol has dissolved, clarify by centrifugation at 5000 x g for 15 minutes, add 2% DABCO (1.4-diazobicyclo[2,2,2]-octane)

Results

Identification of Cdr2 as PHD1 interactor by yeast two-hybrid screenings

Cdr2 was identified in two independent yeast two-hybrid screenings using a mouse and a human testis cDNA library (see pages 45 and 60). Full length mouse Cdr2 (mCdr2) was cloned twice and a human Cdr2 (hCdr2) fragment (hCdr2 aa216-454) once. Alignment of mCdr2 and hCdr2 sequences revealed 89% homology with a highly conserved C-terminus. Figure 17 shows mouse and human Cdr2 full length and the identified hCdr2 fragment 216-454.

```
hCdr2    1   MLAENLVEEFEMKEDEPWYDHQDLQQDLQLAAELGKTLLDRNTELEDSVQQMYTTNQEQLQEIEYLTKQV
mCdr2    1   MLADNLVEEFEM-EDEPWYDHRDLQQDLQLAAELGKTLLDRNTELEDSLQQMYTTNQEQLQEIEYLTKQV

hCdr2    71  ELLRQMNEQHAKVYEQLDVTARELEETNQKLVADSKASQQKILSLTETIECLQTNIDHLQSQVEELKSSG
mCdr2    70  ELLRQMNEQHAKVYEQLDVTARELEETNQKLVAESKASQQKILSLTETIECLQTNIDHLQSQVEELKSSS

hCdr2    141 QGRRSPGKCDQEKPAPSFACLKELYDLRQHFVYDHVFAEKITSLQGQPSPDEEENEHLKKTVTMLQAQLS
mCdr2    140 QGRGRQKACDQEKPAPSFSCLKELYDLRQHFVYDHVFAEKITSLQSQQSPDEEENEHLKKAVTMLQAQLS

hCdr2    211 LERQKRVTMEEEYGLVLKENSELEQQLGATGAYRARALELEAEVAEMRQMLQSEHPFVNGVEKLVPDSLY
mCdr2    210 LERKKRVSVEAEYKVVLKENSELEQQLGATDAYRARALELEAEVAEMRQMLQAEHPFVNGVEKLVPDSLF

hCdr2    281 VPFKEPSQSLLEEMFLTVPESHRKPLKRSSSETILSSLAGSDIVKGHEETCIRRAKAVKQRGISLLHEVD
mCdr2    280 VPFKEPSQSLLEEMFLAAPEAPRKPLKRSSSETALSSLAGDDIVKDHEDTCIRRAKAVKQRGISLLHEVD

hCdr2    351 TQYSALKVKYEELLKKCQEEQDSLSHKAVQTSRAAAKDLTGVNAQSEPVASGWELASVNPEPVSSPTT-P
mCdr2    350 TQYSALKVKYEELLKKCHEEQDSLSHKAVQTSRLLTRDLTGLVTQSEAGASGWEPTPVSPESISSPTTTP

hCdr2    420 PEYKALFKEIFSCIKKTKQEIDEQRTKYRSLSSHS-
mCdr2    420 PEYKALFKEIFSCIKKTKQEIDEQRTKYPSLSSYSY
```

Figure 17: Alignment of hCdr2 and mCdr2 protein sequences
Letters in red represent amino acid mismatches between human and mouse Cdr2 protein sequence. Bold letters correspond to the found hCdr2 sequence in the Matchmaker/Dualsystems screening.

Interaction of Cdr2 and PHDs in yeast

pEXPAD502Cdr2 was transformed in Mav203 yeast strain containing either pDEST32PHD1, pDEST32PHD2 or pDEST32PHD3. As positive control yeast cells were transformed with pDEST22HIF-2α404-569 and pDEST32PHD1 and to exclude self activity of PHD1, pDEST32PHD1 was transformed together with pEXP-AD502 library vector. All combinations of yeast were plated on agar plates with increasing concentrations of 3-AT as well as on uracil-lacking plates. An X-gal assay was carried out to examine the third reporter gene, β-galactosidase. PHD1/Cdr2 showed growth up to 25 mM 3-AT and on uracil-lacking plates and a strong blue staining in the X-gal assay was observed (Fig. 18). Whereas no interaction was seen between PHD2 and Cdr2 , PHD3 weakly interacted with Cdr2 in the presence of up to 10 mM 3-AT (data not shown).

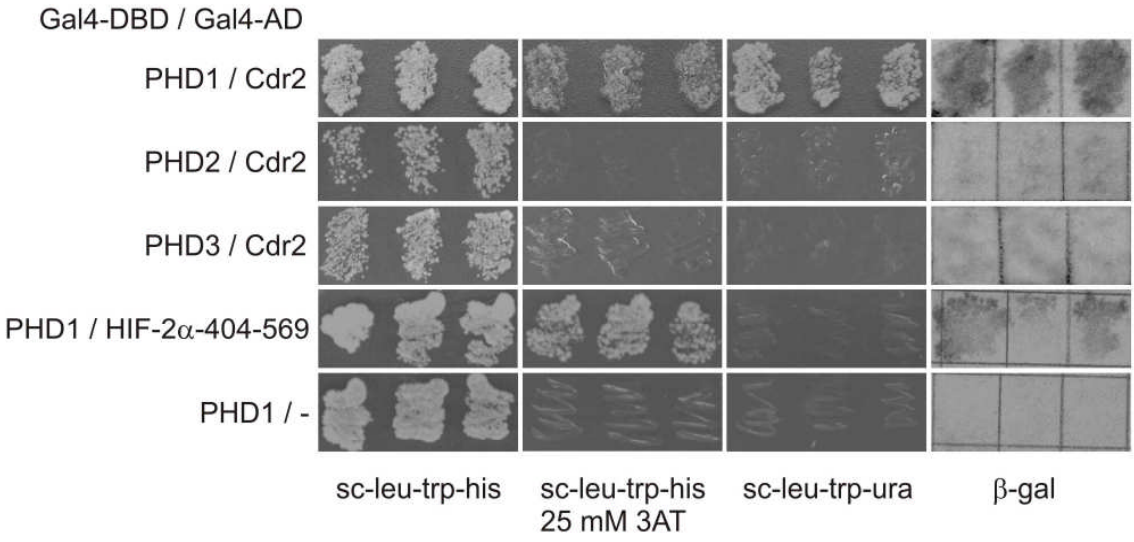

Figure 18: Interaction of Cdr2 and PHDs in yeast. *Yeast reporter strain Mav203 expressing different Gal4-DBD and Gal4-AD fusion proteins was assayed for histidine and uracil auxotrophy as well as for β-galactosidase activity.*

In vitro interaction of Cdr2 and PHD1 in GST pull-down assay

Bacterially expressed and purified GST-PHD1 was incubated with *in vitro* transcribed and translated (IVTT) ^{35}S-Cdr2 and with glutathione sepharose. As positive control served GST-HIF-1α530-826 incubated with ^{35}S-PHD2 and GST alone was used as non-interaction control. PHD1 showed a weak interaction with Cdr2 compared to the positive control (Fig. 19).

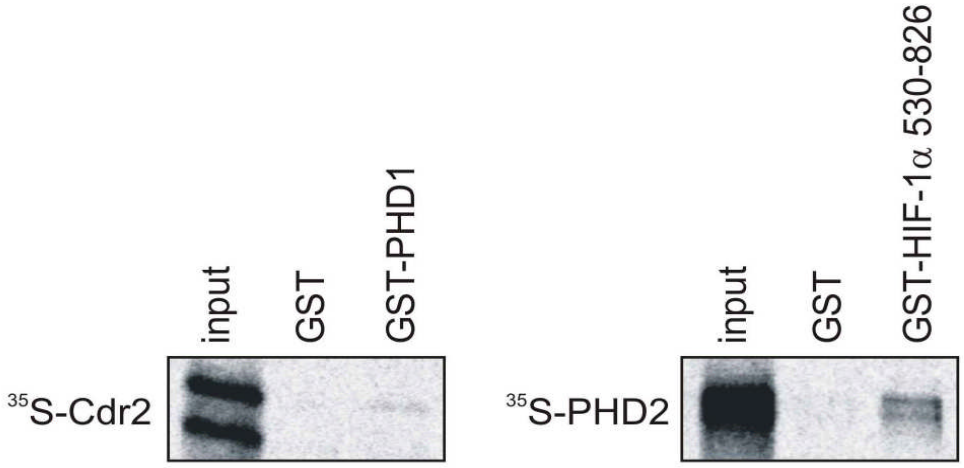

Figure 19: PHD1 and Cdr2 interact in GST pull-down assays. *Protein-protein interaction of in vitro transcribed and translated (IVTT) ^{35}S-labeled Cdr2 or PHD2 and recombinant GST-PHD1 or GST-HIF-1α530-826 fusion proteins, or GST alone were analyzed by GST pull-down with glutathione sepharose. Bound proteins and input controls (5%) were separated by SDS-PAGE and visualized by autoradiography.*

Expression of Cdr2 mRNA

Expression pattern of Cdr2 and PHD1 in mouse tissues

Cdr2 mRNA was shown to be present in almost all tissues with higher expression levels in the brain and in the testis (Corradi *et al.* 1997). To confirm these literature data as well as to compare tissue expression patterns of Cdr2 and PHD1, quantitative PCR was performed. Cdr2 and PHD1 were ubiquitously expressed with higher mRNA levels in testis and brain. Additionally, PHD1 expression levels were higher compared to Cdr2 in skeletal muscle, liver and kidney. Surprisingly, Cdr2 mRNA was similarly high in the bone marrow as in the testis (Fig. 20).

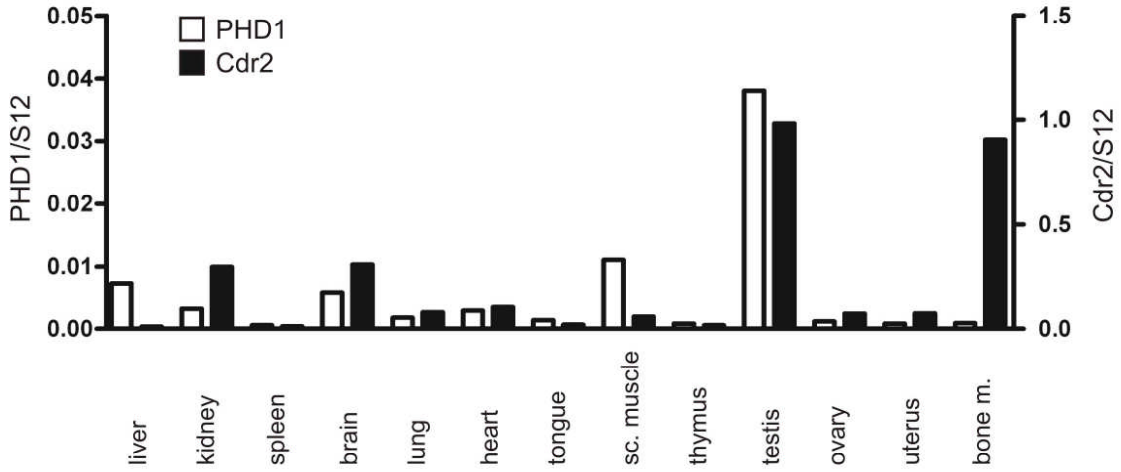

Figure 20: Tissue distribution of mCdr2 and mPHD1 mRNA. *RNA was extracted from mouse tissues and PHD1 as well as Cdr2 mRNA levels determined by quantitative PCR and normalized to S12 mRNA. Note the different scales.*

Cdr2 is not transcriptionally regulated in hypoxia

The fact that Cdr2 is ubiquitously expressed but the protein could only be detected in the brain and the testis, indicated that Cdr2 must be post-transcriptionally regulated (Corradi *et al.* 1997). Brain and testis are tissues with relatively low pO_2 values and we therefore hypothesized that Cdr2 protein might be PHD-dependently regulated under different oxygen conditions. To test whether Cdr2 mRNA is induced under hypoxic conditions, human tumor cell

lines were incubated under normoxic (20% O_2) or hypoxic (0.2% O_2) conditions or treated with the PHD inhibitor dimethyloxalylglycine (DMOG). Whereas Cdr2 gene expression was not upregulated in hypoxia or after DMOG treatment in none of the cell lines tested, PHD3 mRNA levels were highly elevated in a HIF-dependent manner (Fig. 21).

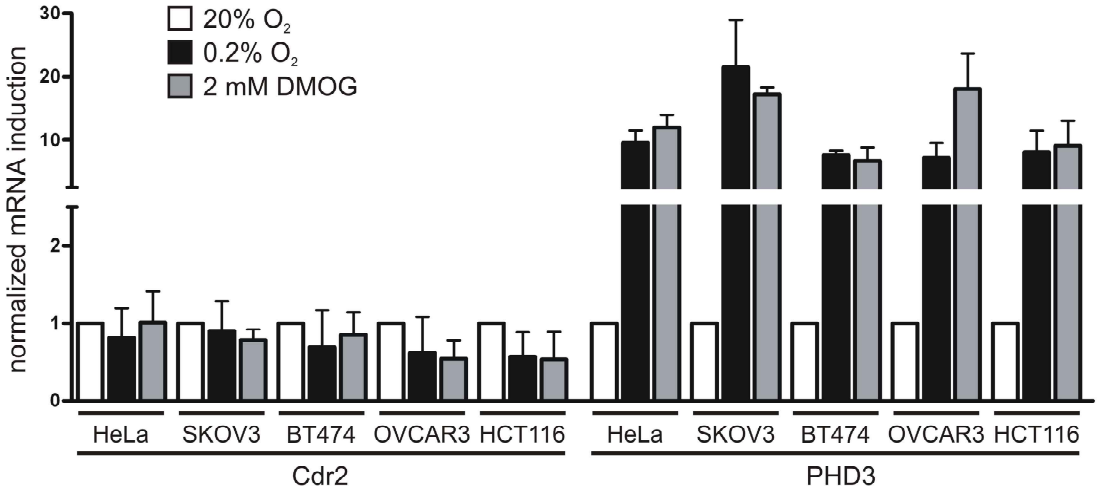

Figure 21: No hypoxic upregulation of Cdr2 mRNA in human cell lines. *HeLa, SKOV3, BT474, OVCAR3 and HCT116 cells were cultured either at 20% or 0.2% oxygen or treated with 2 mM DMOG respectively 1 mM DMOG for SKOV3 for 20 hours. mRNA levels of Cdr2 and PHD3 were quantified by real-time quantitative PCR and normalized to ribosomal L28 mRNA. Data are mean ± SEM of n = 3 independent experiments.*

Possible HIF-1α-dependent Cdr2 regulation was analyzed in mouse embryonic fibroblasts (MEFs) either HIF-1α wild-type (HIF-1$\alpha^{+/+}$) or HIF-1α-deficient (HIF-1$\alpha^{-/-}$). As expected, Cdr2 mRNA levels were not regulated in a HIF-1α- or oxygen-dependent manner, whereas CAP43, a well-known target gene of HIF, was upregulated under hypoxic conditions (Fig. 22).

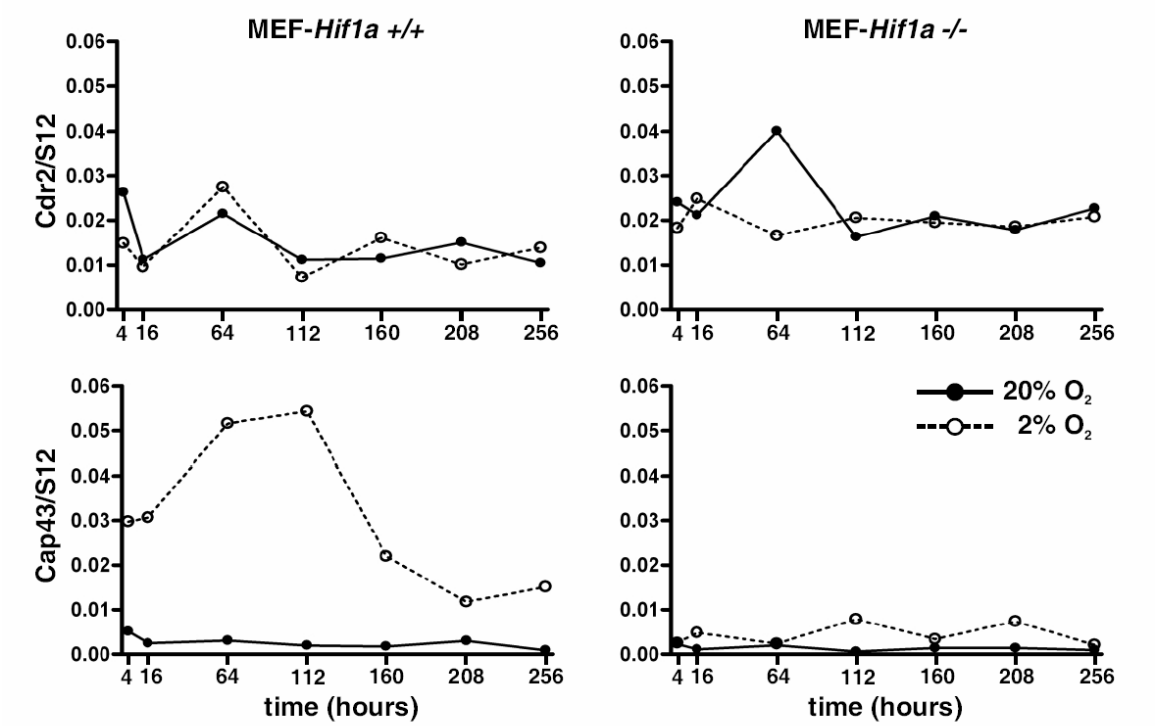

Figure 22: Cdr2 gene expression is not regulated by HIF-1α. *MEF-HIF-1a +/+ and MEF-HIF-1a -/- cells were cultured either at 20% or 2% oxygen for 4 to 256 hours. Cdr2 and CAP43 mRNA levels were quantified by realt-time quantitative PCR and normalized to S12 mRNA levels.*

PHD-dependent Cdr2 protein stabilization in transient transfection assays

To investigate a possible PHD-dependent regulation of Cdr2 protein stability, we transfected HeLa cells with a V5-tagged Cdr2 expression vector. Transient transfection assays were used, because no anti-Cdr2 antibodies were commercially available at this time. After transfection, the cells were split and incubated either under normoxic or hypoxic conditions, or treated with the PHD inhibitors desferrioxamine (DFX) or DMOG. Whereas Cdr2 protein levels were barely detectable by immunoblotting in normoxia, a strong increase was observed in hypoxia or after DFX or DMOG treatment. Transfected HIF-1α and ARNT served as positive and negative control, respectively (Fig. 23A). Similar results were reproduced in MCF7 breast cancer cells (Fig. 23B). This data suggest that Cdr2 protein levels are regulated in a PHD-dependent manner.

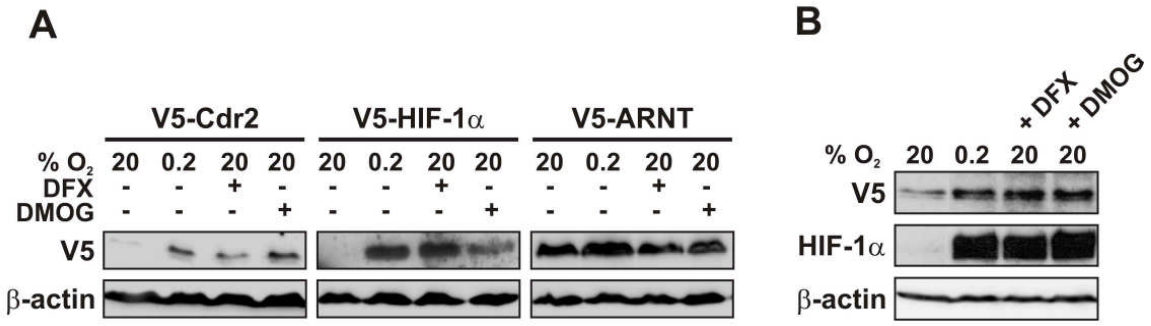

Figure 23: Stabilization of Cdr2 protein in hypoxia and after PHD inhibition*. Total cell extracts of Hela (**A**) and MCF7 (**B**) cells, transfected with V5-Cdr2, V5-HIF-1α or V5-ARNT and incubated under the indicated conditions, were analysed for V5-fusion, endogenous HIF-1α and β-actin protein levels by immunoblotting.*

Proteasomal regulation of V5-Cdr2

The proteolytic regulation of Cdr2 is not known and we analysed whether proteasomal pathways, as for HIF-α subunits, are involved. Therefore, HeLa and MCF7 cells were transiently transfected with V5-tagged Cdr2 and cultured in the presence of the proteasomal inhibitor MG132 (5 μM). As shown in Figure 24, V5-Cdr2 protein stabilization was already observed after 30 minutes in HeLa and 15 minutes in MCF7 cells (Fig. 24A and B), suggesting that Cdr2 protein destruction is regulated by proteasomal pathways. Determination of endogenous HIF-1α protein levels served as positive control.

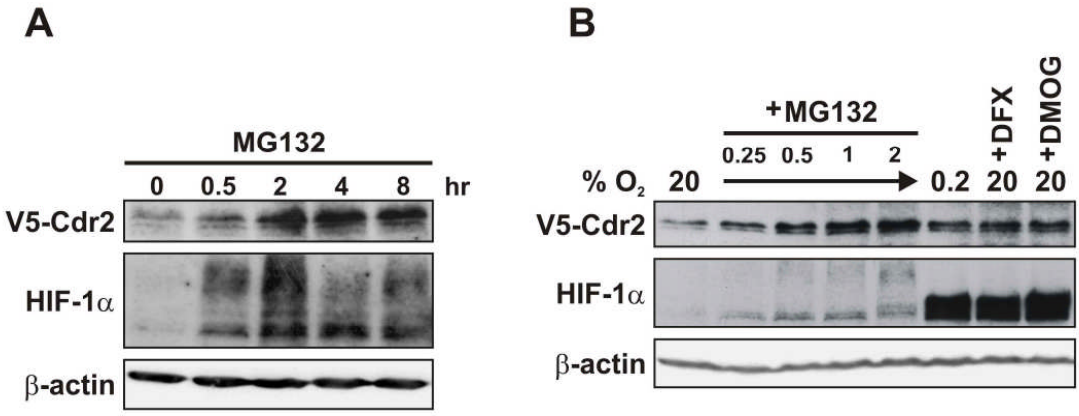

Figure 24: Stabilization of Cdr2 after proteasomal inhibition*. HeLa (**A**) and MCF7 (**B**) cells were transiently transfected with V5-Cdr2 and treated with MG132 (5 μM), DFX (100 μM) or DMOG (2 mM). Transfected V5-Cdr2, endogenous HIF-1α and β-actin levels were determined by immunoblotting.*

Cdr2 shows no transactivation activity

In 1991, Fathallah-Shaykh *et al.* suggested that Cdr2 might be involved in the regulation of gene expression based on its predicted structure, which contains leucine-zipper and zinc-finger motifs (Fathallah-Shaykh *et al.* 1991). Takanaga *et al.* reported that PKN, a fatty acid-activated serine/threonine protein kinase, is an interactor of Cdr2 (Takanaga *et al.* 1998). They fused Cdr2 to the Gal4 DNA-binding domain (Gal4BD) and co-transfected C6 cells with Gal4BD-Cdr2 and the reporter gene plasmid pG5CAT, which contains 5 Gal4 binding sites and a minimal promoter linked to the chloramphenicol acetyltransferase (CAT) gene. Surprisingly, determination of CAT activity showed transcriptional activation when Cdr2 was fused to Gal4BD. Previously, Cdr2 was also reported to be a cytoplasmic protein and no nuclear targeting sequence was identified. To confirm or disprove Cdr2 transactivation activity, we cloned Gal4BD-Cdr2 and transiently co-transfected HeLa cells together with the Gal4 firefly luciferase reporter vector pGRE5xE1b and the renilla luciferase control vector pRL-SV40. The C-terminal part of the oxygen-dependent degradation domain of HIF-1α (amino acid 526-603), cloned between the Gal4BD and the VP16 activation domain (VP16AD), and pGRE5xE1b alone was used as positive and negative control, respectively. Whereas the positive control was induced 3.5x fold after PHD inhibition, no Cdr2 transactivation activity could be measured under normoxic conditions or after DMOG treatment (Fig. 25).

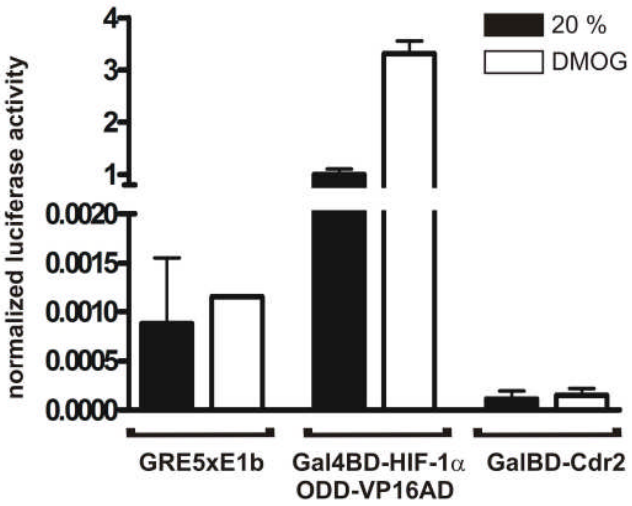

Figure 25: Cdr2 possesses no transactivation activity. *HeLa cells were transiently transfected with Gal4BD-HIF-1α-526-603-VP16AD or Gal4BD-Cdr2 expression vectors, Gal4*

response element-driven firefly luciferase reporter pGRE5xE1b as well as a renilla luciferase control vector. After transfection, cells were cultivated under normoxic conditions in the presence or absence of 2 mM DMOG. Firefly luciferase activities were determined and corrected for renilla luciferase activity and normalized to the normoxic positive control which was arbitrarily defined as 1. Results are mean values of relative luciferase activities ± SEM of 2 independent experiments performed in triplicates.

Mapping the interaction site of Cdr2 and PHD1

The interaction of Cdr2 and PHD1 in yeast and *in vitro* as well as the PHD-dependent stabilization of transfected Cdr2 suggested that Cdr2 could be regulated by PHD1-dependent prolyl-4-hydroxylation. To narrow down the interaction and/or hydroxylation sites of Cdr2, we cloned Cdr2 deletion fragments by using restriction enzyme-mediated cloning and multiple amino acid PCR deletions as depicted in Figure 26. Two proline clusters, amino acid 265-314 and 410-454, were identified and also deleted.

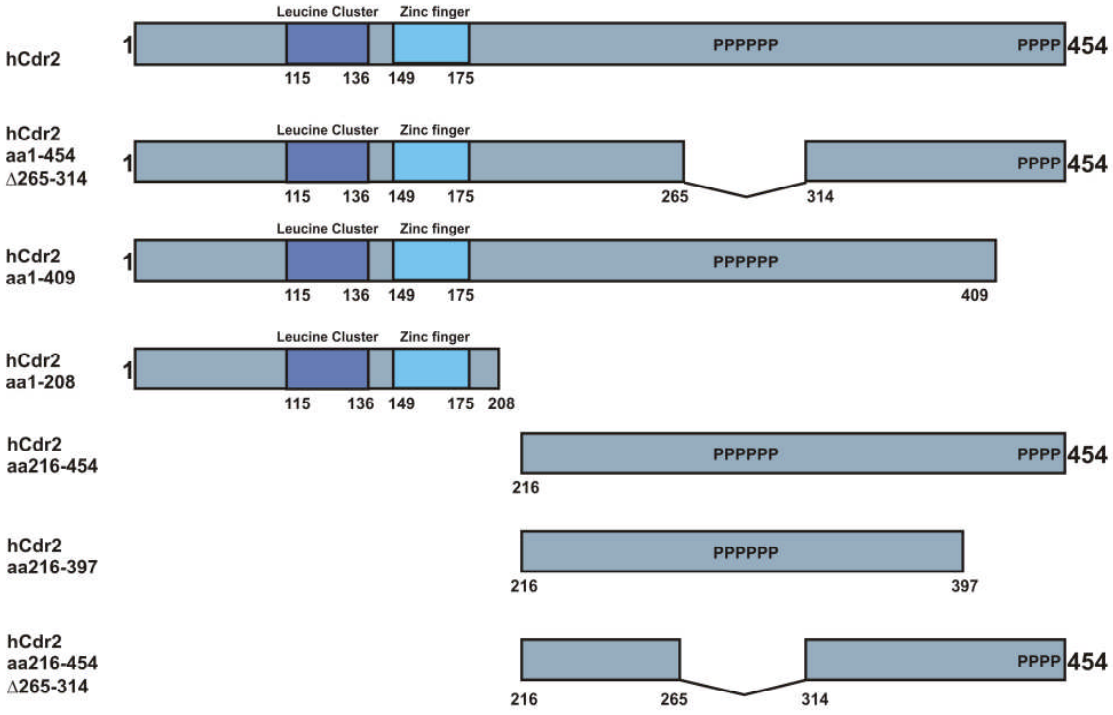

Figure 26: Schematic representation of the predicted Cdr2 domain architecture and cloned fragments thereof. *The leucine cluster, the zinc finger domain and the two conserved proline clusters (P) are indicated.*

To identify the interaction domain in Cdr2 with PHD1, a yeast two-hybrid assay was carried out. Interaction with PHD1 was observed for full length Cdr2 (aa1-454), proline cluster I (aa1-454Δ265-314) and proline cluster II (aa1-409) deletions as well as a fragment (aa1-208) (Fig. 27 and Table 29). No interaction was determined with fragments lacking the first 215 amino acids. Interestingly, the extended N-terminal fragment (aa1-409), including the leucine cluster as well as the zinc finger domain, showed a much stronger interaction compared to the fragment (aa1-208). Of note, the interacting Cdr2 fragment cloned in the human testis, Matchmaker/Dualsystems human cDNA library screening (aa216-454) could not be confirmed in this assay.

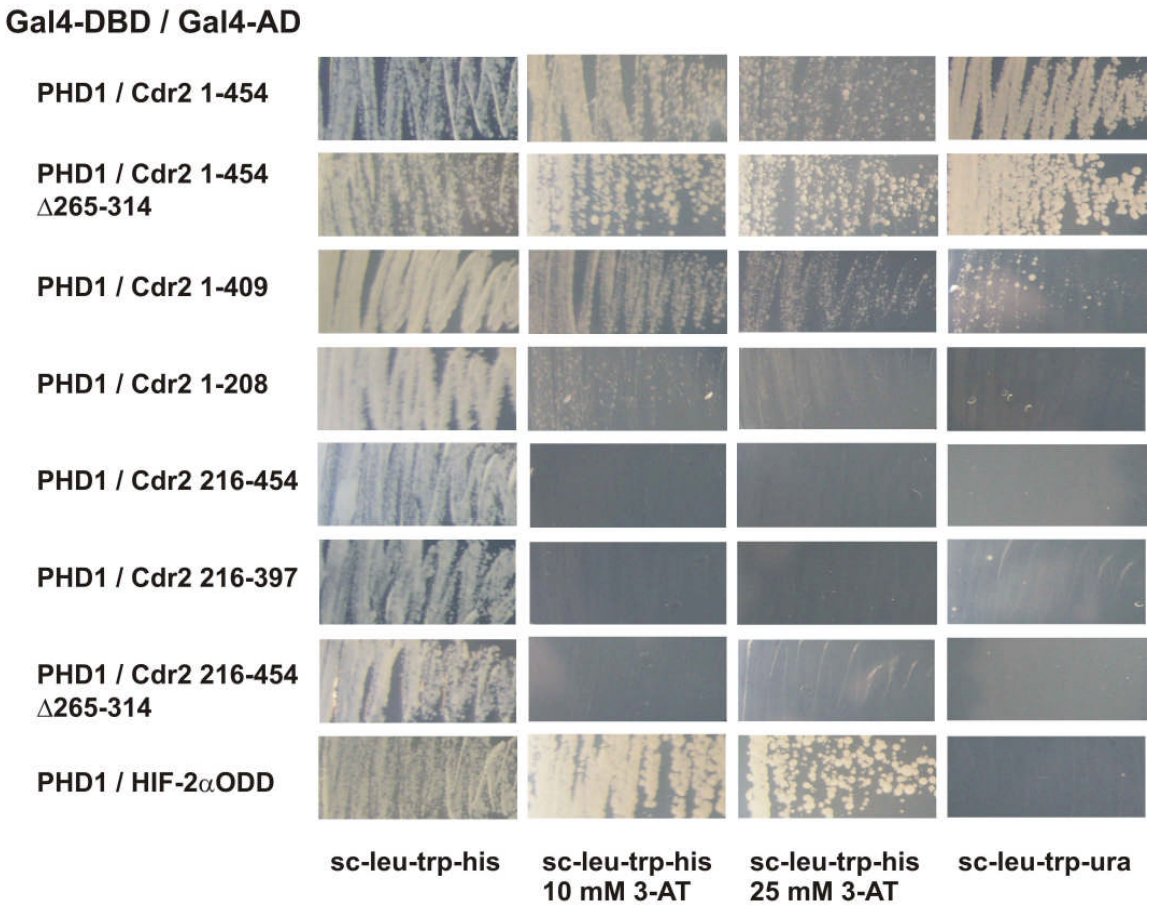

Figure 27: Interaction of PHD1 and Cdr2 fragments in yeast
Yeast reporter strain Mav203 expressing Gal4DB-PHD1 was transformed with the indicated Gal4AD-Cdr2 constructs and subsequently assayed for histidine and uracil auxotrophy.

Cdr2 constructs	histidine auxotrophy growth	uracil auxotrophy growth
hCdr2 1-454	25 mM 3-AT	++
hCdr2 1-454 Δ265-314	25 mM 3-AT	++
hCdr2 1-409	25 mM 3-AT	+
hCdr2 1-208	10 mM 3-AT	-
hCdr2 216-454	No growth	-
hCdr2 216-397	No growth	-
hCdr2 216-454 Δ265-314	No growth	-
Control HIF-2αODD	25 mM 3-AT	-

Table 29: Interaction of PHD1 and Cdr2 fragments in yeast. *Yeast reporter strain Mav203 expressing Gal4DB-PHD1 was transformed with the indicated Gal4AD-Cdr2 constructs and subsequently assayed for histidine and uracil auxotrophy.*

Generation of polyclonal anti-Cdr2 antibodies

To generate polyclonal anti-Cdr2 antibodies, rabbits were immunized with the synthetic peptide PEYKALFKEIFSCIK derived from the conserved C-terminal part of Cdr2 (aa420-434). Pre-immune, immune and affinity-purified immune sera were obtained and used for detection of recombinant as well as transfected Cdr2 by immunoblotting (Fig. 28). Pre-immune serum did not cross-react with recombinant Cdr2 (Fig. 28A) and only detected nonspecific bands in total lysates from HeLa cells (Fig. 28B). As demonstrated previously, transfected Cdr2 protein levels were induced by hypoxia or after DMOG treatment (Fig. 28B).

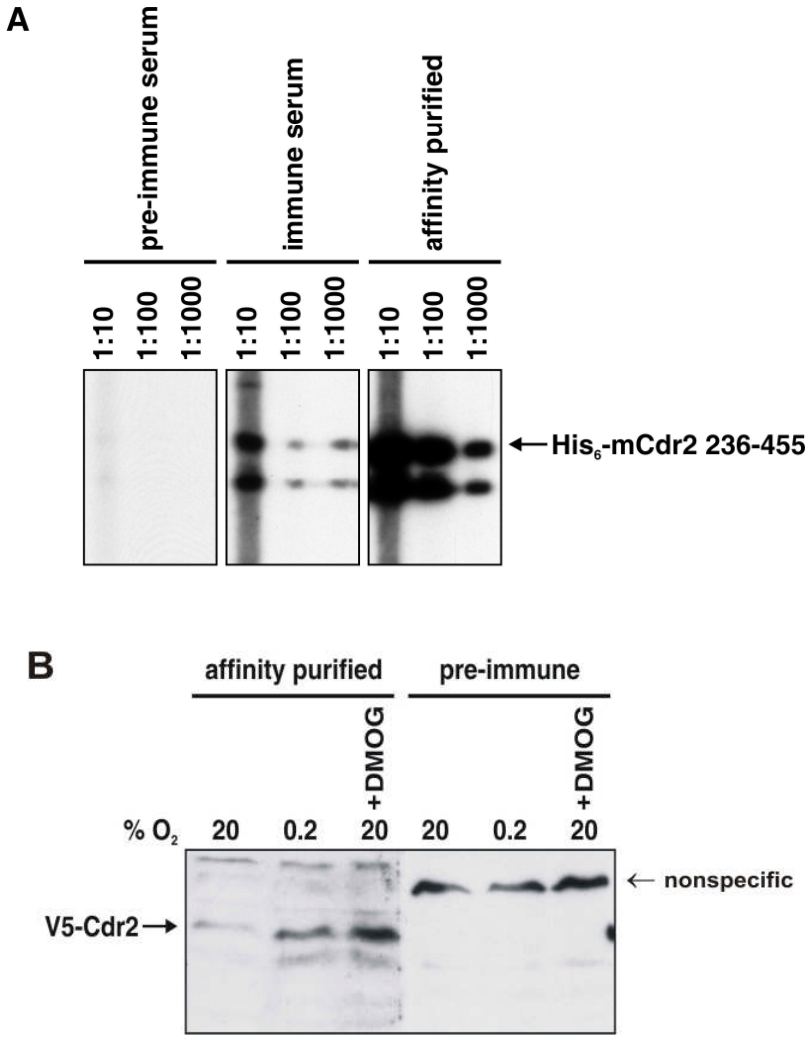

Figure 28: Polyclonal anti-Cdr2 antibodies recognize recombinant as well as transfected Cdr2. A, *Recombinant Cdr2 (aa236-455) was detected by immune- and affinity-purified immune serum but not by pre-immune serum.* ***B,*** *HeLa cells were transfected with V5-Cdr2 and cultivated under normoxic or hypoxic conditions or treated with 2 mM DMOG. Subsequently, total cell extracts were resolved by SDS-PAGE, blotted onto nitrocellulose membranes and incubated with pre-immune or affinity-purified immune serum from rabbits immunized with Cdr2-derived peptides.*

Unfortunately, although polyclonal anti-Cdr2 antibodies were able to detect overexpressed Cdr2, no detection of endogenous Cdr2 was observed in several cell lines (data not shown).

Generation of monoclonal anti-Cdr2 antibodies

Monoclonal antibodies were generated in cooperation with René Fischer (ETH Zürich). Recombinant MBP-Cdr2 was expressed in *E. coli*, purified and used for immunization of mice (Fig. 29). Therefore, MBP-Cdr2 was injected subcutaneously into mice and isolated splenocytes were fused with myeloma cells. Supernatants from the hybridoma cell lines were screened for the presence of specific anti-Cdr2 antibodies by enzyme-linked immunosorbent assay (ELISA). Hybridoma clone #33 was further tested by immunoblotting and detected recombinant MBP-Cdr2 as well as overexpressed V5-Cdr2 (Fig. 30).

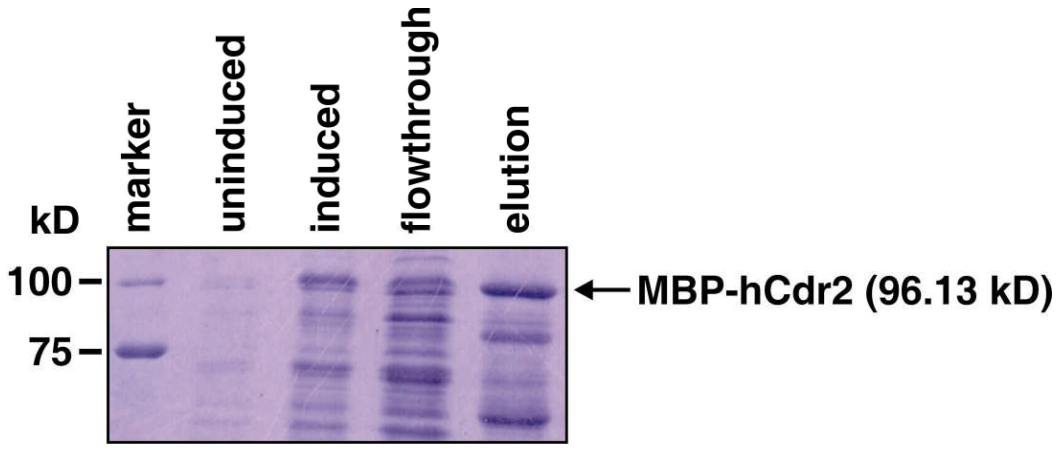

Figure 29: Bacterial expression and purification of recombinant MBP-hCdr2. *Expression of MBP-hCdr2 was induced in E. coli (TB1) with 0.2 mM isopropyl thiogalactoside (IPTG) for 4 hours at 37°C and affinity purified with an amylose-coated matrix (NEB). Indicated fractions were resolved by SDS-PAGE and the gel coomassie stained.*

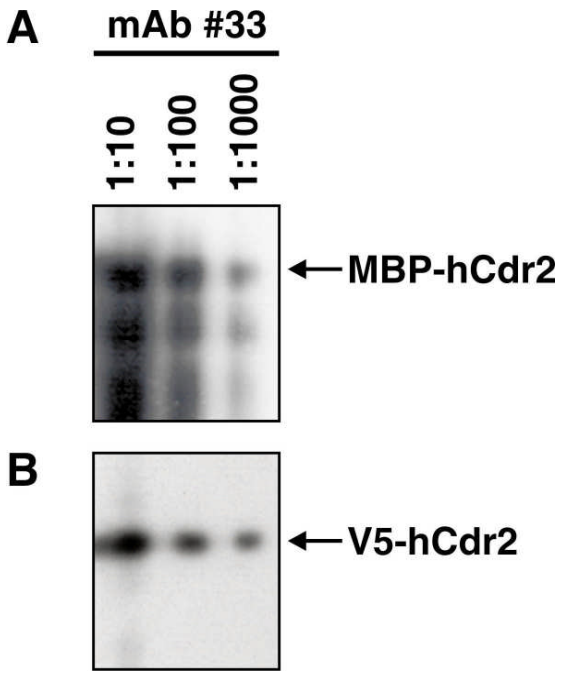

Figure 30: Hybridoma supernatant #33 contains specific anti-Cdr2 antibodies. *Recombinant MBP-hCdr2 (A) or cell extracts from transiently transfected HeLa cells (B) were analyzed by immunoblotting with the indicated dilutions of the hybridoma supernatant #33.*

Monoclonal antibodies specifically recognize hCdr2 but not mCdr2 and hCdr3

Cdr2 and Cdr3 show a 44% homology in their protein sequences. We wanted to exclude a recognizition of hCdr3 by monoclonal anti-Cdr2 antibodies and to investigate if anti-Cdr2 #33 crossreacts with mCdr2. Therefore, V5-tagged hCdr2, mCdr2 and hCdr3 were transcribed and translated *in vitro* (IVTT) and immunoblotted. We showed that hybridoma supernatant #33 only recognizes hCdr2 IVTT but not mCdr2 IVTT and hCdr3 IVTT (Fig. 31).

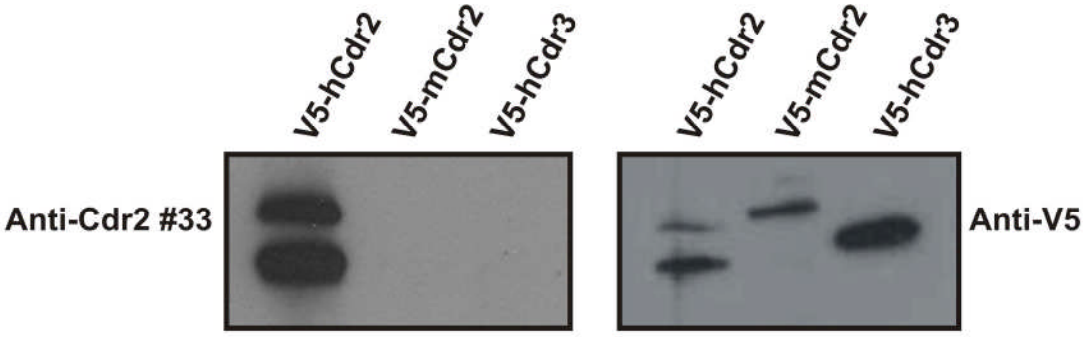

Figure 31: Monoclonal antibodies specifically recognize hCdr2
V5-tagged hCdr2, mCdr2 and hCdr3 were transcribed and translated in vitro and analyzed by immunoblotting with the hybridoma supernatant #33 or with anti-V5 antibodies.

No stabilization of endogenous Cdr2 in hypoxia and upon PHD inhibition

After generation of monoclonal anti-Cdr2 antibodies we investigated the stabilization of endogenous Cdr2 in several cell lines. The ovarian carcinoma cell line SKOV3 showed the highest expression for Cdr2. Cells were incubated for indicated time durations in normoxia or hypoxia or treated with 1 mM DMOG, respectively. In comparison to transient transfected V5-Cdr2, endogenous Cdr2 was very weakly stabilized after 4 up to 72 hours under hypoxia and DMOG treatment (Fig. 32).

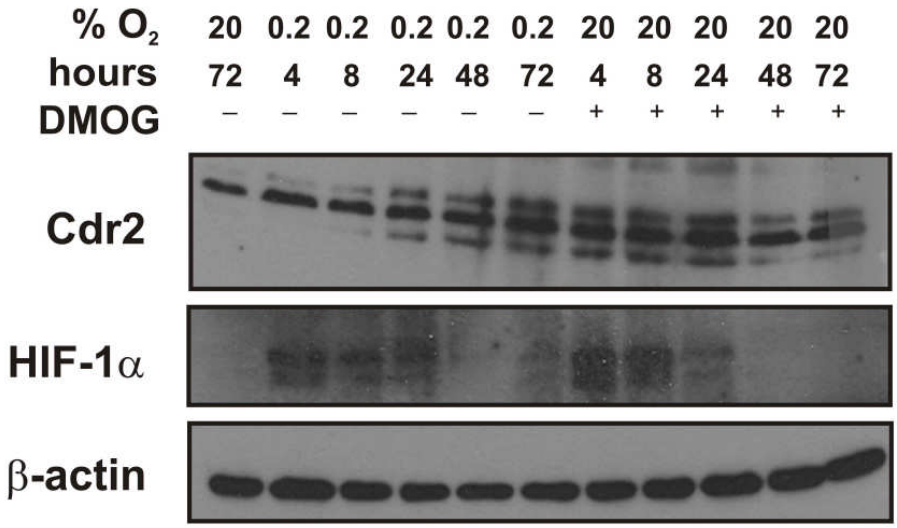

Figure 32: Endogenous Cdr2 is weakly stabilized under hypoxia and PHD inhibition.
SKOV3 cells were incubated for indicated time durations at 20% or 0.2 % oxygen or treated with 1 mM DMOG.

Unfortunately, we were not able to reproduce these data in SKOV3 cells (Fig. 33) and observed no stabilization in any other examined ovarian or breast cancer cell line (data not shown). Further experiments such as preincubation of SKOV3 in FCS-charcoal-stripped medium before treatment could not reconstitute a hypoxic stabilization (data not shown).

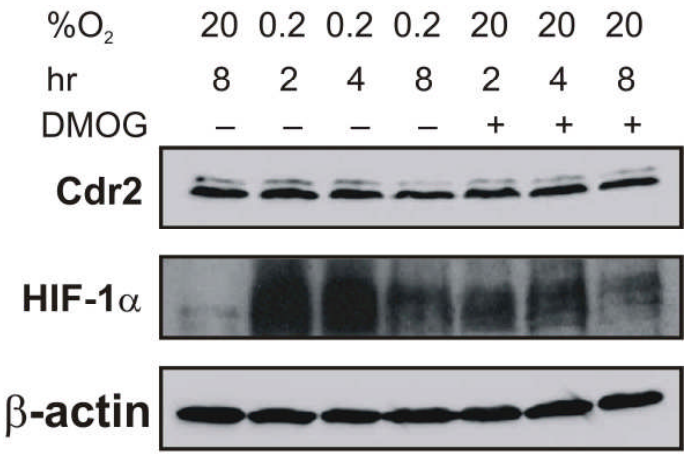

Figure 33: No stabilization of endogenous Cdr2 under hypoxia and PHD inhibition
SKOV3 cells were incubated at either 20% or 0.2% oxygen or in the presence of 1 mM DMOG for the indicated time durations. Cell lysates were immunoblotted and analyzed with anti-Cdr2, anti-HIF-1α and β-actin antibodies.

Increased PHD1 protein levels do not decrease Cdr2 protein levels

Recently, several reports showed that PHD1 mRNA is inducible upon estrogen treatment (Seth *et al*. 2002; Tian *et al*. 2006). In line with these results we investigated Cdr2 protein in estradiol treated BT474 cells. Before treatment cells were incubated for four days in FCS-charcoal-stripped medium (5%). Cells were then incubated for 48 hours without or with 24 respectively 48 hours 20 ng/ml 17-β-estradiol. An increase of PHD1 protein was observed, whereas Cdr2 protein level stayed unchanged (Fig. 34).

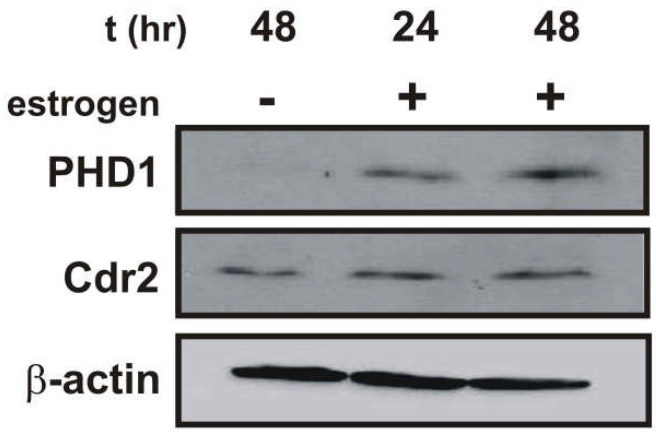

Figure 34: Increased PHD1 protein levels upon estrogen treatment do not alter Cdr2 protein levels. *BT474 cells were incubated with or without 17-β-estradiol for the indicated time durations. Cell lysates were analyzed by immunoblotting with the indicated antibodies.*

Subcellular localization of Cdr2

Immunohistochemical analysis of cerebellar sections and ovarian tumors of PCD patients as well as rat Purkinje cells with PCD antisera showed mainly cytoplasmic staining (Corradi *et al.* 1997; Okano *et al.* 1999). To analyze the subcellular localization of Cdr2, we cultured SKOV3 cells under normoxic or hypoxic conditions or in the presence of DMOG and performed immunofluoresence experiments (Fig. 35).

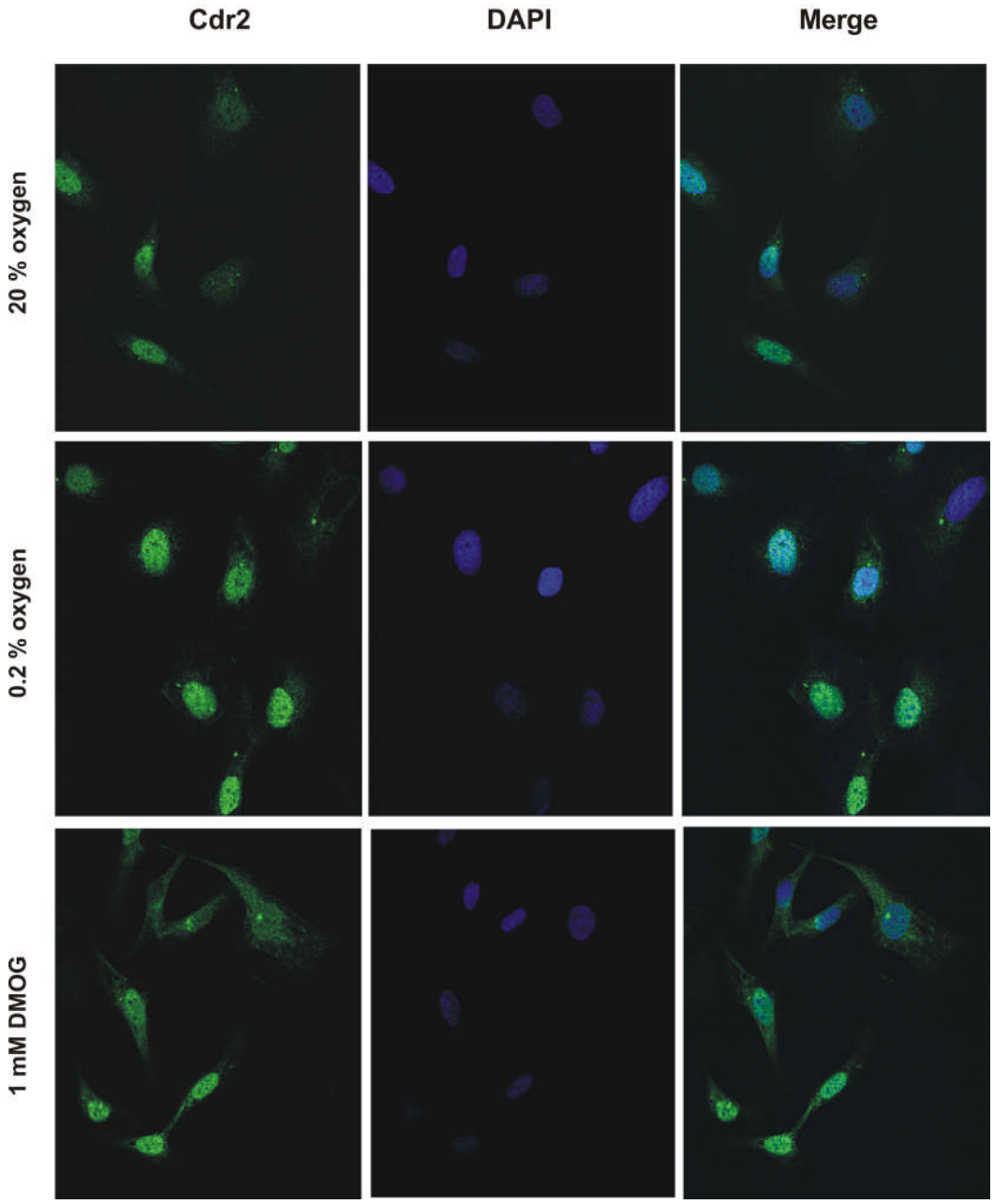

Figure 35: Cdr2 localizes to the nucleus in SKOV3 cells. *Cells were grown on coverslips and incubated for 16 hours at either 20% or 0.2% oxygen or in the presence of 1 mM DMOG. Cells were fixed and indirect confocal immunofluorescence microscopy using anti-Cdr2 primary and anti-mouse Alexa488-coupled secondary antibodies was performed. Nuclei were counterstained with DAPI.*

Surprisingly, Cdr2 was predominantly found in the nucleus and not in the cytoplasm. These data were confirmed in HeLa cells (data not shown). However, no change in the localization of Cdr2 was observed in hypoxia or after DMOG treatment compared to the normoxic control conditions.

Discussion

Interaction of Cdr2 and PHD1 in yeast

Cdr2 but not Cdr3 interacts with PHD1 in yeast

Cdr2 mRNA is known to be ubiquitously expressed whereas the protein is under physiological conditions limited to the brain (cerebellum / Purkinje neurons) and the testis, both tissues with relatively low pO_2. Whereas the anti-Yo antibody of PCD patients is able to detect all three isoforms, Cdr1 (34 kDa), Cdr2 (52 kDa) and Cdr3 (62 kDa) in normal brain and testis, only Cdr2 mRNA and protein was found in ovary or breast tumors of these patients. These findings suggested a major role of Cdr2 as tumor antigen in PCD (Corradi *et al.* 1997). Our results showed no interaction of Cdr3 with PHD1 in yeast (data not shown) and in contrast to Cdr2, Cdr3 showed no hypoxic stabilization when overexpressed in HeLa cells (data not shown). These data suggest that PHD1 interacts specifically with Cdr2. Importantly, our monoclonal antibodies derived from hybridoma clone #33 were specific for Cdr2 and did not recognize IVTT-produced Cdr3 (data not shown).

Expression pattern of Cdr2 protein

Cdr2 mRNA is ubiquitously expressed whereas the protein is under physiological conditions limited to tissues with low oxygen partial pressure

Determination of tissue pO_2 levels is technically challenging. However, different measurement techniques resulted in comparable values and indicated that there are wide variations in tissue pO_2 levels in all organs examined (Vanderkooi *et al.* 1991). Tissue pO_2 values are in general considerable lower than those in mixed venous blood. The cellular demand for oxygen varies among different tissues largely due to variations in energy requirement. Whereas the lung represents the organ with the highest pO_2 of around 100 mm Hg the brain shows a wider spectrum ranging from 1-3 mm Hg (pons) to 6-16 mm Hg (cortex) (Vanderkooi *et al.* 1991). Different assumptions exist why the brain is considered as a tissue with regions of low pO_2 levels. Even the brain has a high heterogeneity, diverse

tissues with different oxygen needs (ATP need), in general it has a high oxygen consumption. In 2001, Stroka *et al*. showed by immunohistochemistry that HIF-1α is present in normal mouse brain in the nucleus under normoxic conditions (Stroka *et al.* 2001). They suggested that HIF-1 may be present in normal tissue for a basal induction of genes that are necessary to provide the cellular energy requirements. In addition to the brain, the testis is also considered as an organ with low pO_2 levels due to its anatomy and high oxygen consumption. Within the testis blood vessels are found exclusively between the tubuli and oxygen reaches the lumen of the tubuli seminiferi only by diffusion. The process of spermatogenesis occurs along the pO_2 gradient in the seminiferi tubuli. In consideration of the high sperm production rate, spermatogonial self-renewal is likely to consume high amounts of oxygen. Due to this two facts luminal pO_2 levels are likely to be very low (Wenger and Katschinski 2005). Indeed, pO_2 values as low as 2 mm Hg have been reported, which are among the lowest values found in the body (Max 1992).

Our results demonstrate that Cdr2 is expressed ubiquitously with high mRNA levels in the testis and the brain. Additionally, we showed that Cdr2 mRNA is not regulated by oxygen, whereas the protein is stabilized under hypoxia in transient transfections. These findings might explain the limited expression of Cdr2 protein in the brain and testis. In contrast to our expectations we could not reproduce a stabilization of endogenous Cdr2 in hypoxia or upon PHD inhibition in the tumor cell line SKOV3. The effect what we have seen with transfected Cdr2 is still an enigma. Genetic modifications of the Cdr2 locus in SKOV3 cells might represent one reason for loss of stability under hypoxia and PHD inhibition. One further approach is the inducibility of PHD1 by estrogen which was shown in BT474 cells. Cdr2 expression is thought to be limited to gynecological tumors which are estrogen-dependent tissues. It might be that Cdr2 protein in estrogen sensitive tissue undergoes no stabilization due to high expression of PHD1. So far, it is not clear if Cdr2 is expressed in other tumors which underlie no hormonal influence or estrogen influence, respectively and if stabilization of Cdr2 can be observed in these tissues.

Cdr2 protein expressed in tumor tissues functions as onconeural antigen

Low oxygen partial pressure is a characteristic of all solid tumors. It is now well established that most tumors have lower median oxygen partial pressure than their tissues of origin. Microelectrode oxygen measurements revealed that the mean oxygen tension of normal tissue lies between 40 – 50 mm Hg, whereas tumors reach values between 5 and 10 mm Hg or even lower (Vaupel *et al.* 1989). In addition, clinical studies show that in many cases invasive growth and metastatic spread are associated with the degree of tumor hypoxia. Explanations for tumor hypoxia are primitive and unstructured tumor microcirculation and high oxygen consumption due to rapidly growing tumor cells. Neoplastic vascularization occurs uncoordinatedly, resulting in functionally poor vasculature incapable of meeting tumor demands for oxygen, thereby giving rise to hypoxic areas within tumors. The cellular responses to hypoxia to improve cell oxygenation and survival are angiogenesis, improved glycolytic flux enhancing energy production and an upregulation of molecules related to cell survival and apoptosis. HIF activation is seen throughout tumors and is likely to explain the marked vascularity and high level of expression of glycolytic genes (Semenza 2003). Usually, tumor hypoxia occurs at a distance farther than 100 – 200 μm from blood vessels and cells which are not able to adapt to oxygen and nutrient deprivation finally undergo cell death by apoptosis and / or necrosis (Zhou *et al.* 2006). Figure 36 shows tumor hypoxia and its consequences on a molecular level.

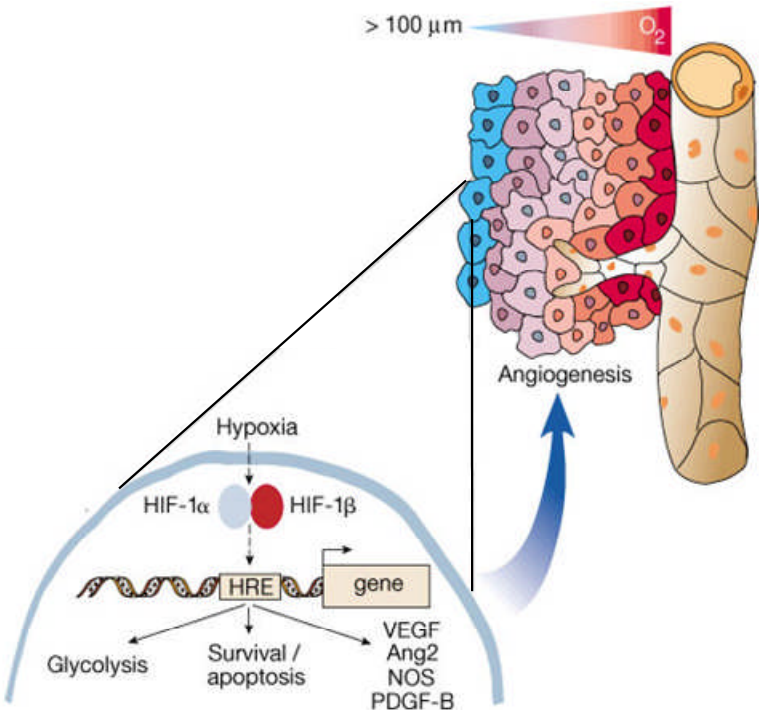

Figure 36: Uncoordinated neoplastic vascularization in tumors resulting in functionally poor vasculature incapable of meeting tumor demands of oxygen *(Carmeliet and Jain 2000). Some tumor cells are due to the uncoordinated neoplastic vascularization located more than 100 µm (diffusion limit for oxygen) away from blood vessels (red-to-blue gradient indicates progressive hypoxia). These cells become hypoxic and HIF stabilization leads to upregulation of genes involved in angiogenesis (i.e. VEGF, Ang2, NOS and PDGF-B), to improved glycolytic flux and upregulation of molecules related to cell survival and apoptosis.*

Furthermore, hypoxia can also affect tumor growth positively by local adaptation. Graeber *et al.* showed that hypoxia represents a physiological selective pressure in tumor tissue. On one hand hypoxic conditions induce apoptosis in tumor cells but on the other hand it induces genetic alterations, for example loss of the *p53* tumor-suppressor gene or overexpression of Bcl-2, an apoptosis-inhibitor protein, and thereby decreases hypoxia-induced cell death. Additionally, these hypoxic conditions select for cells with defects in apoptosis (Graeber *et al.* 1996). The consequence is often a more aggressive tumor phenotype in combination with chemoresistance (Unruh *et al.* 2003). One example for local hypoxic adaptation is increased anaerobic glycolysis which is facilitated by increased expression of glucose transporters and glycolytic enzymes and induced angiogenesis. Hypoxia seems to be able to induce pro- and anti-apoptotic cellular mechanism and particularly the impact of HIF-1 is still not elucidated (Zhou *et al.* 2006). Figure 37 summarizes HIF-1 dependent and HIF-1 independent responses towards survival or cell death.

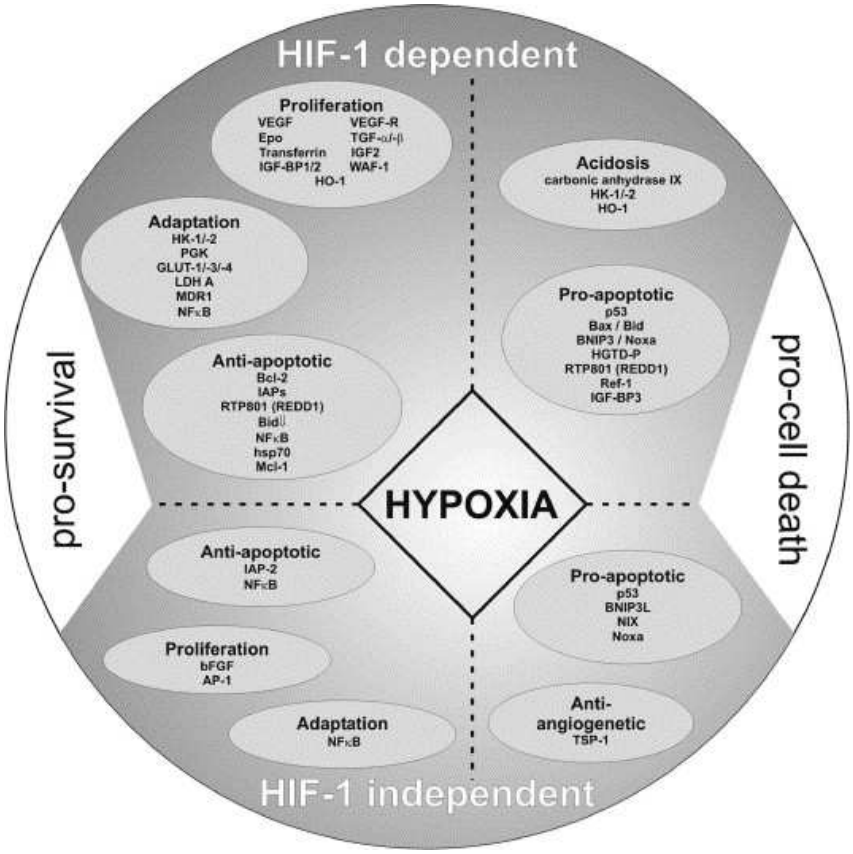

Figure 37: Pro-survival and pro-apoptotic mechanisms as response to hypoxia in tumor cells *(Zhou et al. 2006) Abbreviations: AP-1: activator protein-1; bFGF: basic fibroblast growth factor; BNIP3: Bcl-2/adenovirus E1B 19 kDa interacting protein 3; BNIP3L: Bcl-2 19 kDa interacting protein like; Epo: erythropoietin; GLUT-1/-3/-4: glucose transporter-1/-3/-4; HK-1/-2: hexokinase-1/-2; HO-1: heme oxygenase-1; hsp70: heat shock protein 70; IAPs: inhibitors of apoptosis; IGF2: insulin-like growth factor; IGF-BP1/2/3: IGF-factor-binding protein 1/2/3; LDH A: lactate dehydrogenase A; Mcl-1: myeloid cell factor-1; MDR1: multidrug resistance 1; NFκB: nuclear factor κB; NIX: Nip3-like protein X; NOXA: NADPH oxidase activator; PGK-1: phosphoglycerate kinase 1; TGF-α/-β: transforming growth factor-α/-β; TSP-1: thrombospondin-1; VEGF: vascular endothelial growth factor; VEGF-R: VEGF-receptor*

Cdr2 is found mainly on the surface of ovarian and breast tumors. It is important to mention that Cdr2 is not limited to PND connected tumors, but is found in 60% of ovarian and more than 25% of all breast cancer tumors. Interestingly, Cdr2 expression in tumors does not always lead to PCD (Peterson *et al.* 1992). It is unclear under which conditions the antigen is targeted by the immune system. Additionally, studies with the antigen Hu showed that the antibody production and antibody titer in patients was correlated with the onset of PND (Dalmau *et al.* 1990). We showed that overexpressed Cdr2 is stabilized in HeLa and MCF-7 cells in hypoxia and after PHD inhibition. Therefore, tumor hypoxia

might be the trigger for Cdr2 protein stabilization in tumor tissues resulting from reduced PHD1 hydroxylation activity.

In the proposed pathogenesis and mechanism of paraneoplastic cerebellar degeneration it is thought that apoptotic tumor cells are internalized by tissue dendritic cells. Apoptosis of tumor cells is assumed to be due to excessive signaling in cell-cycle and DNA-repair pathways. Our findings that Cdr2 interacts with PHD1 and the hypoxic stabilization of transfected Cdr2 protein suggest that tumor cells might undergo apoptosis due to hypoxia and glucose deprivation. Hypoxia might be one trigger for apoptosis of tumor cells and stabilization of Cdr2 and thereby internalization of tumor cells via dendritic cells. It is still unclear if Cdr2 is also directly involved in apoptosis of tumor cells. So far, it has not been shown that expression of Cdr2 in tumor cells is involved in the recognition of apoptotic tumor cells by tissue dendritic cells.

Hydroxylations sites of Cdr2

The LXXLAP PHD hydroxylation site in HIF-α is highly conserved. Our database search revealed no conserved LAP motif for Cdr2. Nevertheless, a recent publication of Li *et al.* showed amino acid substitutions in a HIF-1α peptide caused only minor changes in its hydroxylation. Alanine was the strictest requirement for hydroxylation and no other amino acids was able to fully substitute for it in case of PHD2, whereas in case of PHD1 and PHD3 it could only be substituted by serine or isoleucine or valine and serine (Li *et al.* 2004). These data were confirmed independently (Huang *et al.* 2002; Hirsilä *et al.* 2003). Cdr2 contains two conserved proline cluster in the C-terminal amino acid sequence. We carried out multiple amino acid deletions to generate constructs which contain either a single or no proline cluster. Cdr2 fragments including only the N-terminal part of the zinc finger domain show a much weaker interaction with PHD1 in yeast suggesting that the zinc finger is necessary for interaction. No interaction was observed with the C-terminal part of Cdr2 including two conserved proline cluster. In contrast, the C-terminal part 216-454 was found as interactor in the yeast two-hybrid screening. These data suggest that Cdr2 binds with its N-terminal part to PHD1 whereas the hydroxylation site is still unclear. Furthermore, we expressed and purified these sequences in bacterial

expression systems to analyze these recombinant proteins in hydroxylation assays and by mass spectrometry.

Subcellular localization of Cdr2

In contrast to previous reports, we detected endogenous Cdr2 predominantly in the nucleus of different cell lines rather than in the cytoplasm. This finding is contradictive to previous immunohistochemical localization data of Cdr2 in the cytoplasm (Corradi *et al.* 1997; Okano *et al.* 1999). Okano *et al.* suggested that Cdr2 sequesters c-Myc in the cytoplasm and thereby regulates c-Myc dependent transactivation of target genes. We investigated whether hypoxia might trigger a change in the subcellular localization of Cdr2. But no change of Cdr2 was observed when cells were incubated under hypoxic conditions or after DMOG treatment. PHD1 was found exclusively in the nucleus when fused to GFP (Metzen *et al.* 2003) whereas endogenous PHD1 was shown to be localized in the cytoplasm and nucleus (Soilleux *et al.* 2005).

IκB kinase-β (IKKβ) is a hydroxylation target of PHD1

The transcription factor NFκB is involved in promotion and progression of tumor development and survival (Karin and Greten 2005). Several pro-inflammatory cytokines and chemokines, such as TNF, IL-1 and IL-6 are target genes of the IKK-β-dependent NFκB-activation pathway and are known to be associated with tumor development and progression. Two different pathways of distinct NFκB-activation, the classical and the alternative pathway, are distinguished. Both pathways are involved in tumor development but the recent knowledge suggests that the pro-carcinogenic function is mostly related to the classical pathway. Figure 38 shows the classical activation pathway of NFκB and its target genes (Karin and Greten 2005). This pathway is triggered by infections, bacterial or viral, as well by pro-inflammatory cytokines. First, the IKK complex is activated, when pro-inflammatory cytokines, bacterial cell-wall components or viruses are binding to the cellular receptor. The IKK complex consists of two catalytic subunits, IKK-α and IKK-β and a regulatory subunit, IKK-γ (NEMO). The IKK complex is able to phosphorylate NFκB-bound IκBs which leads to a proteasomal degradation of IκB and thereby a liberation of NFκB dimers,

composed of REL-A (p65) and p50. Now, the transcription factor is able to enter the nucleus and to induce its target genes involved in inflammation, innate immunity and cell survival.

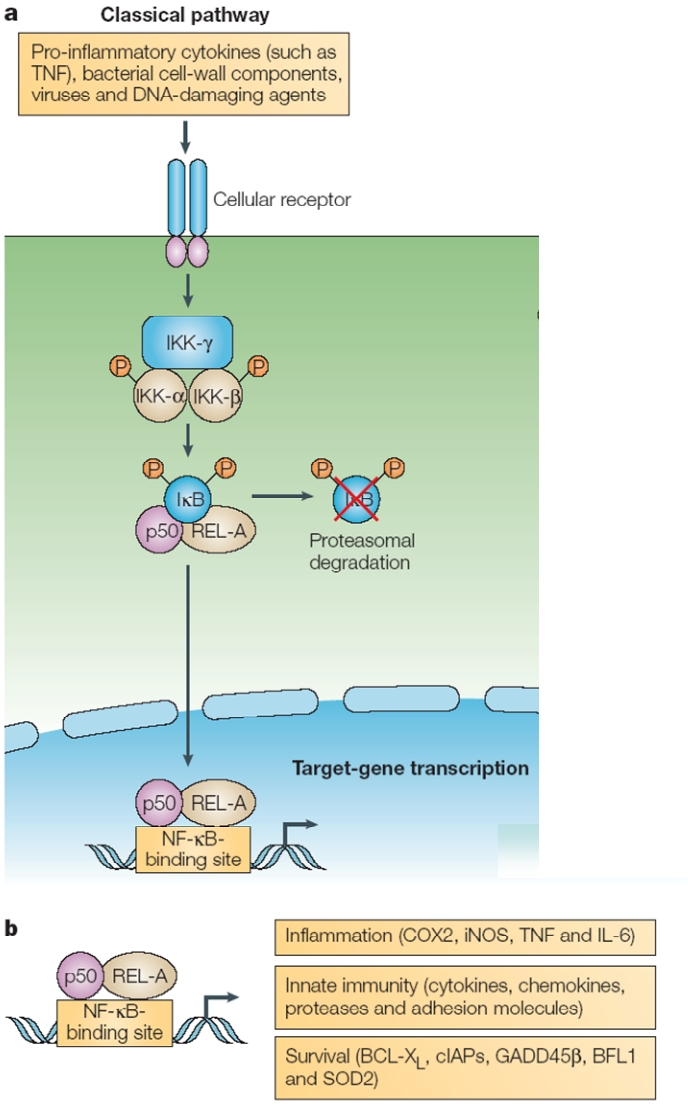

Figure 38: Classical signaling pathway of NFκB *modified from (Karin and Greten 2005) NFκB dimers consisting of p50 and REL-A are bound in the cytoplasm to IκB. Phosphorylation of IκB by IKK-β leads to proteasomal degradation of IκB and a liberation of the transcription factor NFκB, which enters the nucleus and induces its target genes.* BCL-X_L: B-cell lymphoma X_L, BFL1: a B cell-lymphoma-2-related protein, cIAPs: cellular inhibitors of apoptosis, COX2: cyclooxygenase-2, iNOS: inducible nitric-oxide synthase, GADD45β: growth arrest and DNA-damage-inducible 45β, SOD2: superoxide dismutase 2.

Even it was known that NFκB is activated in hypoxia the underlying mechanism was still unclear (Ryan *et al.* 2005). A recent report of Cummins *et al.* confirmed previous studies and showed that the response of NFκB in hypoxia and under DMOG treatment is due to an inhibition of the PHDs, respectively mainly PHD1 (Cummins 2006). They identified a LXXLAP consensus motif in the IKKα and

IKKβ subunit of the IKK complex and found increased IKKβ protein levels under hypoxia in HeLa cells. The mechanism was shown to be HIF-1α-independent by using siRNA against HIF-1α, which did not alter hypoxia-induced IκBα phosphorylation. Overexpressing of PHD1 decreased cytokine-stimulated NFκB reporter activity. Site-directed mutagenesis of IKKβ of putative IKKβ hydroxylation site resulted in a loss of hypoxic inducibility. To summarize these data the authors suggest that hypoxia increases NFκB activity through PHD inhibition and thereby inhibition of IKKβ hydroxylation. These results might explain one further molecular mechanism how hypoxia contributes to tumor development and progression (Cummins 2006). Furthermore these data show that PHD1 regulates additional to HIF-1α another transcription factor, NFκB. Although we could not confirm a transactivation activity of Cdr2, Cdr2 might represent an additional transcription factor regulated by PHD1.

Conclusion and Outlook

Taken together, we identified the onconeural antigen Cdr2 as an interactor of the oxygen-sensing PHD1. We showed that Cdr2 protein is stabilized in hypoxia and upon PHD inhibition when overexpressed in different cell lines. These findings were letting us assume that the limited expression of Cdr2 protein to the brain and to the testis, organs known as tissues with low oxygen partial pressure, is due to a hypoxic stabilization of Cdr2 by inhibition of PHD1. The generation of monoclonal antibodies enabled us to detect endogenous Cdr2 in several breast and ovarian cancer cell lines. However, we could not reproduce the stabilization of endogenous Cdr2 in hypoxia or upon PHD inhibition. Furthermore, the induction of PHD1 under estrogen treatment showed no change in endogenous Cdr2 protein level. The effect what we have seen with transfected Cdr2 is still an enigma. Genetic modifications of the Cdr2 locus in SKOV3 cells might represent one reason for loss of stability under hypoxia and PHD inhibition. Therefore we started a selection of clones based on a limited dilution. Nethertheless the investigation of Cdr2 interaction with PHD1 allow new insights in the ectopic expression of Cdr2 in tumor tissue. Furthermore it broadens the understanding of naturally occurring tumor immunity in paraneoplastic cerebellar degeneration.

References

Albert, M. L., L. M. Austin and R. B. Darnell (2000). "Detection and treatment of activated T cells in the cerebrospinal fluid of patients with paraneoplastic cerebellar degeneration." Ann Neurol **47**(1): 9-17.

Albert, M. L., J. C. Darnell, A. Bender, L. M. Francisco, N. Bhardwaj and R. B. Darnell (1998). "Tumor-specific killer cells in paraneoplastic cerebellar degeneration." Nat Med **4**(11): 1321-4.

Albert, M. L. and R. B. Darnell (2004). "Paraneoplastic neurological degenerations: keys to tumour immunity." Nat Rev Cancer **4**(1): 36-44.

Albert, M. L., M. Jegathesan and R. B. Darnell (2001). "Dendritic cell maturation is required for the cross-tolerization of $CD8^+$ T cells." Nat Immunol **2**(11): 1010-7.

Albert, M. L., B. Sauter and N. Bhardwaj (1998). "Dendritic cells acquire antigen from apoptotic cells and induce class I-restricted CTLs." Nature **392**(6671): 86-9.

Amano, M., H. Mukai, Y. Ono, K. Chihara, T. Matsui, Y. Hamajima, K. Okawa, A. Iwamatsu and K. Kaibuchi (1996). "Identification of a putative target for Rho as the serine-threonine kinase protein kinase N." Science **271**(5249): 648-50.

An, W. G., M. Kanekal, M. C. Simon, E. Maltepe, M. V. Blagosklonny and L. M. Neckers (1998). "Stabilization of wild-type p53 by hypoxia-inducible factor 1α." Nature **392**(6674): 405-408.

Anderson, N. E., C. Budde-Steffen, R. G. Wiley, L. Thurman, M. K. Rosenblum, S. E. Nadeau and J. B. Posner (1988). "A variant of the anti-Purkinje cell antibody in a patient with paraneoplastic cerebellar degeneration." Neurology **38**(7): 1018-26.

Appelhoff, R. J., Y. M. Tian, R. R. Raval, H. Turley, A. L. Harris, C. W. Pugh, P. J. Ratcliffe and J. M. Gleadle (2004). "Differential function of the prolyl hydroxylases PHD1, PHD2, and PHD3 in the regulation of hypoxia-inducible factor." J Biol Chem **279**(37): 38458-65.

Aprelikova, O., G. V. Chandramouli, M. Wood, J. R. Vasselli, J. Riss, J. K. Maranchie, W. M. Linehan and J. C. Barrett (2004). "Regulation of HIF prolyl hydroxylases by hypoxia-inducible factors." J Cell Biochem **92**(3): 491-501.

Arnesen, T., X. Kong, R. Evjenth, D. Gromyko, J. E. Varhaug, Z. Lin, N. Sang, J. Caro and J. R. Lillehaug (2005). "Interaction between HIF-1α (ODD) and hARD1 does not induce acetylation and destabilization of HIF-1α." FEBS Lett **579**(28): 6428-32.

Bae, S. H., J. W. Jeong, J. A. Park, S. H. Kim, M. K. Bae, S. J. Choi and K. W. Kim (2004). "Sumoylation increases HIF-1α stability and its transcriptional activity." Biochem Biophys Res Commun **324**(1): 394-400.

Baek, J. H., P. C. Mahon, J. Oh, B. Kelly, B. Krishnamachary, M. Pearson, D. A. Chan, A. J. Giaccia and G. L. Semenza (2005). "OS-9 interacts with hypoxia-inducible factor 1α and prolyl hydroxylases to promote oxygen-dependent degradation of HIF-1α." Mol Cell **17**(4): 503-12.

Bai, M. K., J. S. Costopoulos, B. P. Christoforidou and C. S. Papadimitriou (1994). "Immunohistochemical detection of the c-myc oncogene product in normal, hyperplastic and carcinomatous endometrium." Oncology **51**(4): 314-9.

Bardos, J. I. and M. Ashcroft (2005). "Negative and positive regulation of HIF-1: a complex network." Biochim Biophys Acta **1755**(2): 107-20.

Berra, E., E. Benizri, A. Ginouves, V. Volmat, D. Roux and J. Pouysségur (2003). "HIF prolyl-hydroxylase 2 is the key oxygen sensor setting low steady-state levels of HIF-1α in normoxia." EMBO J **22**(16): 4082-90.

Bhattacharya, S., C. L. Michels, M. K. Leung, Z. P. Arany, A. L. Kung and D. M. Livingston (1999). "Functional role of p35srj, a novel p300/CBP binding protein, during transactivation by HIF-1." Genes Dev **13**(1): 64-75.

Bilton, R., N. Mazure, E. Trottier, M. Hattab, M. A. Dery, D. E. Richard, J. Pouyssegur and M. C. Brahimi-Horn (2005). "Arrest-defective-1 protein, an acetyltransferase, does not alter stability of hypoxia-inducible factor (HIF)-1α and is not induced by hypoxia or HIF." J Biol Chem **280**(35): 31132-40.

Blachere, N. E., R. B. Darnell and M. L. Albert (2005). "Apoptotic cells deliver processed antigen to dendritic cells for cross-presentation." PLoS Biol **3**(6): e185.

Blancher, C. and A. L. Harris (1998). "The molecular basis of the hypoxia response pathway: tumour hypoxia as a therapy target." Cancer Metastasis Rev **17**(2): 187-94.

Bruick, R. K. and S. L. McKnight (2001). "A conserved family of prolyl-4-hydroxylases that modify HIF." Science **294**(5545): 1337-40.

Buckanovich, R. J., Y. Y. Yang and R. B. Darnell (1996). "The onconeural antigen Nova-1 is a neuron-specific RNA-binding protein, the activity of which is inhibited by paraneoplastic antibodies." J Neurosci **16**(3): 1114-22.

Burnet, M. (1957). "Cancer; a biological approach. I. The processes of control." Br Med J **1**(5022): 779-86.

Carmeliet, P. and R. K. Jain (2000). "Angiogenesis in cancer and other diseases." Nature **407**(6801): 249-57.

Casciola-Rosen, L. A., G. Anhalt and A. Rosen (1994). "Autoantigens targeted in systemic lupus erythematosus are clustered in two populations of surface structures on apoptotic keratinocytes." J Exp Med **179**(4): 1317-30.

Chan, D. A., P. D. Sutphin, S. E. Yen and A. J. Giaccia (2005). "Coordinate regulation of the oxygen-dependent degradation domains of hypoxia-inducible factor 1α." Mol Cell Biol **25**(15): 6415-26.

Chandel, N. S., E. Maltepe, E. Goldwasser, C. E. Mathieu, M. C. Simon and P. T. Schumacker (1998). "Mitochondrial reactive oxygen species trigger hypoxia-induced transcription." Proc Natl Acad Sci U S A **95**(20): 11715-20.

Cioffi, C. L., X. Q. Liu, P. A. Kosinski, M. Garay and B. R. Bowen (2003). "Differential regulation of HIF-1α prolyl-4-hydroxylase genes by hypoxia in human cardiovascular cells." Biochem Biophys Res Commun **303**(3): 947-53.

Cobb, R. R., J. McClary, W. Manzana, S. Finster, B. Larsen, E. Blasko, J. Pearson, S. Biancalana, K. Kauser, P. Bringmann, D. R. Light and S. Schirm (2005). "Cloning and characterization of the rat HIF-1α prolyl-4-hydroxylase-1 gene." Protein Expr Purif **42**(2): 295-304.

Corradi, J. P., C. Yang, J. C. Darnell, J. Dalmau and R. B. Darnell (1997). "A post-transcriptional regulatory mechanism restricts expression of the

paraneoplastic cerebellar degeneration antigen Cdr2 to immune privileged tissues." J Neurosci **17**(4): 1406-15.

Costas, M., M. P. Mehn, M. P. Jensen and L. Que, Jr. (2004). "Dioxygen activation at mononuclear nonheme iron active sites: enzymes, models, and intermediates." Chem Rev **104**(2): 939-86.

Cummins (2006). "Prolyl hydroxylase-1 negatively regulates IκB kinase-β, giving insight into hypoxia-induced NFkB activity." Proc Natl Acad Sci U S A **103**(48).

Dalgard, C. L., H. Lu, A. Mohyeldin and A. Verma (2004). "Endogenous 2-oxoacids differentially regulate expression of oxygen sensors." Biochem J **380**(Pt 2): 419-24.

Dalmau, J., H. M. Furneaux, R. J. Gralla, M. G. Kris and J. B. Posner (1990). "Detection of the anti-Hu antibody in the serum of patients with small cell lung cancer - a quantitative western blot analysis." Ann Neurol **27**(5): 544-52.

Dalmau, J., F. Graus, M. K. Rosenblum and J. B. Posner (1992). "Anti-Hu-associated paraneoplastic encephalomyelitis/sensory neuronopathy. A clinical study of 71 patients." Medicine (Baltimore) **71**(2): 59-72.

Darnell, J. C., M. L. Albert and R. B. Darnell (2000). "Cdr2, a target antigen of naturally occuring human tumor immunity, is widely expressed in gynecological tumors." Cancer Res **60**(8): 2136-9.

Darnell, R. B. (2004). "Paraneoplastic neurologic disorders: windows into neuronal function and tumor immunity." Arch Neurol **61**(1): 30-2.

Darnell, R. B. and L. M. DeAngelis (1993). "Regression of small-cell lung carcinoma in patients with paraneoplastic neuronal antibodies." Lancet **341**(8836): 21-2.

Darnell, R. B. and J. B. Posner (2003). "Observing the invisible: successful tumor immunity in humans." Nat Immunol **4**(3): 201.

Darnell, R. B. and J. B. Posner (2003). "Paraneoplastic syndromes involving the nervous system." N Engl J Med **349**(16): 1543-54.

de Beukelaar, J. W. and P. A. Sillevis Smitt (2006). "Managing paraneoplastic neurological disorders." Oncologist **11**(3): 292-305.

Dropcho, E. J. (2005). "Update on paraneoplastic syndromes." Curr Opin Neurol **18**(3): 331-6.

Dropcho, E. J., Y. T. Chen, J. B. Posner and L. J. Old (1987). "Cloning of a brain protein identified by autoantibodies from a patient with paraneoplastic cerebellar degeneration." Proc Natl Acad Sci U S A **84**(13): 4552-6.

Dupuy, D., I. Aubert, V. G. Dupérat, J. Petit, L. Taine, M. Stef, B. Bloch and B. Arveiler (2000). "Mapping, characterization, and expression analysis of the SM-20 human homologue, c1orf12, and identification of a novel related gene, SCAND2." Genomics **69**(3): 348-54.

Epstein, A. C., J. M. Gleadle, L. A. McNeill, K. S. Hewitson, J. O'Rourke, D. R. Mole, M. Mukherji, E. Metzen, M. I. Wilson, A. Dhanda, Y. M. Tian, N. Masson, D. L. Hamilton, P. Jaakkola, R. Barstead, J. Hodgkin, P. H. Maxwell, C. W. Pugh, C. J. Schofield and P. J. Ratcliffe (2001). "C. elegans EGL-9 and mammalian homologs define a family of dioxygenases that regulate HIF by prolyl hydroxylation." Cell **107**(1): 43-54.

Erez, N., M. Milyavsky, R. Eilam, I. Shats, N. Goldfinger and V. Rotter (2003). "Expression of prolyl-hydroxylase-1 (PHD1/EGLN2) suppresses hypoxia

inducible factor-1α activation and inhibits tumor growth." Cancer Res **63**(24): 8777-83.
Erez, N., M. Milyavsky, N. Goldfinger, E. Peles, A. V. Gudkov and V. Rotter (2002). "Falkor, a novel cell growth regulator isolated by a functional genetic screen." Oncogene **21**(44): 6713-21.
Erez, N., P. Stambolsky, I. Shats, M. Milyavsky, T. Kachko and V. Rotter (2004). "Hypoxia-dependent regulation of PHD1: cloning and characterization of the human PHD1/EGLN2 gene promoter." FEBS Lett **567**(2-3): 311-5.
Evan, G. and T. Littlewood (1998). "A matter of life and cell death." Science **281**(5381): 1317-22.
Fathallah-Shaykh, H., S. Wolf, E. Wong, J. B. Posner and H. M. Furneaux (1991). "Cloning of a leucine-zipper protein recognized by the sera of patients with antibody-associated paraneoplastic cerebellar degeneration." Proc Natl Acad Sci U S A **88**(8): 3451-4.
Feddersen, R. M., R. Ehlenfeldt, W. S. Yunis, H. B. Clark and H. T. Orr (1992). "Disrupted cerebellar cortical development and progressive degeneration of Purkinje cells in SV40 T antigen transgenic mice." Neuron **9**(5): 955-66.
Feldman, D. E., V. Thulasiraman, R. G. Ferreyra and J. Frydman (1999). "Formation of the VHL-elongin BC tumor suppressor complex is mediated by the chaperonin TRiC." Mol Cell **4**(6): 1051-61.
Fisher, T. S., S. D. Etages, L. Hayes, K. Crimin and B. Li (2005). "Analysis of ARD1 function in hypoxia response using retroviral RNA interference." J Biol Chem **280**(18): 17749-57.
Furneaux, H. F., L. Reich and J. B. Posner (1990). "Autoantibody synthesis in the central nervous system of patients with paraneoplastic syndromes." Neurology **40**(7): 1085-91.
Galaktionov, K., X. Chen and D. Beach (1996). "Cdc25 cell-cycle phosphatase as a target of c-Myc." Nature **382**(6591): 511-7.
Gerald, D., E. Berra, Y. M. Frapart, D. A. Chan, A. J. Giaccia, D. Mansuy, J. Pouysségur, M. Yaniv and F. Mechta-Grigoriou (2004). "JunD reduces tumor angiogenesis by protecting cells from oxidative stress." Cell **118**(6): 781-94.
Gnarra, J. R., K. Tory, Y. Weng, L. Schmidt, M. H. Wei, H. Li, F. Latif, S. Liu, F. Chen, F. M. Duh and et al. (1994). "Mutations of the VHL tumor suppressor gene in renal carcinoma." Nat Genet **7**(1): 85-90.
Goldberg, M. A., S. P. Dunning and H. F. Bunn (1988). "Regulation of the erythropoietin gene: evidence that the oxygen sensor is a heme protein." Science **242**(4884): 1412-5.
Graeber, T. G., C. Osmanian, T. Jacks, D. E. Housman, C. J. Koch, S. W. Lowe and A. J. Giaccia (1996). "Hypoxia-mediated selection of cells with diminished apoptotic potential in solid tumours." Nature **379**(6560): 88-91.
Graus, F. (1992). "Purkinje cell antibodies in a patient with cerebellar disorder." J Neurol **239**(4): 237.
Guermonprez, P., J. Valladeau, L. Zitvogel, C. Thery and S. Amigorena (2002). "Antigen presentation and T cell stimulation by dendritic cells." Annu Rev Immunol **20**: 621-67.
Guzy, R. D., B. Hoyos, E. Robin, H. Chen, L. Liu, K. D. Mansfield, M. C. Simon, U. Hammerling and P. T. Schumacker (2005). "Mitochondrial complex III

is required for hypoxia-induced ROS production and cellular oxygen sensing." Cell Metab **1**(6): 401-408.
Hagen, T., C. T. Taylor, F. Lam and S. Moncada (2003). "Redistribution of intracellular oxygen in hypoxia by nitric oxide: effect on HIF1α." Science **302**(5652): 1975-8.
Hausinger, R. P. (2004). "FeII/α-ketoglutarate-dependent hydroxylases and related enzymes." Crit Rev Biochem Mol Biol **39**(1): 21-68.
Heath, W. R. and F. R. Carbone (2001). "Cross-presentation, dendritic cells, tolerance and immunity." Annu Rev Immunol **19**: 47-64.
Hirsilä, M., P. Koivunen, V. Günzler, K. I. Kivirikko and J. Myllyharju (2003). "Characterization of the human prolyl 4-hydroxylases that modify the hypoxia-inducible factor." J Biol Chem **278**(33): 30772-80.
Hirsilä, M., P. Koivunen, L. Xu, T. Seeley, K. I. Kivirikko and J. Myllyharju (2005). "Effect of desferrioxamine and metals on the hydroxylases in the oxygen sensing pathway." FASEB J **19**(10):1308-10.
Hopfer, U., H. Hopfer, K. Jablonski, R. A. Stahl and G. Wolf (2006). "The novel WD-repeat protein Morg1 acts as a molecular scaffold for hypoxia-inducible factor prolyl hydroxylase 3 (PHD3)." J Biol Chem **281**(13): 8645-55.
Huang, L. E., E. A. Pete, M. Schau, J. Milligan and J. Gu (2002). "Leu-574 of HIF-1α is essential for the von Hippel-Lindau (VHL)-mediated degradation pathway." J Biol Chem **277**(44): 41750-5.
Huang, L. E., W. G. Willmore, J. Gu, M. A. Goldberg and H. F. Bunn (1999). "Inhibition of hypoxia-inducible factor 1 activation by carbon monoxide and nitric oxide. Implications for oxygen sensing and signaling." J Biol Chem **274**(13): 9038-44.
Isaacs, J. S., Y. J. Jung, D. R. Mole, S. Lee, C. Torres-Cabala, Y. L. Chung, M. Merino, J. Trepel, B. Zbar, J. Toro, P. J. Ratcliffe, W. M. Linehan and L. Neckers (2005). "HIF overexpression correlates with biallelic loss of fumarate hydratase in renal cancer: novel role of fumarate in regulation of HIF stability." Cancer Cell **8**(2): 143-53.
Ivan, M., T. Haberberger, D. C. Gervasi, K. S. Michelson, V. Gunzler, K. Kondo, H. Yang, I. Sorokina, R. C. Conaway, J. W. Conaway and W. G. Kaelin, Jr. (2002). "Biochemical purification and pharmacological inhibition of a mammalian prolyl hydroxylase acting on hypoxia-inducible factor." Proc Natl Acad Sci U S A **99**(21): 13459-64.
Jeong, J. W., M. K. Bae, M. Y. Ahn, S. H. Kim, T. K. Sohn, M. H. Bae, M. A. Yoo, E. J. Song, K. J. Lee and K. W. Kim (2002). "Regulation and destabilization of HIF-1α by ARD1-mediated acetylation." Cell **111**(5): 709-20.
Jiang, B. H., E. Rue, G. L. Wang, R. Roe and G. L. Semenza (1996). "Dimerization, DNA binding, and transactivation properties of hypoxia-inducible factor 1." J Biol Chem **271**(30): 17771-8.
Karin, M. and F. R. Greten (2005). "NF-κB: linking inflammation and immunity to cancer development and progression." Nat Rev Immunol **5**(10): 749-59.
Kitagawa, M., H. Mukai, H. Shibata and Y. Ono (1995). "Purification and characterization of a fatty acid-activated protein kinase (PKN) from rat testis." Biochem J **310 (Pt 2)**: 657-64.

Kivirikko, K. I. and R. Myllyla (1982). "Posttranslational enzymes in the biosynthesis of collagen: intracellular enzymes." Methods Enzymol **82 Pt A**: 245-304.

Knowles, H. J., R. R. Raval, A. L. Harris and P. J. Ratcliffe (2003). "Effect of ascorbate on the activity of hypoxia-inducible factor in cancer cells." Cancer Res **63**(8): 1764-8.

Koivunen, P., M. Hirsila, K. I. Kivirikko and J. Myllyharju (2006). "The length of peptide substrates has a marked effect on hydroxylation by the hypoxia-inducible factor prolyl 4-hydroxylases." J Biol Chem **281**(39): 28712-20.

Lando, D., D. J. Peet, D. A. Whelan, J. J. Gorman and M. L. Whitelaw (2002). "Asparagine hydroxylation of the HIF transactivation domain: a hypoxic switch." Science **295**(5556): 858-61.

Li, D., M. Hirsila, P. Koivunen, M. C. Brenner, L. Xu, C. Yang, K. I. Kivirikko and J. Myllyharju (2004). "Many amino acid substitutions in a hypoxia-inducible transcription factor (HIF)-1α-like peptide cause only minor changes in its hydroxylation by the HIF prolyl 4-hydroxylases: substitution of 3,4-dehydroproline or azetidine-2-carboxylic acid for the proline leads to a high rate of uncoupled 2-oxoglutarate decarboxylation." J Biol Chem **279**(53): 55051-9.

Lieb, M. E., K. Menzies, M. C. Moschella, R. Ni and M. B. Taubman (2002). "Mammalian EGLN genes have distinct patterns of mRNA expression and regulation." Biochem Cell Biol **80**(4): 421-6.

Lipscomb, E. A., P. D. Sarmiere and R. S. Freeman (2001). "SM-20 is a novel mitochondrial protein that causes caspase-dependent cell death in nerve growth factor-dependent neurons." J Biol Chem **276**(7): 5085-92.

Madden, S. L., E. A. Galella, D. Riley, A. H. Bertelsen and G. A. Beaudry (1996). "Induction of cell growth regulatory genes by p53." Cancer Res **56**(23): 5384-90.

Martin, F., T. Linden, D. M. Katschinski, F. Oehme, I. Flamme, C. K. Mukhopadhyay, K. Eckhardt, J. Tröger, S. Barth, G. Camenisch and R. H. Wenger (2005). "Copper-dependent activation of hypoxia-inducible factor (HIF)-1: implications for ceruloplasmin regulation." Blood **105**(12): 4613-9.

Masson, N., R. J. Appelhoff, J. R. Tuckerman, Y. M. Tian, H. Demol, M. Puype, J. Vandekerckhove, P. J. Ratcliffe and C. W. Pugh (2004). "The HIF prolyl hydroxylase PHD3 is a potential substrate of the TRiC chaperonin." FEBS Lett **570**(1-3): 166-70.

Max, B. (1992). "This and that: hair pigments, the hypoxic basis of life and the Virgilian journey of the spermatozoon." Trends Pharmacol Sci **13**(7): 272-6.

Maxwell, P. H., M. S. Wiesener, G. W. Chang, S. C. Clifford, E. C. Vaux, M. E. Cockman, C. C. Wykoff, C. W. Pugh, E. R. Maher and P. J. Ratcliffe (1999). "The tumour suppressor protein VHL targets hypoxia-inducible factors for oxygen-dependent proteolysis." Nature **399**(6733): 271-5.

McNeill, L. A., E. Flashman, M. R. Buck, K. S. Hewitson, I. J. Clifton, G. Jeschke, T. D. Claridge, D. Ehrismann, N. J. Oldham and C. J. Schofield (2005). "Hypoxia-inducible factor prolyl hydroxylase 2 has a high affinity for ferrous iron and 2-oxoglutarate." Mol Biosyst **1**(4): 321-4.

Metzen, E., U. Berchner-Pfannschmidt, P. Stengel, J. H. Marxsen, I. Stolze, M. Klinger, W. Q. Huang, C. Wotzlaw, T. Hellwig-Burgel, W. Jelkmann, H. Acker and J. Fandrey (2003). "Intracellular localisation of human HIF-1α

hydroxylases: implications for oxygen sensing." J Cell Sci **116**(Pt 7): 1319-26.
Metzen, E. and P. J. Ratcliffe (2004). "HIF hydroxylation and cellular oxygen sensing." Biol Chem **385**(3-4): 223-30.
Metzen, E., D. P. Stiehl, K. Doege, J. H. Marxsen, T. Hellwig-Bürgel and W. Jelkmann (2005). "Regulation of the prolyl hydroxylase domain protein 2 (*phd2/egln-1*) gene: identification of a functional hypoxia-responsive element." Biochem J **387**(Pt 3): 711-7.
Metzen, E., J. Zhou, W. Jelkmann, J. Fandrey and B. Brüne (2003). "Nitric oxide impairs normoxic degradation of HIF-1α by inhibition of prolyl hydroxylases." Mol Biol Cell **14**(8): 3470-81.
Myllyharju, J. and K. I. Kivirikko (1997). "Characterization of the iron- and 2-oxoglutarate-binding sites of human prolyl 4-hydroxylase." EMBO J **16**(6): 1173-80.
Myllyla, R., K. Majamaa, V. Gunzler, H. M. Hanauske-Abel and K. I. Kivirikko (1984). "Ascorbate is consumed stoichiometrically in the uncoupled reactions catalyzed by prolyl 4-hydroxylase and lysyl hydroxylase." J Biol Chem **259**(9): 5403-5.
Nakayama, K., I. J. Frew, M. Hagensen, M. Skals, H. Habelhah, A. Bhoumik, T. Kadoya, H. Erdjument-Bromage, P. Tempst, P. B. Frappell, D. D. Bowtell and Z. Ronai (2004). "Siah2 regulates stability of prolyl-hydroxylases, controls HIF1α abundance, and modulates physiological responses to hypoxia." Cell **117**(7): 941-52.
Oehme, F., P. Ellinghaus, P. Kolkhof, T. J. Smith, S. Ramakrishnan, J. Hutter, M. Schramm and I. Flamme (2002). "Overexpression of PH-4, a novel putative proline 4-hydroxylase, modulates activity of hypoxia-inducible transcription factors." Biochem Biophys Res Commun **296**(2): 343-9.
Okano, H. J. and R. B. Darnell (1997). "A hierarchy of Hu RNA binding proteins in developing and adult neurons." J Neurosci **17**(9): 3024-37.
Okano, H. J., W. Y. Park, J. P. Corradi and R. B. Darnell (1999). "The cytoplasmic Purkinje onconeural antigen Cdr2 down-regulates c-Myc function: implications for neuronal and tumor cell survival." Genes Dev **13**(16): 2087-97.
Ozer, A., L. C. Wu and R. K. Bruick (2005). "The candidate tumor suppressor ING4 represses activation of the hypoxia inducible factor (HIF)." Proc Natl Acad Sci U S A **102**(21): 7481-6.
Pescador, N., Y. Cuevas, S. Naranjo, M. Alcaide, D. Villar, M. O. Landazuri and L. Del Peso (2005). "Identification of a functional hypoxia-responsive element that regulates the expression of the *egl nine* homologue 3 (*egln3/phd3*) gene." Biochem J **15**;390:189-97
Peterson, K., M. K. Rosenblum, H. Kotanides and J. B. Posner (1992). "Paraneoplastic cerebellar degeneration. I. A clinical analysis of 55 anti-Yo antibody-positive patients." Neurology **42**(10): 1931-7.
Posner, J. B. (2003). "Immunology of paraneoplastic syndromes: overview." Ann N Y Acad Sci **998**: 178-86.
Prives, C. (1998). "Signaling to p53: breaking the MDM2-p53 circuit." Cell **95**(1): 5-8.
Ravi, R., B. Mookerjee, Z. M. Bhujwalla, C. H. Sutter, D. Artemov, Q. Zeng, L. E. Dillehay, A. Madan, G. L. Semenza and A. Bedi (2000). "Regulation of

tumor angiogenesis by p53-induced degradation of hypoxia-inducible factor 1α." Genes Dev **14**(1): 34-44.
Richard, D. E., E. Berra, E. Gothie, D. Roux and J. Pouysségur (1999). "p42/p44 mitogen-activated protein kinases phosphorylate hypoxia-inducible factor 1α (HIF-1α) and enhance the transcriptional activity of HIF-1." J Biol Chem **274**(46): 32631-7.
Roberts, W. K. and R. B. Darnell (2004). "Neuroimmunology of the paraneoplastic neurological degenerations." Curr Opin Immunol **16**(5): 616-22.
Rojas, I., F. Graus, F. Keime-Guibert, R. Rene, J. Y. Delattre, J. M. Ramon, J. Dalmau and J. B. Posner (2000). "Long-term clinical outcome of paraneoplastic cerebellar degeneration and anti-Yo antibodies." Neurology **55**(5): 713-5.
Royds, J. A., R. M. Sharrard, M. A. Parsons, J. Lawry, R. Rees, D. Cottam, B. Wagner and I. G. Rennie (1992). "C-myc oncogene expression in ocular melanomas." Graefes Arch Clin Exp Ophthalmol **230**(4): 366-71.
Ryan, S., C. T. Taylor and W. T. McNicholas (2005). "Selective activation of inflammatory pathways by intermittent hypoxia in obstructive sleep apnea syndrome." Circulation **112**(17): 2660-7.
Sakai, K., M. Gofuku, Y. Kitagawa, T. Ogasawara and G. Hirose (1995). "Induction of anti-Purkinje cell antibodies in vivo by immunizing with a recombinant 52-kDa paraneoplastic cerebellar degeneration-associated protein." J Neuroimmunol **60**(1-2): 135-41.
Sakai, K., Y. Kitagawa, Y. Li, T. Shirakawa and G. Hirose (2001). "Suppression of the transcriptional activity and DNA binding of nuclear factor κB by a paraneoplastic cerebellar degeneration-associated antigen." J Neuroimmunol **119**(1): 10-5.
Sakai, K., T. Ogasawara, G. Hirose, K. A. Jaeckle and J. E. Greenlee (1993). "Analysis of autoantibody binding to 52-kd paraneoplastic cerebellar degeneration-associated antigen expressed in recombinant proteins." Ann Neurol **33**(4): 373-80.
Sakai, K., T. Shirakawa, Y. Kitagawa, Y. Li and G. Hirose (2001). "Induction of cytotoxic T lymphocytes specific for paraneoplastic cerebellar degeneration-associated antigen in vivo by DNA immunization." J Autoimmun **17**(4): 297-302.
Salnikow, K., S. P. Donald, R. K. Bruick, A. Zhitkovich, J. M. Phang and K. S. Kasprzak (2004). "Depletion of intracellular ascorbate by the carcinogenic metals nickel and cobalt results in the induction of hypoxic stress." J Biol Chem **279**(39): 40337-44.
Sandau, K. B., J. Fandrey and B. Brune (2001). "Accumulation of HIF-1α under the influence of nitric oxide." Blood **97**(4): 1009-15.
Schofield, C. J. and P. J. Ratcliffe (2004). "Oxygen sensing by HIF hydroxylases." Nat Rev Mol Cell Biol **5**(5): 343-54.
Schofield, C. J. and P. J. Ratcliffe (2005). "Signalling hypoxia by HIF hydroxylases." Biochem Biophys Res Commun.
Selak, M. A., S. M. Armour, E. D. MacKenzie, H. Boulahbel, D. G. Watson, K. D. Mansfield, Y. Pan, M. C. Simon, C. B. Thompson and E. Gottlieb (2005). "Succinate links TCA cycle dysfunction to oncogenesis by inhibiting HIF-α prolyl hydroxylase." Cancer Cell **7**(1): 77-85.

Semenza, G. (2002). "Signal transduction to hypoxia-inducible factor 1." Biochem Pharmacol **64**(5-6): 993-8.
Semenza, G. L. (2003). "Targeting HIF-1 for cancer therapy." Nat Rev Cancer **3**(10): 721-32.
Seth, P., I. Krop, D. Porter and K. Polyak (2002). "Novel estrogen and tamoxifen induced genes identified by SAGE (Serial Analysis of Gene Expression)." Oncogene **21**(5): 836-43.
Sillevis Smitt, P., G. Manley, J. Dalmau and J. Posner (1996). "The HuD paraneoplastic protein shares immunogenic regions between PEM/PSN patients and several strains and species of experimental animals." J Neuroimmunol **71**(1-2): 199-206.
Sogawa, K., K. Numayamatsuruta, M. Ema, M. Abe, H. Abe and Y. Fujiikuriyama (1998). "Inhibition of hypoxia-inducible factor 1 activity by nitric oxide donors in hypoxia." Proc Natl Acad Sci U S A **95**(13): 7368-7373.
Soilleux, E. J., H. Turley, Y. M. Tian, C. W. Pugh, K. C. Gatter and A. L. Harris (2005). "Use of novel monoclonal antibodies to determine the expression and distribution of the hypoxia regulatory factors PHD-1, PHD-2, PHD-3 and FIH in normal and neoplastic human tissues." Histopathology **47**(6): 602-10.
Stiehl, D. P., W. Jelkmann, R. H. Wenger and T. Hellwig-Bürgel (2002). "Normoxic induction of the hypoxia-inducible factor-1α by insulin and interleukin-1β involves the phosphatidylinositol 3-kinase pathway." FEBS Lett. **512**: 157-162.
Stiehl, D. P., R. Wirthner, J. Koditz, P. Spielmann, G. Camenisch and R. H. Wenger (2006). "Increased prolyl-4-hydroxylase domain (PHD) proteins compensate for decreased oxygen levels: evidence for an autoregulatory oxygen-sensing system." J Biol Chem.
Stroka, D. M., T. Burkhardt, I. Desbaillets, R. H. Wenger, D. A. Neil, C. Bauer, M. Gassmann and D. Candinas (2001). "HIF-1 is expressed in normoxic tissue and displays an organ-specific regulation under systemic hypoxia." FASEB J **15**(13): 2445-53.
Sumbayev, V. V., A. Budde, J. Zhou and B. Brune (2003). "HIF-1α protein as a target for S-nitrosation." FEBS Lett **535**(1-3): 106-12.
Takanaga, H., H. Mukai, H. Shibata, M. Toshimori and Y. Ono (1998). "PKN interacts with a paraneoplastic cerebellar degeneration-associated antigen, which is a potential transcription factor." Exp Cell Res **241**(2): 363-72.
Tanaka, M., K. Tanaka, S. Tsuji, A. Kawata, S. Kojima, T. Kurokawa, J. Kira and M. Takiguchi (2001). "Cytotoxic T cell activity against the peptide, AYRARALEL, from Yo protein of patients with the HLA A24 or B27 supertype and paraneoplastic cerebellar degeneration." J Neurol Sci **188**(1-2): 61-5.
Takeda, K., V. C. Ho, H. Takeda, L. J. Duan, A. Nagy and G. H. Fong (2006). "Placental but not heart defects are associated with elevated hypoxia-inducible factor alpha levels in mice lacking prolyl hydroxylase domain protein 2." Mol Cell Biol **26**(22): 8336-46.
Taylor, M. S. (2001). "Characterization and comparative analysis of the EGLN gene family." Gene **275**(1): 125-32.

Tian, Y. M., D. R. Mole, P. J. Ratcliffe and J. M. Gleadle (2006). "Characterization of different isoforms of the HIF prolyl hydroxylase PHD1 generated by alternative initiation." Biochem J **397**(1): 179-86.

Tuckerman, J. R., Y. Zhao, K. S. Hewitson, Y. M. Tian, C. W. Pugh, P. J. Ratcliffe and D. R. Mole (2004). "Determination and comparison of specific activity of the HIF prolyl hydroxylases." FEBS Lett **576**(1-2): 145-50.

Ulrich, E., A. Duwel, A. Kauffmann-Zeh, C. Gilbert, D. Lyon, B. Rudkin, G. Evan and D. Martin-Zanca (1998). "Specific TrkA survival signals interfere with different apoptotic pathways." Oncogene **16**(7): 825-32.

Unruh, A., A. Ressel, H. G. Mohamed, R. S. Johnson, R. Nadrowitz, E. Richter, D. M. Katschinski and R. H. Wenger (2003). "The hypoxia-inducible factor-1α is a negative factor for tumor therapy." Oncogene **22**(21): 3213-20.

Vanderkooi, J. M., M. Erecinska and I. A. Silver (1991). "Oxygen in mammalian tissue: methods of measurement and affinities of various reactions." Am J Physiol **260**(6 Pt 1): C1131-50.

Vaupel, P., F. Kallinowski and P. Okunieff (1989). "Blood flow, oxygen and nutrient supply, and metabolic microenvironment of human tumors: a review." Cancer Res **49**(23): 6449-65.

Vomastek, T., H. J. Schaeffer, A. Tarcsafalvi, M. E. Smolkin, E. A. Bissonette and M. J. Weber (2004). "Modular construction of a signaling scaffold: MORG1 interacts with components of the ERK cascade and links ERK signaling to specific agonists." Proc Natl Acad Sci U S A **101**(18): 6981-6.

Vriz, S., J. M. Lemaitre, M. Leibovici, N. Thierry and M. Mechali (1992). "Comparative analysis of the intracellular localization of c-Myc, c-Fos, and replicative proteins during cell cycle progression." Mol Cell Biol **12**(8): 3548-55.

Wang, G. L., B. H. Jiang and G. L. Semenza (1995). "Effect of protein kinase and phosphatase inhibitors on expression of hypoxia-inducible factor 1." Biochem Biophys Res Commun **216**(2): 669-75.

Wang, G. L. and G. L. Semenza (1995). "Purification and characterization of hypoxia-inducible factor 1." J Biol Chem **270**(3): 1230-7.

Wax, S. D., C. L. Rosenfield and M. B. Taubman (1994). "Identification of a novel growth factor-responsive gene in vascular smooth muscle cells." J Biol Chem **269**(17): 13041-7.

Welford, R. W., J. M. Kirkpatrick, L. A. McNeill, M. Puri, N. J. Oldham and C. J. Schofield (2005). "Incorporation of oxygen into the succinate co-product of iron(II) and 2-oxoglutarate dependent oxygenases from bacteria, plants and humans." FEBS Lett **579**(23): 5170-4.

Wenger, R. H. (2002). "Cellular adaptation to hypoxia: O_2-sensing protein hydroxylases, hypoxia-inducible transcription factors, and O_2-regulated gene expression." FASEB J **16**(10): 1151-62.

Wenger, R. H., G. Camenisch, I. Desbaillets, D. Chilov and M. Gassmann (1998). "Up-regulation of hypoxia-inducible factor-1α is not sufficient for hypoxic/anoxic p53 induction." Cancer Res **58**(24): 5678-80.

Wenger, R. H. and D. M. Katschinski (2005). "The hypoxic testis and post-meiotic expression of PAS domain proteins." Semin Cell Dev Biol **16**(4-5): 547-53.

Wenger, R. H., D. P. Stiehl and G. Camenisch (2005). "Integration of oxygen signaling at the consensus HRE." Sci STKE **2005**(306): re12.

Zhang, Z., J. Ren, K. Harlos, C. H. McKinnon, I. J. Clifton and C. J. Schofield (2002). "Crystal structure of a clavaminate synthase-Fe(II)-2-oxoglutarate-substrate-NO complex: evidence for metal centered rearrangements." FEBS Lett **517**(1-3): 7-12.

Zhou, J., T. Schmid, S. Schnitzer and B. Brune (2006). "Tumor hypoxia and cancer progression." Cancer Lett **237**(1): 10-21.

Zindy, F., C. M. Eischen, D. H. Randle, T. Kamijo, J. L. Cleveland, C. J. Sherr and M. F. Roussel (1998). "Myc signaling via the ARF tumor suppressor regulates p53-dependent apoptosis and immortalization." Genes Dev **12**(15): 2424-33.

Zundel, W., L. M. Swiersz and A. Giaccia (2000). "Caveolin 1-mediated regulation of receptor tyrosine kinase-associated phosphatidylinositol 3-kinase activity by ceramide." Mol Cell Biol **20**(5): 1507-14.

Acknowledgements

I express my special thanks to Dr. Gieri Camenisch, for his supervision and support and his enduring patience with me and this project.

I would like to thank my Doktorvater Prof. Dr. Roland Wenger, his gift of teaching and his open door and willingness for answering questions.

I express my gratitude to Dr. Ingo Flamme, for his support as a member of the promotion committee, his review of my PhD thesis and a great scientific exchange at the “Bayer–HIF prolyl-hydroxylase–Workshop”.

I thank Dr. René Fischer (ETH Zürich) for the help in generation of anti-Cdr2 antibodies.

I thank Bala for one and a half good years of cooperation and scientific exchange in this project and his outstanding helpfulness.

I thank all the members of the “Wenger research group” for their great support. Especially I would like to thank Daniel for his helpful inputs and discussions and his encouragement.

I thank Patrick, the “soul of the lab”, for his patience and practical support in all situations.

I express my appreciation for Sandra, for all the good exchanges and her constant willingness to help.

I would like to thank my great parents and siblings Andrea and Michael and all my friends especially Haiqiong for their support and encouragement.

I express my deep gratitude and love for my husband Dennis, his prayers and his constant support.

Curriculum vitae

Personal Data

Name	HOFMANN, Verena Simone
Academic title	Dipl. Oecotrophologin
Place and date of birth	Lindau (Germany), 11.02.1978
Nationality	German
Working address	Institute of Physiology, Unversity of Zürich Winterthurerstr. 190, 8057 Zürich, Switzerland Tel. (office): +41-44-636-5021 e-mail: Verena.Hofmann@access.unizh.ch
Private address	Regensbergstr. 80 8050 Zürich Tel.: +41-43-5363026 e-mail: V.S.Hofmann@web.de

Education

1.10.2003 – Present	University of Zürich, Switzerland **PhD in Molecular Physiology** at the Physiology Institute • Yeast two-hybrid screenings of novel interactors of the oxygen sensor HIF prolyl hydroxylase 1 • Analysis and characterization of the interactor Cerebellar degeneration-related protein 2
1.10.2001 – 1.08.2002	University of Giessen, Germany **Master thesis** at the Institute of Biochemistry • Cloning, expression and characterization of the human Thioredoxin reductase (SeC498Cys)
1.10.1997 – 1.6.2003	University of Giessen, Germany **Master in Nutritional Science** Main subjects: Biochemistry, Pathophysiology, Nutrition in Developing countries and Home economics
09.1994 - 07.1997	Abitur (University Entrance qualification) Droste-Hülshoff-Gymnasium, Friedrichshafen, Germany

Internships

2002	Department of Studies and Research Affairs, Scholarship transfer and International Relations, University of Giessen, Germany • Assistant in National and EU research promotion programme • Preparation of the annual research report of the University of Giessen
2001	Medical Center Vazatehope, Kerala, India (2 months)

- Internship in Health Care and Nursing

2000 — Federal Research Centre of Nutrition & Food, Karlsruhe, Germany (BfE), Institute of Nutritional Physiology (6 months)
- Internship working on "Influence of carotinoids and retinoids on proliferation of colon carcinoma cells"

1998 — Oncology Rehabilitation Hospital, Aulendorf, Germany (1 month)
- Internship in Food and Nutrition Management

Teaching

Winter Semester 2000/2001	Practical course in physiology for nutritional science students at the Institute for Animal nutrition and Nutritional physiology University Giessen
Winter Semester 2003/2004	Practical course in physiology for medical students (Topic Blood) at the Institute of Physiology, University Zürich
Summer Semester 2004	Practical course in physiology for medical students (Topic CNS) at the Institute of Physiology, University Zürich
Winter Semester 2004/2005	Practical course in physiology for medical students (Topic Respiration) at the Institute of Physiology, University Zürich
Winter Semester 2004/2005	Practical course in physiology for human biology students (Topic Blood/Topic Membrane transport) at the Institute of Physiology, University Zürich
Winter Semester 2005/2006	Practical course in physiology for medical students (Topic signal transduction) at the Institute of Physiology, University Zürich
Summer Semester 2006	Practical course in physiology for medical students (Topic Ergometrie) at the Institute of Physiology, University Zürich

Congresses and presentations

22.09.2006 — Symposium of the Zürich Center of Integrative Human Physiology (ZIHP), Zürich, Switzerland
Junior researcher ***oral communication*** competition: "Protein stability of the onconeural antigen Cdr2 is regulated by PHD1"

22.-24.03.2006 — German Physiology Society Congress, Munich, Germany
Poster presentation: "The onconeural antigen Cdr2 is a novel oxygen regulated protein".

18.10.2005	Workshop of research group Prof. RH Wenger and Bayer AG, Wuppertal, Germany. ***Oral presentation***: "The onconeural antigen Cdr2 is a novel oxygen regulated protein"
6.10.2005	Swiss Physiological Society, Bern, Switzerland Asher-Hess Prize Young Investigator Award Competition ***Oral presentation***: "Cerebellar degeneration-related protein 2 is an interactor of oxygen sensing HIF prolyl hydroxylase 1
29.09.2005	Symposium of the Zürich Center of Integrative Human Physiology (ZIHP), Zürich, Switzerland ***Poster presentation*****:** "The onconeural antigen Cdr2 is a novel oxygen regulated protein".
21.06.2005	Seminar - Institute of Physiology, Zürich, Switzerland ***Oral presentation***: "Identification and analysis of interactors of the oxygen-sensing HIF-prolyl hydroxylase 1 (PHD1)"

Grants

2005 – 2007	Grant for consumables within the University Research Priority Program (URPP) "Zürich Integrative Human Physiology (ZIHP)"